Dissertation

submitted to the

Combined Faculties for the Natural Sciences and for Mathematics

of the Ruperto-Carola University of Heidelberg, Germany

for the degree of

Doctor of Natural Sciences

Presented by M.Sc. Xiulian Yu

Born in Datong, Shanxi Province, China

Oral-examination: 29th Nov 2016

The role of dorsoventral cell type boundaries in controlling Arabidopsis leaf development

Referees:

Dr. Alexander Aulehla

Prof. Dr. Jan Lohmann

To my parents

Zusammenfassung

Einen wichtigen entwicklungsbiologischen Mechanismus der Metazoa stellt die Etablierung von spezialisierten Zellen oder Organisatoren, welche die Musterbildung in Geweben in nicht-zellautonomer Weise bewirken, dar. Bei Pflanzen entwickelte sich Multizellularität hingegen unabhängig und die Mechanismen der Musterbildung in pflanzlichen Geweben sind weitgehend unbekannt. In der vorliegenden Dissertation wird die Rolle der adaxial-abaxialen Grenzflächen als mutmaßliche Organisatoren der Blattentwicklung untersucht. Zunächst wird gezeigt, dass Grenzflächen zwischen dem adaxial exprimierten Klasse III HD-ZIP und dem abaxial exprimierten KANADI Gens in Sprossmeristemen wichtig für die Positionierung neuer Blätter und die Bestimmung ihrer späteren morphogenetischen Muster sind. Diese und vorherige Ergebnisse unterstützen ein Model, wonach ad-ab Grenzflächen die Organogenese dadurch beeinflussen, dass zwischen der Class III HD-ZIP- und der KAN-exprimierenden Domäne ein Bereich vorhanden ist, in welchem keines der beiden Gene exprimiert wird. Um dieses Model zu verifizieren, werden mittels Mosaikanalyse ektopische REV/KAN-Grenzflächen, in denen Class III HD-ZIP- und KAN-Expressionsdomänen direkt benachbart sind, generiert. Die daraus gewonnenen Ergebnisse zeigen, dass das Vorhandensein eines Bereichs zwischen REV- und KAN-Expressionsdomänen wichtig für örtlich begrenztes Wachstum an den Grenzflächen und für die Morphogenese der Blattlamina ist, und unterstützen damit das postulierte Model. Andererseits werden Hinweise auf eine nicht-zellautonome Signaltransduktion ausgehend von REV-exprimierenden Zellklonen deutlich. Diese unterstützt die Identität der Grenzflächen auch unabhängig vom Vorhandensein einer separierten Grenzregion. Insgesamt zeigen diese Erkenntnisse deutliche Ähnlichkeiten aber auch Unterschiede in der Entwicklung von Pflanzen und Tieren auf und schaffen die Grundlage für einen integrativen konzeptionellen Bezugsrahmen zur Aufklärung allgemeiner Aspekte der Pflanzenarchitektur.

Summary

An important developmental mechanism utilized by metazoans is the establishment of specialized cells, or organizers that act to pattern tissues in a non-cell autonomous manner. In plants, for which multicellularity evolved independently, the mechanisms that organize tissue level patterning are not well understood. In this thesis, I investigate the role of adaxial-abaxial boundaries as putative organizers of leaf development. Firstly, I show that boundaries between adaxial Class III HD-ZIP and abaxial KANADI gene expression in the shoot apical meristem play an instructive role in positioning new leaves and determining their subsequent patterns of morphogenesis. These data, together with previous results, suggest a model in which ad-ab boundaries influence organogenesis due to the presence of a domain in between Class III HD-ZIP and KAN expression domains where neither set of genes is expressed. Using mosaic analysis I test this model by generating ectopic REV / KAN boundaries in which the Class III HD-ZIP and KAN expression domains are directly juxtaposed. My results indicate that the presence of a region in between REV and KAN expression is important for localized growth at the boundary and lamina morphogenesis, supporting the proposed model. However I also find evidence of non-cell autonomous signaling from REV expressing clones that promotes boundary identity regardless of whether a separated boundary region is present or not. Taken together, these findings reveal striking similarities and differences in the development of plants and animals and start to provide an integrative conceptual framework that helps clarify broad aspects of plant architecture.

Acknowledgement

I would like to thank sincerely to my PhD supervisor, Dr. Marcus Heisler for offering me such a great opportunity to work on this exciting project. It's a very valuable experience to have him as my supervisor during the last four years. I am very grateful for his kind guidance in many aspects of my research adventures. I also very much appreciate his time and effort in the critical reviewing of this thesis.

I would also like to thank Dr. Monica Pia Caggiano, who initiated this project, for her excellent pioneer work. Besides, I would like to thank Dr. Carolyn Ohno who generated most of the transgenic plants in this work, for her support and dedication to make sure the day-to-day running of the whole lab. This project wouldn't be achieved without their help. I also want to thank all the members in the lab, for their great helps and fruitful discussions.

Also, I want to thank all the members on my Thesis Advisory Committee, Dr. Alexander Aulehla, Dr. Eileen Furlong and Prof. Dr. Jan Lohmann for their brilliant ideas and valuable suggestions for my project.

Particularly, it has been such a memorable experience at EMBL in the last four years, together with a group of open-minded and warm-hearted people. I have been exposed with various training opportunities to improve myself. I am very thankful to all my friends here, especially Bingqing Zhao and Yang Bai for accompanying with me to share the joys and overcome frustrations. Also, I really appreciate the helps of Ximing Ding and Daniel Krueger for their translation of the abstract from English to German. I have also been cheered up by the drivers of EMBL shuttle bus and the Chefs in EMBL canteen for their greetings.

I would express my deeply gratitude to my parents, my sister and twin brother for their persistent love and support. Lastly, I am grateful to have the accompany of my fiancé in the last five years; his love and support has been always enlightening in my life and it has been and will continue to be exciting and adventurous to explore the world together.

Table of Contents

List of Figures:

Chapter 1 Introduction

Development usually involves the successive subdivision of tissues into distinct cell types, which ultimately differentiate to form parts of adult structures. It is now well established that cells located in boundary regions between these cell types often act as long-range organizers of further tissue patterning during animal development (Dahmann et al., 2011; Lawrence and Struhl, 1996; Meinhardt, 1983).

1.1 The identification of boundaries between adjacent cells types

The existence of boundaries between different cell types was first reported in relation to the *Drosophila* wing imaginal disc by García-Bellido in the year 1973. In his work, clones of cells created by mitotic recombination and distinguished by the presence of cuticular cell markers were found to have restricted fates within either the anterior or posterior regions (termed compartments according to cell-lineage) of the imaginal disc. Interestingly, when the clones met at the anterior-posterior border, they never crossed it but instead formed a straight line along the border (García-Bellido et al., 1973). This finding revealed the existence of compartmental boundaries that restrict the mixing of different cell types, in this case anterior and posterior cell populations (García-Bellido et al., 1973). Later, *in situ* localization analysis of the *engrailed* transcript revealed that the boundary of the *engrailed* expression domain corresponded to the anterior-posterior (A-P) compartment boundary (Kornberg et al., 1985) supporting a developmental role for compartment boundaries. Subsequently, compartment boundaries were also found in vertebrates during the development of chick, mouse and zebrafish embryos (Dahmann et al., 2011).

1.2 Boundaries – the organizing center

From the studies of compartment boundaries in *Drosophila* Meinhardt proposed the concept that the boundary regions between compartments may act as organizers to pattern surrounding tissues through the production of long range diffusible signals (Meinhardt, 1983). Subsequent experimental studies further supported Meinhardt's boundary model and led Lawrence and Struhl to propose a beautiful three-step

mechanism for tissue patterning (also referred to as the "central dogma" for tissue patterning) (Lawrence and Struhl, 1996). First, a tissue is subdivided into different cell groups (termed compartments) in response to a morphogen gradient. This is the so-called "allocation of cells" step. Second, these compartments get specified through the regulation of compartment-specific genes (termed "selector genes"), which is the so-called "acquirement of the genetic address" step. Lastly, boundary cell types are specified as a result of short-range signaling between adjacent compartments, which then become a source of long-range signals that pattern the surrounding tissues (Lawrence and Struhl, 1996). Although this "central dogma" for tissue patterning is based on findings in *Drosophila*, the idea of boundary localized long-range organizers has been widely adopted in numerous experimental studies in both invertebrates and vertebrates (Kiecker and Lumsden, 2005).

In the section below, I will briefly introduce two examples to illustrate the instructive role of compartment boundaries in tissue patterning, including the anterior-posterior (A-P) and dorsal-ventral (D-V) boundaries of the *Drosophila* wing (as an example for insects) and the dorsal-ventral (D-V) boundary of vertebrate limb.

1.2.1 Anterior-Posterior (A-P) and Dorsal-Ventral (D-V) compartment boundaries in the Drosophila wing

The *Drosophila* wing primordium is derived from the border between parasegment 4 and 5 of the embryo and is subdivided into anterior and posterior compartments (García-Bellido et al., 1973). The establishment of the A-P compartment boundary in the wing disc is dependent on the expression of selector genes and short-range signals. Specifically, expression of the posterior cell fate determinants, *engrailed* and *invected* induce the expression of *Hedgehog* (*Hh*) and repress the transcription factor *cubitus interruptus* (*Ci*) that responds to Hh within the posterior compartment (Coleman et al., 1987; García-Bellido and Santamaría, 1972; Schwartz et al., 1995; Tabata et al., 1995; Zecca et al., 1995). Hedgehog is a secreted protein that acts as a short-rang signal by diffusing across the border to the anterior compartment (Tabata and Kornberg, 1994). The expression of *cubitus interruptus* (*Ci*) is restricted to the anterior compartment by the repression of *engrailed* in the posterior domain, thus restricting the response to Hh to the anterior compartment (Schwartz et al., 1995). Since Hh can only diffuse over a distance of about 10 cell diameters, cells just

anterior to the A-P border respond to Hh signal and produce *Decapentaplegic* (Dpp) in a stripe along the A-P boundary (Zecca et al., 1995). Dpp then spreads towards both anterior and posterior sides, acting as a long-range morphogen to pattern surrounding tissues (Fig 1.1 A and B) (Lecuit et al., 1996) (also reviewed by (Hamaratoglu et al., 2014).

The *Drosophila* wing is also subdivided into dorsal and ventral compartments after the wing disc is formed, during second larval instar (García-Bellido et al., 1976). A similar mechanism for tissue patterning is utilized along the D-V compartment boundary but with more complicated short-range signalling. In particular, *apterous* (*ap*) acts as a selector gene that determines dorsal cell fate (Diaz-Benjumea and Cohen, 1993). Apterous activates the Notch ligand Serrate within dorsal compartments and represses another ligand, Delta, such that Delta is restricted to the ventral compartment. At the same time, Apterous induces the glycosyltransferase Fringe, which modifies Notch to inhibit its response to Serrate within the dorsal compartment but promote it for Delta (Brückner et al., 2000; Doherty et al., 1996; Kim et al., 1995; Panin et al., 1997). Notch is present throughout both D-V compartments and can interact with both Serrate and Delta, whereas dorsally modified Notch can only act with Delta but not Serrate. Both Serrate and Delta are thought to interact with Notch only in cell neighbours. Therefore, Notch signalling occurs in a narrow region in the vicinity of the D-V border, where dorsal modified Notch meets ventral Delta and ventral Notch meets dorsal Serrate (Blair, 2003). Then the signalling of Notch induces the expression of *wingless* (*wg*) as a stripe at the D-V boundary (Fig 1.1 A and C), which similar to Dpp, acts as a long-range morphogen for wing patterning (Neumann and Cohen, 1997), although this role has come under recent scrutiny (Swarup and Verheyen, 2012).

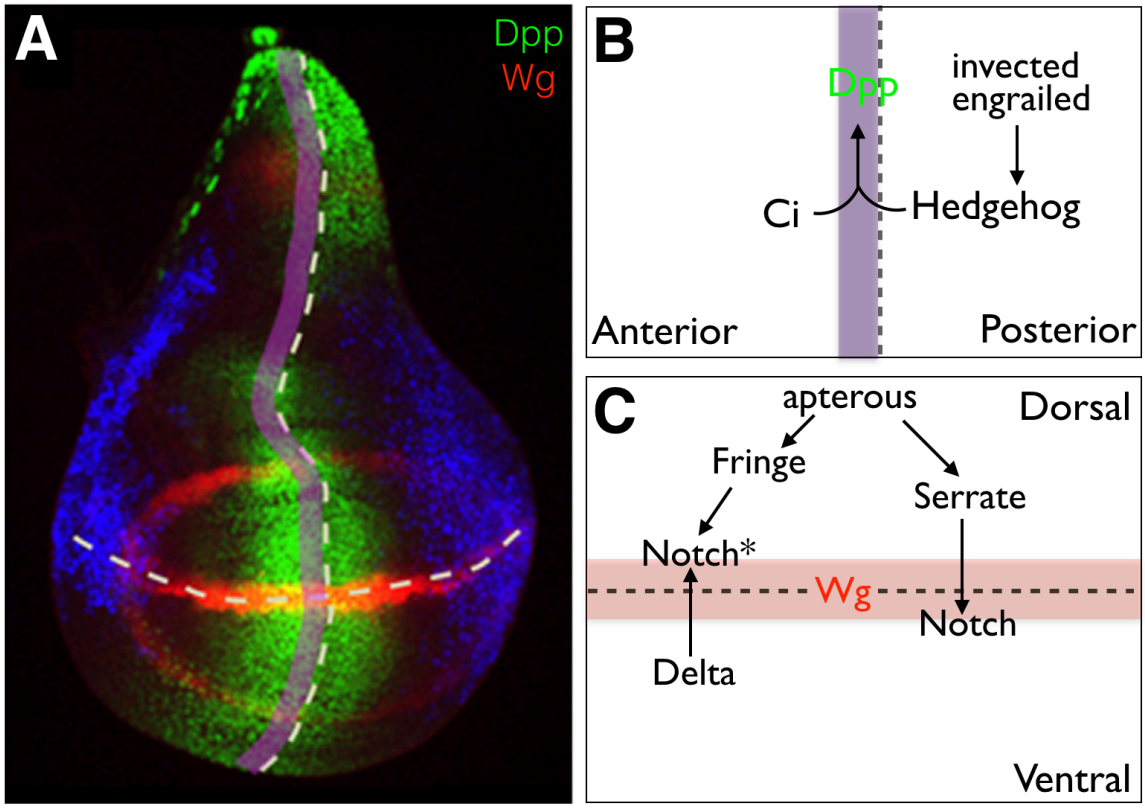

Figure 1.1 Boundary-localized organizers Dpp and Wg.

(A) Confocal image of *Drosophila* wing disc showing Dpp activity gradient (green) and Wg expression (red), dashed lines mark the A-P and D-V compartments borders, purple strip indicates the narrow region in which Dpp is produced, adapted from (Hamaratoglu et al., 2014) **(B)** Signalling pathway at the anterior-posterior compartment border (dashed line) and induction of Dpp (green), cells just anterior to the A-P border produce Dpp in response to Hedgehog. **(C)** Notch signalling (marked with light red stripe) in the vicinity of D-V border (dashed line). "Notch* indicates modified Notch by Fringe which is preferential to Delta. Modified from (Blair, 2003).

1.2.2 Dorsal-Ventral (D-V) boundary in vertebrate limb

Organizers have also been found at compartments borders in vertebrates, such as at the junction of the dorsal and ventral compartments of the limb bud. Vertebrate limb buds initiate as a protrusion containing both mesodermal and ectodermal cells. They are further patterned along three axes: the anterior-posterior (A-P), proximal-distal (P-D), and dorsal-ventral (D-V) axes. At the tip of the limb bud, there is a thickened ectoderm region along the dorsal-ventral borders, which is called the apical ectodermal ridge (AER). Surgical experiments involving removal of the AER during

chick limb bud development revealed an essential role of the AER in limb bud proximal-distal growth, since removal of the AER resulted in truncation of the chick wing (Saunders, 1948; Summerbell, 1974). Subsequently, fibroblast growth factors (FGFs) were identified as molecules produced by AER that promote limb growth, as the developmental arrest resulting from AER removal could be rescued by application of FGF-soaked beads (Fallon et al., 1994; Niswander et al., 1993).

The formation of AER involves the regulation of both bone morphogenetic protein (BMP) signaling and the *Wnt* genes (*Wnt-2b*, *Wnt-8c* and *Wnt-3a*) mediated by an FGF-8/FGF-10 feedback loop (Ahn et al., 2001; Kawakami et al., 2001; Pizette et al., 2001). In particular, the AER is formed through three steps: Firstly the induction of *Fgf8* expression in the ectoderm AER precursors is promoted by Fgf10, Wnt3a and BMP signaling; Secondly AER precursors within both the dorsal and ventral ectoderm (in chick, while located in the ventral ectoderm in mouse) become centered at the distal tip, possibly due to cell migration or downregulation of *Fgf8* in the cells surrounding the distal tip; lastly *Fgf8* expression induces cells to elongate and compact to form a columnar epithelium (Niswander, 2003). Although a direct link between AER formation and signalling along the distal D-V border remains unclear, there is evidence that proper AER formation is dependent on the compartmentalization of dorsal and ventral cell types (Kimmel et al., 2000).

In contrast to the cell-lineage compartmentalization along both the A-P and D-V axes of the *Drosophila* wing, compartmentalization only occurs along the D-V axis in the vertebrate limb bud (Arques et al., 2007). In addition, the compartments occur both within ectoderm and mesenchymal tissue unlike D-V compartments in the *Drosophila* wing, which only occur in epithelial tissues. Cell lineage analysis in the mouse limb revealed that compartmentalization of limb ectoderm divides it into three regions: the dorsal ectoderm; the dorsal AER; and the ventral ectoderm (Kimmel et al., 2000). The dorsal ectoderm expresses Wnt7a, which encodes a secreted protein that induces the expression of *Lmx1b* in the mesenchyme underling the dorsal ectoderm (Dealy et al., 1993; Parr et al., 1993; Riddle et al., 1995; Vogel et al., 1995). *Lmbx1* encodes a LIM-homeodomain transcription factor that acts to specify dorsal cell fate during limb development (Riddle et al., 1995; Vogel et al., 1995). Conversely, the transcription factor *Engrailed1* (*En1*) induced by BMP signalling is expressed in the ventral ectoderm and the ventral half of the AER (Ahn et al., 2001; Kimmel et al., 2000;

Pizette et al., 2001). En1 was found to repress the expression of *Wnt7a*, since in *En1* mutant limbs, *Wnt7a* is misexpressed in the ventral ectoderm resulting in the formation of bi-dorsal limb (Loomis et al., 1996). The dorsal AER is characterized by the absence of both Wnt7a and En1 (Kimmel et al., 2000). It has been reported that the dorsal ectoderm border, the transit middle border (corresponding to the boundary of *En1* expression domain) within the AER and the ventral ectoderm border are required for the compaction of the pre-AER cells (Kimmel et al., 2000). In addition, early transplanting experiments revealed a direct link between AER formation and the D-V axis. For instance, transplanting cells between the dorsal and ventral compartments in the chick limb results in ectopic AER formation and limb-like outgrowths are induced at the novel D-V boundaries (Fig 1.2 C) (Laufer et al., 1997a; Tanaka et al., 1997). This juxtaposition induced organ growth also occurs in the *Drosophila* wing. When the activity of the dorsal selector gene *apterous* is lost in clones of cells (ap^- clones adapted ventral cell identity) within the dorsal compartment (ap^+ cells), ectopic wing blades are formed at the clonal boundaries (Fig 1.2 A and B) (Diaz-Benjumea and Cohen, 1993). Hence juxtaposition dependent growth is a hallmark of boundary-localized organizers.

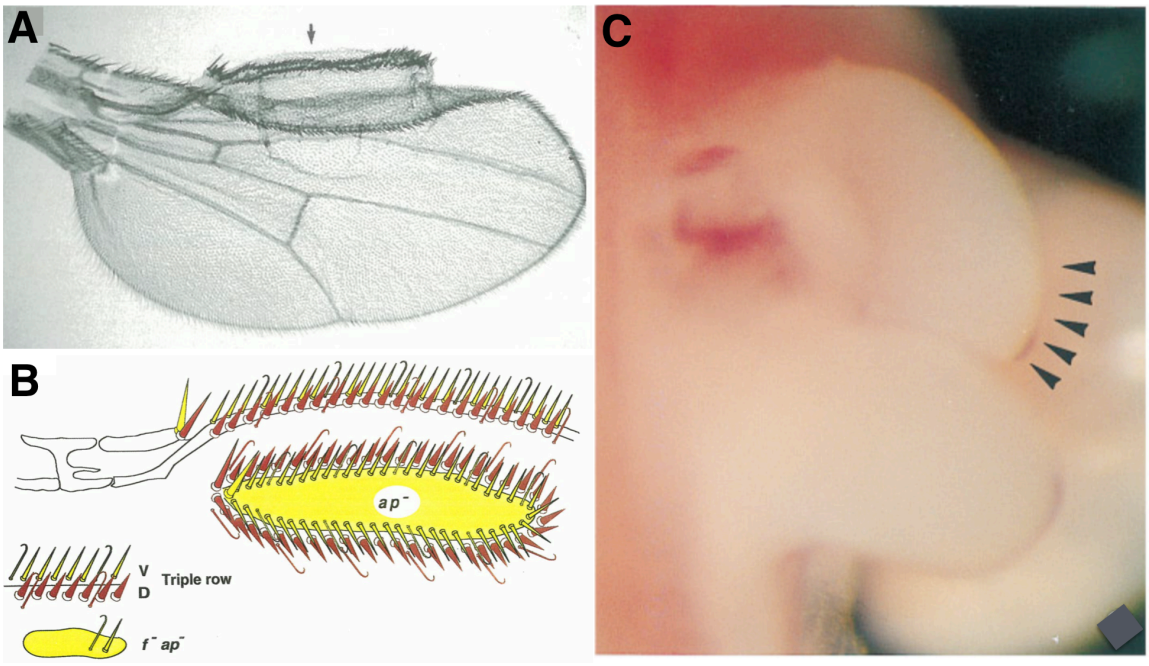

Figure 1.2 Juxtaposition dependent organ formation.

(A and B) Ectopic wing blade surrounding the ap^- clone with ectopic wing margin at the tip, indicated by arrow in (A) and the ectopic margin resembled that of normal wing margin as

shown in the schematic drawing (B) (Diaz-Benjumea and Cohen, 1993). **(C)** Ectopic limb bud formation with ectopic AER at the tip (arrowheads) at 36hr after transplanting presumptive dorsal tissue to the ventral domain of stage 12/13 chick embryo wing bud (Tanaka et al., 1997).

Taken together, although the molecular mechanism underlining the formation of boundary organizers is quite different in *Drosophila* wing and vertebrate limb, in both cases, lineage boundaries serve as the location for long-range organizers.

1.3 Dorsal-Ventral patterning in plant leaves

Similar to the *Drosophila* wing and vertebrate limb bud, the lateral organs of seed plants, such as leaves, are also flattened along the dorsal (top) - ventral (bottom) axis. The cell types in the upper and lower halves of leaves are also quite distinct. Most importantly, over twenty years ago, based on the phenotype of the *phan* mutant (discussed further below) Richard Waites and Andrew Hudson proposed that boundary regions between dorsal and ventral leaf tissues may control leaf development in a similar way in which boundary regions control wing and limb development in animals (Waites and Hudson, 1995). This was a very important proposal since it suggested a specific developmental mechanism, already quite well characterized in animals, that might also underlie leaf development. Below I review the literature on dorsoventral patterning in plants before stating the aims of my thesis.

1.3.1 The Shoot Apical Meristem (SAM)

Plants generate all their aboveground tissues through the activity of the shoot apical meristem (SAM), which is located at the tip of the shoot (Fig 1.3 A). The SAM is divided into three different zones according to cytological differences: the central zone (CZ) where the stem cells reside contains cells that divide infrequently; the periphery zone (PZ) is where lateral organs of the plant initiate and this region contains cells that divide more rapidly. Lastly, the rib zone (RZ) is located beneath the central zone and contains cells that also divide rapidly to give rise to the stem (Fig 1.3 B) (Steeves and Sussex, 1989). Apart from these subdivisions, the SAM is also organized into different cell layers according to their cell division patterns. In the SAM of *Arabidopsis*, the tunica contains two adjacent cell layers, the epidermal layer or layer 1 (L1) and Layer 2 (L2), where cells divide anticlinally. The corpus or layer 3

(L3), located beneath the tunica, contains cells that divide in variable planes (Fig 1.3 C) (Steeves and Sussex, 1989).

The SAM is formed during early embryogenesis and after germination it goes through a vegetative phase (vegetative meristem) that involves the production of leaves, before entering a reproductive phase (inflorescence meristem) during which the SAM produces flowers (Steeves and Sussex, 1989). The establishment and maintenance of the SAM depends on several phytohormones (such as auxin, cytokinin and gibberellin) and gene regulatory networks such as the *CLAVATA* (*CLV*)-*WUSCHEL* (*WUS*) and KNOX1 pathways (reviewed by (Gaillochet and Lohmann, 2015; Hudson, 2005; Jenik and Barton, 2005)).

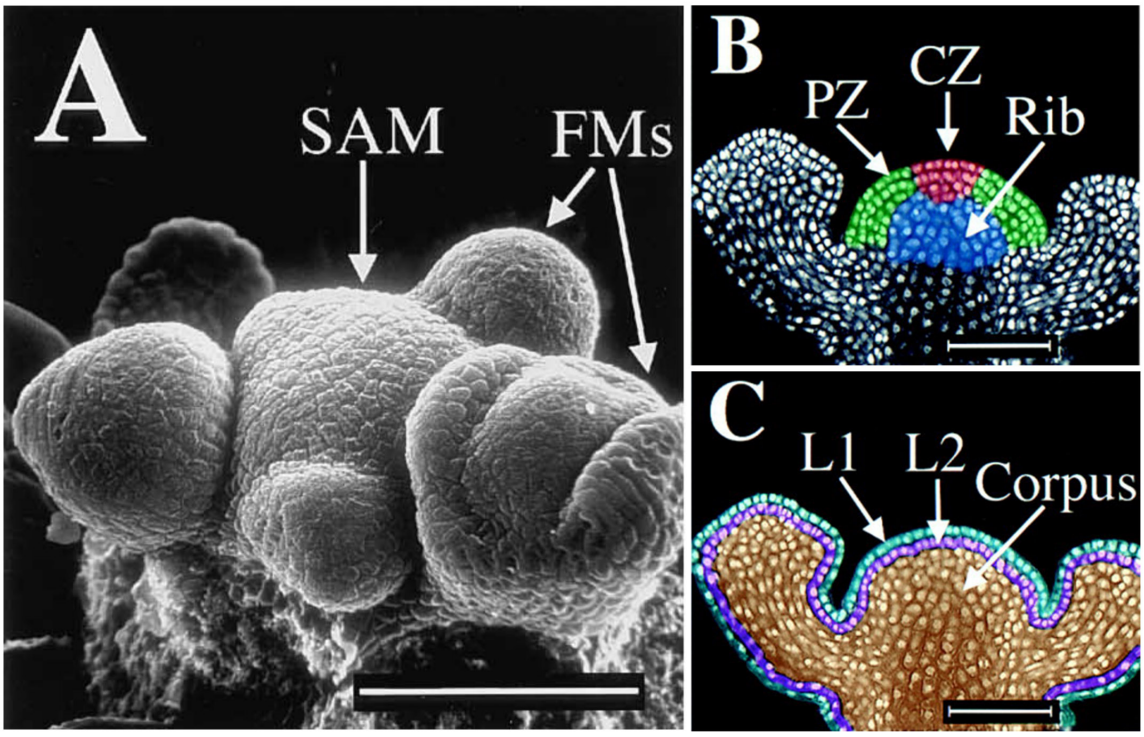

Figure 1.3 Arabidopsis shoot apical meristem (SAM).

(A) Scanning electron micrograph of the shoot apical meristem of *Arabidopsis* with flower buds at the periphery. **(B)** Longitudinal section of the SAM with colors indicating three different zones of the SAM. Red marks the central zone (CZ), green labels the periphery zone (PZ) and blue marks the rib zone (Rib). **(C)** Longitudinal section with colors indicating the layered structure of the SAM. Bars = 50 µm. Adapted from (Meyerowitz, 1997).

1.3.2 Lateral organ initiation

Lateral organs such as leaves or flowers initiate at the periphery of the SAM. The role of auxin transport in this process was first revealed by the phenotypes of plants treated with the auxin transport inhibiter *N*-1-naphthylphthalamic acid (NPA). These plants developed a shoot apex devoid of flowers (Okada et al., 1991). In the same study the *pin1-1* mutant was described, which developed the same pin-shaped inflorescence stem phenotype (Okada et al., 1991). Subsequently, molecular cloning of the *PIN1* gene showed that it encodes a 622 amino acids protein with 8 to 12 predicted transmembrane domains, similar to the bacterial and eukaryotic carrier proteins (Gälweiler et al., 1998). PIN1 localize to the plasma membrane in a polar fashion, which is consistent with the predicted role in auxin transport (Gälweiler et al., 1998). Further experiments in which exogenous IAA (the natural auxin indole-3-acetic acid) was applied manually to tomato apices previously treated with NPA and *pin1-1* meristems revealed that organ formation could be rescued by such treatments, indicating that the local distribution of auxin, as patterned by auxin transport, plays an instructive role in determining organ position (Reinhardt et al., 2000). Later studies detailing the expression pattern of PIN1 in the SAM revealed that PIN1 is mainly expressed in the epidermal layer of the SAM as well as in the provasculature (Heisler et al., 2005; Reinhardt et al., 2003). In the vicinity of organ initiation sites, PIN1 is asymmetrical localized on the plasma membrane on the sides of epidermal cells facing the initiation site. This type of arrangement is call a polarity convergence pattern and it results in the local accumulation of auxin, which in turn promotes organ formation (Benková et al., 2003; Heisler et al., 2005; Reinhardt et al., 2003). Such polarity arrangements are now known to be the result of a feedback loop in which cells containing high levels of auxin, signal to neighboring cells via the Auxin Response Factor (ARF) MONOPTEROS to transport more auxin towards those cells (Bhatia et al., 2016).

1.3.3 Establishment of Dorsal-Ventral (Adaxial-Abaxial) polarity

Since lateral organs initiate at the periphery of the SAM, they have one side facing the meristem and this is called adaxial side. The side facing away from the meristem is called the abaxial side (Steeves and Sussex, 1989). During development the leaf primordium becomes blade or lamina shaped with the adaxial side corresponding to

the upper or dorsal side and the abaxial side corresponding to the bottom or ventral side. The developmental mechanisms underlying this typical bifacial structure have long been of interest to biologists.

1.3.3.1 Sussex signal – a signal from the shoot apical meristem

Early in 1950s, Ian Sussex conducted elegant experiments on *Solanum tuberosum* (potato) in which he surgically isolated leaf primordia from the shoot apical meristem (SAM). These leaf primordia subsequently developed into radially symmetric structures consisting of ventral cell types (Sussex, 1951). Based on this observation, he proposed that dorsal cell fate is specified by a mobile signal derived from the meristem (later named "Sussex signal") which is blocked upon wounding. More recently, Reinhardt and coworkers performed similar surgical experiments using a more sophisticated laser ablation method on the tomato shoot apex (Reinhardt, 2004). They observed that wounds restricted to the L1 layer of the SAM were sufficient to cause similar phenotypes (Reinhardt, 2004). The nature of the putative mobile signal remains unknown.

1.3.3.2 Dorsal and ventral determinants

Work conducted over many years has resulted in the identification of several key genes involved in specifying dorsoventrality, thereby providing important new molecular insights into the genetic regulation of leaf polarity. In addition to transcription factors, two types of small RNAs were also found to play key roles.

1.3.3.2.1 Determination of dorsal identity

***PHANTASTIC* (*PHAN*)**

PHANTASTICA (*PHAN*) from *Antirrhinum majus* was the first gene discovered in the plant kingdom with an obvious role in controlling leaf polarity. The *phan* mutant develops a needle-like leaf consisting of only ventral cell types, indicating that *phan* is necessary for specifying dorsal cell identity (Waites and Hudson, 1995). Furthermore, it was observed that clonal patches of ventral epidermal tissue often developed ectopically on dorsal leaf surfaces and that ridges or protuberances often formed at the boundary between these patches and the surrounding dorsal tissue.

These observations led Waites and Hudson to propose that juxtaposition of dorsal and ventral cell types may promote lamina growth analogously to the way in which juxtaposition of different cells types causes ectopic wing development in Drosophila (Waites and Hudson, 1995). Although subsequent cloning of the *PHAN* gene revealed it was expressed ubiquitously (Waites et al., 1998), the proposal that juxtaposition of dorsal and ventral cell types promotes lamina development has now been supported by many other studies where it has been shown that both dorsal and ventral tissues need to be present for a leaf blade to develop (Kidner and Timmermans, 2010).

ASYMMETRIC LEAVES1 and *2* (*AS1* and *AS2*)

In *Arabidopsis*, the orthologue of *PHAN* is *ASYMMETRIC LEAVES1* (*AS1*), which encodes a myb-like transcription factor (Byrne et al., 2000). In contrast to the radially symmetric, abaxialized leaf phenotype of the *phan* mutant (Waites and Hudson, 1995), *as1* mutants of *Arabidopsis* exhibit rumpled and lobed leaves without obvious leaf polarity defects (Byrne et al., 2000; Tsukaya and Uchimiya, 1997). Interestingly, mutations in *ASYMMETRIC LEAVES2* (*AS2*), which encodes a LATERAL ORGAN BOUNDARIES (LOB) domain protein that also contains a leucine-zipper motif (Iwakawa et al., 2002), has a very similar phenotype (Ori et al., 2000; Semiarti et al., 2001). And, although only overexpression of *AS2* leads to polarity defects (Xu et al., 2003) this phenotype depends on the presence of *AS1* (Iwakawa et al., 2002; Lin et al., 2003; Xu et al., 2003). Perhaps explaining these data *in vitro* assays show that AS1 and AS2 interact physically (Xu et al., 2003). Since *AS1* is expressed throughout leaf primordia (Byrne et al., 2000), while transcripts of *AS2* are mainly detected in the dorsal domain (Iwakawa et al., 2002), an AS1-AS2 protein complex would be predicted to only form in the dorsal domain of the leaf. Thus the function of AS1 in leaf dorsoventrality may largely depend on its interaction with AS2 (Xu et al., 2003).

The Class III HD-ZIPs

In *Arabidopsis*, the class III homeodomain-leucine zipper (HD-ZIPIII) family of transcription factors comprises five members including ATHB8, PHAVOLUTA (PHV), PHABULOSA (PHB), CORONA (CNA) and REVOLUTA (REV). These proteins contain three different domains: an HD-Zip domain that determines DNA binding specificities and protein dimerization (Sessa et al., 1998), a START domain

for putative lipid or steroid binding (Ponting and Aravind, 1999), and a conserved MEKHLA domain at the C-terminus.

Among the five members of HD-ZIP III family transcription factors, three of them including *PHB*, *PHV*, and *REV* exhibit similar expression patterns in the center of the meristem, in the vasculature and in the dorsal domain of the developing leaves, which is consistent with their function in the maintenance of the meristem and specification of the dorsal cell fate (Emery et al., 2003; Heisler et al., 2005; McConnell et al., 2001; Otsuga et al., 2001). A large number of mutant alleles for these genes have been isolated. Gain of function mutants with lesions in the miR165/166 regulatory site of *phb* (e.g. *phb-1d*), *phv* (e.g. *phv-1d*) and *rev* (e.g. *rev-10d*) exhibit a dramatic dorsalization phenotype (Emery et al., 2003; McConnell and Barton, 1998; McConnell et al., 2001) In contrast, single recessive mutations in the *PHB* and *PHV* genes result in normal looking plants (Emery et al., 2003). However *rev* loss-of-function alleles such as *rev-1* and *rev-6*, displayed defects in organ development as well as axillary and floral meristem formation (Otsuga et al., 2001; Talbert et al., 1995). Although the single loss-of-function mutant does not show a defect in leaf dorsoventrality, the triple mutant (*phb-6 phv-5 rev-9*) displays a dramatic phenotype with a lack of SAM and occasionally only a single ventralized (abaxialized) cotyledon (Emery et al., 2003). The triple mutant phenotype together with the expression patterns of *PHB*, *PHV* and *REV*, indicate that they act redundantly to maintain the meristem and specify dorsal cell fate (Emery et al., 2003). The activity of Class III HD-ZIPs is not only regulated by miR165/166 (describe below), but also by four LITTLE ZIPPER (ZPR1-4) proteins that prevent the binding of Class III HD-ZIPs to the DNA due to the formation of Class III HD-ZIPs/ZPR heterodimers (Wenkel et al., 2007).

1.3.3.2.2 Determination of ventral identity

The specification of ventral identity is controlled by several key factors, including the *YABBY* gene family, the *KANADI* (*KAN*) gene family and two members of auxin response factors: *ARF3/ETT* and *ARF4*.

The *YABBY* (*YAB*) genes

There are six members in the *Arabidopsis* YABBY transcription factor family including *CRABS CLAW* (*CRC*), *FILAMENTOUS FLOWER* (*FIL*)/*YABBY1* (*YAB1*), *YABBY2* (*YAB2*), *YABBY3* (*YAB3*), *INNER NO OUTER (INO)/YABBY4* (*YAB4*) and *YABBY5* (*YAB5*) (Siegfried et al., 1999). *CRC* and *INO* are expressed only within the floral organs, with *CRC* expression being detected in the carpels and nectaries, and *INO* expression in the ventral/abaxial region of outer integument during ovule development (Bowman and Smyth, 1999; Villanueva et al., 1999). Consistent with its expression pattern within flowers, *CRC* functions to regulate carpel and nectary development, while *INO* plays an essential role in promoting outer integument growth (Bowman and Smyth, 1999; Villanueva et al., 1999). In contrast, the remaining four members *FIL*, *YAB2*, *YAB3* and *YAB5* are so-called "vegetative YABBY genes" as they have similar expression patterns in the abaxial domain of cotyledons, leaves and leaf-derived floral organs (Sarojam et al., 2010; Sawa et al., 1999; Siegfried et al., 1999). None of the single mutants of these four genes show obvious vegetative phenotypes, although some *fil* alleles displayed partial radialization in the leaf-derived floral organs (Kumaran et al., 2002; Sawa et al., 1999; Stahle et al., 2009). However, triple (*fil yab3 yab5*) and quadruple mutants (*fil yab2 yab3 yab5*) show a dramatic loss of lamina expansion in leaves including a complete radialization of organs in later produced leaves (Sarojam et al., 2010; Stahle et al., 2009). Furthermore, overexpression of *FIL* or *YAB3* is sufficient to transform dorsal epidermal cell types to ventral cell identities, further supporting a role for these genes in determining ventral cell fate (Sawa et al., 1999; Siegfried et al., 1999). The expression of "vegetative YABBY genes" is restricted to the ventral/abaxial side only gradually during leaf development (Sarojam et al., 2010; Sawa et al., 1999; Siegfried et al., 1999), indicating that specification of dorsoventrality may be a gradual process.

The *KANADI* (*KAN*) genes

The *KANADI* (*KAN*) gene family is composed of four members: *KAN1* to *KAN4/ABERRANT TESTA SHAPE* (*ATS*), encoding GARP-domain transcription factors (Eshed et al., 2001; Kerstetter et al., 2001; McAbee et al., 2006). Expression analyses reveal that the *KAN* genes are expressed in the abaxial domain of lateral organs and at the periphery of the SAM (*KAN1* and *KAN2*), while the expression of *KAN4* was only examined in floral organs with expression detected at the boundary between the inner and outer integuments (Eshed et al., 2004; Kerstetter et al., 2001;

McAbee et al., 2006; Yadav et al., 2013). Mutant studies indicate that members of the KAN gene family act redundantly to promote abaxial identities since none of the single mutants of these genes exhibit dramatic alteration in leaf polarity (Eshed et al., 2001). However, higher order loss-of-function mutants cause dramatic adaxialization of leaves correlated with a reduction of lamina and the formation of ectopic outgrowths in different locations (Eshed et al., 2001; 2004; Izhaki and Bowman, 2007). In particular, *kan1kan2* double mutants exhibit narrow, cup-shaped cotyledons and narrow leaves with ectopic finger-shaped outgrowths on their abaxial side (Eshed et al., 2001). Moreover, the *kan1kan2kan3* triple mutants show a further reduction in lamina growth and a radialized leaf structure excluding the distal tips compared to that of the *kan1kan2* double mutants (Eshed et al., 2004). Interestingly, the *kan1kan2kan4* triple mutants develop ectopic radial leaf-like organs on the hypocotyl and outgrowth not only on the abaxial side of the leaves but also on the cotyledons (Izhaki and Bowman, 2007). Furthermore, the quadruple mutant *kan1kan2kan3kan4* display an additive phenotype with partially radialized lateral organs similar to *kan1kan2kan3* and ectopic outgrowth on cotyledons and hypocotyl similar to that of *kan1kan2kan4*, indicating that KAN3 and KAN4 act redundantly with KAN1 and KAN2 in distinct regions during plant vegetative development (Izhaki and Bowman, 2007). Although all KAN activity is lost in the quadruple mutant, leaves still only display a partially reduced lamina at the tip, indicating that KAN genes are not absolutely required for leaf lamina development. However, overexpression of *KAN1* or *KAN2* driven by the *AS1* promoter results in complete radialization and abaxialization of leaves and the inhibition of vasculature formation, indicating that KAN genes are sufficient to specify abaxial cell fate (Eshed et al., 2001). When any of *KAN1*, *KAN2* or *KAN3* is overexpressed using the constitutive CaMV35S promoter, the meristem is arrests and vasculature tissues fail to form (Eshed et al., 2001; Kerstetter et al., 2001). Taken together, these studies shows that the KAN genes act redundantly to promote ventral cell fate and define organ positions.

Auxin Response Factor3* (*ARF3*)/*ETTIN* (*ETT*) and *ARF4

Two members of the auxin response factor family of transcription factors, ARF3/ETTIN (ETT) and ARF4 are known to act redundantly in the establishment of leaf abaxial cell fate with overlapping expression patterns in the abaxial side of leaves (Pekker et al., 2005). Although the single mutant for either *ETT* or *ARF4* displays no

obvious leaf polarity defect, the *ett arf4* double mutant exhibits a strikingly similar phenotype to that of the *kan1kan2* double mutant (Pekker et al., 2005). Additionally, abaxialized leaf phenotype caused by overexpression of KAN is suppressed in the *ett* mutant background. However the *kan1kan2* double mutant phenotype can not be rescued by ectopic expression of either *ARF3* or *ARF4*, indicating that ARF3 and ARF4 possibly act together with KAN rather than downstream to promote abaxial cell identity (Pekker et al., 2005). Later studies have also shown that both KAN1 and KAN4 can interact with ETT in a yeast two-hybrid assay, further supporting the idea that they play a common role in the determination of leaf polarity (Kelley et al., 2012).

1.3.3.2.3 Small RNAs

In addition to the transcription factor families described above, the establishment of leaf dorsoventral polarity in *Arabidopsis* also involves small RNAs such as miR165/166 and tasiR-ARFs, which regulate some of the key transcription factors described above.

MIR165/166

In *Arabidopsis*, miR165 and miR166, which differ by only one nucleotide, contain almost perfect complementary sequences to a region present within the START domain of Class III HD-ZIPs (Reinhart et al., 2002; Rhoades et al., 2002) and regulate the Class III HD-ZIPs post transcriptionally. There are two genes in the *Arabidopsis* genome that encode miR165 (*MIR165A* and *MIR165B*), while seven genes encode miR166 (*MIR166A* to *MIR166G*) (Reinhart et al., 2002). Transcripts of MIR165/166 are detected in the ventral leaf epidermis and this specific expression pattern is controlled by two-types of cis-acting elements within their promoters (Yao et al., 2009). In particular, the type I element controls transcription throughout the epidermal layer of the leaf, while the type II element helps to restrict the transcripts specifically to the ventral side (Yao et al., 2009). The critical role of miR165/166 in leaf dorsoventrality is to spatially restrict Class III HD-ZIPs expression to the dorsal domain of leaves, since disruption of this regulation results in severe leaf polarity defects with radial and adaxialized leaves (McConnell and Barton, 1998). In fact the regulation goes both ways as it has recently been shown that the Class III HD-ZIPs

together with the related Class II HD-ZIPs directly repress these MIRs via their type II element (Merelo et al., 2016).

Trans-acting short-interfering RNA–auxin response factors (tasiR-ARFs)

The tasiR-ARFs are small RNAs that direct the degradation of *ARF3/ETT* and *ARF4* transcripts (Allen et al., 2005; Williams et al., 2005). The tasiR-ARFs are processed from the transcript of *TAS3* through miR390- ARGONAUTE7/ZIPPY (AGO7/ZIP) complex mediated cleavage (Montgomery et al., 2008). The cleavage fragments are then converted into double-stranded RNAs (dsRNAs) via the activities of SUPPRESSOR OF GENE SILENCING3 (SGS3) and RNA-DEPENDENT RNA POLYMERASE6 (RDR6), respectively. The DICER-LIKE4 (DCL4) protein further cleaves these dsRNAs into 21-nucleotide ta-siRNAs (Chapman and Carrington, 2007). Although *Arabidopsis* mutants in tasiR-ARF biogenesis display increased expression levels of *ARF3* and *ARF4*, they do not show obvious alteration in leaf dorsoventrality in contrast to that of maize and rice (Nagasaki et al., 2007; Nogueira and Timmermans, 2007). Further studies show that TAS3 ta-siARF pathway may act partially redundantly with the AS1-AS2 pathways, as mutants defective in tasiR-ARF production enhance the *as1* and *as2* mutant phenotypes (Garcia et al., 2006; Xu et al., 2006). It has been reported that miR390 is present broadly throughout the SAM and leaves, whereas tasiR-ARFs production is restricted to the dorsal cell layers of the leaf due to the localized expression of *AGO7* and *TAS3A* dorsally (Chitwood et al., 2009). The tasiR-ARFs are also considered to be a mobile signal during leaf development based on the observation that they move from where they are produced to restrict the expression of *ARF3* and *ARF4* (Chitwood et al., 2009).

1.3.3.2.4 Antagonistic interactions between dorsal and ventral factors

Class III HD-ZIPs* and *KANs

In *kan1kan2* double and *kan1kan2kan3* triple mutants, the Class III HD-ZIP genes *REV* and *PHB* are ectopically expressed throughout the leaves (Eshed et al., 2001; 2004). Conversely, when KAN is ectopically expressed throughout the leaf primodia, the expression of PHB is lost in the radial and abaxialized leaves (Eshed et al., 2004). Therefore, *KANs* negatively regulate *Class III HD-ZIPs* expression. Recently, it has been found that KAN1 directly binds to the promoters of both *MIR166A* and

MIR166F, indicating that KAN1 may regulate the expression of Class III HD-ZIP via these *MIRs* (Merelo et al., 2013). So far, there is not so much evidence that the *KAN* genes are regulated by the Class III HD-ZIP genes. One such piece of evidence however is based on the observation that the loss of bilateral symmetry phenotype of *phb phv rev* mutants with is partially rescued by the loss of *kan1 kan2 kan4* activities, suggesting that Class III HD-ZIPs also possibly repress KAN expression (Izhaki and Bowman, 2007).

AS2* and *KANs

The discovery of a gain-of-function allele for *AS2*, *as2-5D,* containing a G-to-A mutation in the *AS2* promoter reveals an antagonistic interaction between *AS2* and *KANs* (Wu et al., 2008). It has been reported that KAN1 directly down-regulates the expression of *AS2* through a site within the promoter that is mutated in *as2-5D*. Although there is no direct evidence for the binding of KAN2 to the promoter of *AS2*, KAN2 acts redundantly with KAN1 to repress *AS2* in the ventral domain of cotyledons and leaves (Wu et al., 2008). Conversely, plants overexpressing *AS2* show a reduction in both KAN1 and KAN2 transcripts and their leaf phenotype resembles that of the *kan1kan2* double mutant with outgrowths from ventral leaf tissues (Lin et al., 2003). Further support for this relationship comes from the finding that in the *as2-1* mutant, *KAN1* expression extends to the dorsal side of young leaf primodia. Also, *kan-11 as2-5D* (gain-of-function *AS2* mutant) plants exhibit a similar phenotype to that of the *kan1kan2* double mutant, further indicating that *AS2* represses both *KAN1* and *KAN2* activity (Wu et al., 2008).

AS1-AS2* and *ARF3-ARF4

It's likely that the *AS1-AS2* and *ARF3-ARF4* pathways also antagonize each other. Plants highly expressing tasiR-ARFs-insensitive *ARF3,* driven by the 35S promoter display a similar phenotype to that of *as2* mutants, indicating that *ARF3* may negatively regulate *AS2* (Hunter et al., 2006). However, whether the expression of *AS2* is ectopic in the *arf3* or *arf3arf4* double mutants is still unknown. More recent studies reveal the existence of dual regulation of *ARF3* expression by the AS1-AS2 pathway. Specifically, AS1 represses *ARF3* expression by directly binding to the promoter of *ARF3*, whereas the binding of AS2 to the *ARF3* promoter is much weaker (Iwasaki et al., 2013). AS1-AS2 also acts indirectly to repress *ARF3* and *ARF4* via

activation of miR390 and RDR6-depedent tasiR-ARF production, which negatively regulates the activities of both *ETT/ARF3* and *ARF4* (Iwasaki et al., 2013).

Taken together, these antagonistic interactions between dorsal and ventral determinants are expected to create mutually exclusive and opposing cell identities.

1.3.3.3 Leaf boundary specific genes: WUSCHEL-RELATED HOMEOBOX1 (WOX1) and PRESSED FLOWER (PRS)/WOX3

In *Arabidopsis*, two members of the WUSCHEL-RELATED HOMEOBOX (WOX) gene family, *WOX1* and *PRESSED FLOWER (PRS)/WOX3* are expressed at the leaf dorsal-ventral boundary where they function redundantly to promote leaf blade outgrowth and margin-specific cell identity (Haecker et al., 2004; Matsumoto and Okada, 2001; Nakata et al., 2012). In the *prs wox1* double mutant, dorsal and ventral-genes are co-expressed in the vicinity of the leaf margin and this is associated with a loss of margin-specific cell types. Specifically genes such as *AS2* and *FIL* are miss-expressed and partially overlap at the leaf margin (Nakata et al., 2012), revealing that *PRS* and *WOX1* act to maintain the separation of these two distinct domains. In addition, the expression of *WOX1* but not *PRS* is positively regulated by *FIL*, while KAN represses the expression of both *WOX1* and *PRS* (Nakata et al., 2012). These findings suggest that the *WOX* genes possibly act downstream of dorsal-ventral polarity to promote lamina growth by maintaining the restricted expression domains of dorsal and ventral factors. (Nakata and Okada, 2012; Nakata et al., 2012).

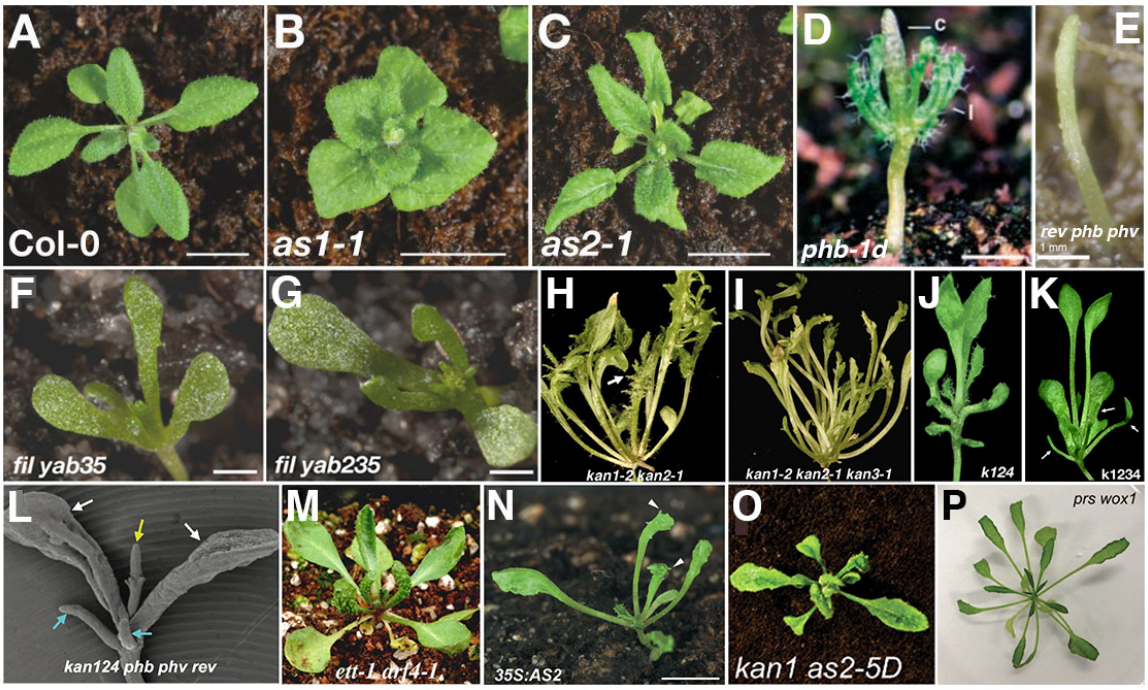

Figure 1.4 Arabidopsis mutants with leaf polarity defects.

(A) Wild-type plant. **(B and C)** *as2-1* mutant (C) shows very similar phenotype as *as1-1* mutant (B) but with longer petioles, bars =10mm in A to C, adapted from (Ishibashi et al., 2012). **(D)** Gain-of-function *phb1-d* mutant. "c" represents cotyledons and "l" represents leaves, bar = 1.25mm (McConnell and Barton, 1998). **(E)** *rev-9 phb-6 phv-5* triple mutant displays a single radial and ventralized cotyledon distal to the hypocotyl (Emery et al., 2003). **(F and G)** *fil yab35* triple mutants (F) and *fil yab235* quadruple mutants (G) bar =1mm (Sarojam et al., 2010). **(H and K)** Mutant phenotype of *kan12*, *kan123* (Eshed et al., 2004), *kan124* and *kan1234* (Izhaki and Bowman, 2007), respectively. **(L)** Seedling phenotype of *kan124 phv phb rev* hextuple mutants (Bowman and Floyd, 2008). **(M)** *ett arf4* double mutants show similar phenotype as that of *kan12* with outgrowth on the ventral side of leaves (Pekker et al., 2005). **(N)** Plants transformed with *35::AS2* in col-0 background develop outgrowths similar to those of *kan12* double mutants (Lin et al., 2003). **(O)** *kan1 as2-5D* double mutants exhibit similar phenotype to the *kan12* double mutant (Wu et al., 2008). **(P)** The phenotype of *prs wox1* double mutant with reduced lamina growth (Nakata and Okada, 2012).

1.4 Aim of the project

So far, most of the data on dorsoventrality I've described for plants relates to the phenotypes of gain or loss of function mutants for various factors that either promote dorsal or ventral identity. In addition, much of the literature describes the function of these genes in terms of their regulation of other regulatory factors. Hence the

fundamental question of how these genes actually function to alter leaf development or morphogenesis has remained essentially un-addressed since the seminal paper by Waites and Hudson over twenty years ago. In particular, considering the startling phenotypes caused by juxtaposition of distinct cell types in animals, further investigation of this potential phenomenon in plants is sorely lacking. Do plant leaves actually utilize a similar logic to that of fly wings or vertebrate limbs to pattern their development? If so, this would be quite a significant finding considering that plants evolved multicellularity quite independently of animals. Furthermore, detailed analysis of what happens when distinct dorsal and ventral cell types are juxtaposed could provide critical insight into how these boundaries actually control plant tissue growth.

In this thesis, I would like to address these issues by:

1. Determining how D-V patterning in lateral organs is initially established

2. Determining what actually happens when dorsal and ventral cell types are juxtaposed – in detail.

Chapter 2 Materials and Methods

2.1 Plant growth conditions

Arabidopsis plants were grown under constant light-conditions at 22 °C for all experiments. The seeds were surface sterilized using two different methods before sowing and the plants were cultivated either on plates for the experiments performed at a seedling stage or in soil for the reproductive stage.

2.1.1 Bleach vapor sterilization of seeds

Chlorine gas was utilized for sterilization of large amount of seeds (T1 generation) or lager numbers of lines (T2 or T3 generation). Open tubes of seeds were placed on a rack inside a sealable plastic container together with a glass container filled with 100 mL sodium hypochlorite solution (50 mL for T2 seeds). The plastic container was sealed immediately after adding 3mL concentrated HCL (1.5mL for T2 seeds) to the bleach solution. The sterilization process lasts for 4-6 hours for T1 seeds and 3hrs for T2 or T3 seeds in the fumehood.

2.1.2 Liquid sterilization of seeds

Liquid sterilization is a quick method to sterilize a few seed lines at a time. Briefly, seeds in 1.5mL Eppendorf tubes were soaked in 70% ethanol for 15mins, and subsequently, the seeds were sucked up and placed on the autoclaved filter papers to dry.

2.1.3 Growth medium preparation

After sterilization, the seeds were sowed on GM plus Vitamins (GM+Vit) medium which was composed of 1 % sucrose (Affymetrix), 1× Murashige and Skoog basal salt mixture (Sigma, M5524), 0.05% MES 2-(MN-morpholino)-ethane sulfonic acid (Sigma, M2933), 0.8 % Bacto Agar (BD), 1 % MS vitamins (Sigma, M3900) and pH 5.7 adjusted with 1 M KOH.

For selection of transgenic plants with different antibiotic resistances, antibiotics were added to the GM+Vit medium and the concentrations used were listed below.

Table1. Concentrations of the antibiotics used in growth media

Antibiotics/Herbicide	**Company**	**Concentration**
Kanamycin (Kan)	Sigma, K1377	50mg/L
Sulfadizine (Sulf)	Sigma, S8626	7.5mg/L
Hygromycin (Hyg)	Sigma, H0654	35mg/L
Basta	Molekula	15mg/L

2.1.4 Soil preparation

The "soil" used for growing the plants was a mixture of soil (Einheitserde Typ T), vermiculite (vermiculite 2-3 mm) and Perlite (Raiffeisen perlite 0-6 mm) in a ratio of 4:3:2. The mixture was placed loosely in rectangular pots (TEKU TK914 S pot 14.3 × 9.6 cm) with holes in the bottom and the pots were placed in a tray (50 × 32 × 6 cm) filled with 2 L water. After transplanting the seedlings grown on plates to soil, the tray was covered by a plastic dome with a similar size. The plastic dome was removed a couple of days later after transferring the tray in the growth room.

2.2 Plant transformation

Arabidopsis transgenic lines were generated by Agrobacterium-mediated ''floral dip'' method (Clough and Bent, 1998). Flowering plants were immersed in the solution of C58 strain of Agrobacterium tumefaciens containing the desired vector for 1 to 3 min. The dipped plants were then covered with a plastic wrap until the next day.

All the transgenic lines and mutants used in this thesis are list in Appendix 1.

2.3 Dexamethasone (DEX) treatment

Dexamethasone (Sigma, D4902) was dissolved in 100 % Ethanol to make up a 10 mM frozen stock solution. This stock was then diluted to a final concentration of 10 μM in GM+Vit growth medium or applied using droplets as described below.

2.3.1 Drops on inflorescences

For induction of gene expression during reproductive stage, 10 μM DEX solution (diluted in ddH_2O) containing 0.015% Silwet L-77 was applied onto the inflorescences every second day for three times before imaging. Each time, the DEX solution was freshly prepared and applied with 20 μl for each sample.

2.3.2 Induction at seedling stage

For inducible gene perturbations in the vegetative meristem (VM), seeds were germinated directly on GM+Vit medium containing 10 μM DEX. Seedlings were then dissected for imaging at 4, 5 or 7 days after stratification (DAS) depending on the experiment.

2.4 FM4-64 staining

For imaging of *kan1 kan2 kan4* multiple mutants at 6 DAS and 13 DAS, seedlings were stained with 10 μg/mL FM4-64 (Molecular Probes, T13320) in water for 10 min after removing of one cotyledon.

2.5 Whole-mount Immunolocalization of PIN1

Whole-mount immunolocalization of PIN1 on *kan1kan2kan4* multiple mutants was performed with a protocol from the lab of Teva Vernoux, which is a modified version as described (Besnard et al., 2014). And I greatly appreciate my colleague Neha Bhatia for teaching me this technique. Here the protocol is described briefly.

The pin-shaped apexes of *kan1kan2kan4* multiple mutants were chopped off leaving a length of 5 - 8 mm of stem under a Zeiss dissection microscope (Stemi 2000-C) and fixed immediately in FAA (4% formaldehyde, 5% acetic acid and 50% ethanol) for 1

h at room temperature. The samples were firstly dehydrated in a serial of 70%, 90% and 100% ethanol (twice) for 10min each and rehydrated through a serial of 75%, 50%, 25% and 0% ethanol in microtubule-stabilising buffer plus Triton (MTSB-T: 50 mM PIPES, 5 mM EGTA, 5 mM $MgSO_4$, pH 7.0 plus 0.1% Triton X-100) for 5 min each. A partial cell wall digestion was performed for 45 min using an enzymatic mixture (0.5% Macerozyme R10 (Duchefa, M8002.0005), 0.5% cellulase RS (Duchefa, C8003.0005), 0.25%, pectolyase Y23 (Duchefa, P8004.0001), 0.75% pectinase (Sigma, 17389) in water) diluted four times in MTSB. Then, the digested samples were washed with MTSB-T three times for 10 min each and subsequently treated with a mixture of 10% DMSO, 3% NP-40 in MTSB-T for 1h. The samples were then washed shortly for 2 min with MTSB-T and blocked with 3% BSA (Sigma, A8022) prepared in MTSB-T for 1h at room temperature. Samples were then incubated at 4°C overnight with Ap20 anti-PIN1 antibody (Santa Cruz), with a dilution of 1:100 in MTSB-T containing 3% BSA. Samples were washed 4 times for 15 min each in MTSB-T before being incubated for 4h at 37 °C with a secondary antibody (Alexa 488 antibody, Invitrogen) with a dilution of 1:500 in MTSB-T containing 3% BSA. After five washes of 15 min, samples were carefully mounted approximately upright with 1% low melt agarose (Starlab) and then imaged with confocal microscopy.

2.6 Sample preparation for live imaging

2.6.1 Seedling dissection

At the seedling stage, the vegetative meristem tissue is located centrally between the two cotyledons (the embryonic leaves) and covered by leaves later on. In order to observe the VM and the first pair of leaves, one of the cotyledons has to be removed carefully without damaging the seedling. The method for seedling dissection was established by Dr. Pia Sappl (a former postdoc in the lab) and Dr. Monica Pia Caggiano (a former PhD student). In Monica's thesis, the protocol was described in great detail and therefore only described here briefly with slight modifications.

Different staged seedlings grown on plates with GM+Vit or GM+Vit+DEX medium were first transferred to a new GM+Vit or GM+Vit+DEX plate. The root and part of the hypocotyl were embedded into the medium before sterile water was added to the

plate to immerse the seedlings completely. With two tweezers (No5.5 and No5, Dumont) grasping the cotyledons, a downward force is applied on one cotyledon only to carefully remove it without splitting the hypocotyl. The detached cotyledons are then removed by pouring the water away gently. The seedlings were then positioned upright with the remaining cotyledon bent backwards to obtain a clear view from above or bent vertically to get a side view of the leaves. Before imaging, fresh sterile water was added to the plate. To remove the grown out leaf primordia that covered the VM, such as the first pair of leaves at 4DAS or 5DAS, a needle (BD, 30G × 1/2) attached to a syringe (BD, 1 mL) was utilized to remove the leaves by pushing each leaf away from the meristem.

To image the ventral side of the leaves, water was removed completely after removing one of the cotyledons. A small hole was made by removing some media next to the seedling (Fig. 2.1 A, red dashed circle), providing space for the first pair of leaves after turning the seedling towards right (for imaging the leaf on the left side) or left (for imaging the other leaf). Then the remaining cotyledon, part of the hypocotyl and root (the parts outside the red dashed circle in Fig. 2.1 B) were embedded into the medium outside the hole, which makes the ventral side of the leaf face upright without any contact with the media. Fresh sterile water was added to the plate before imaging.

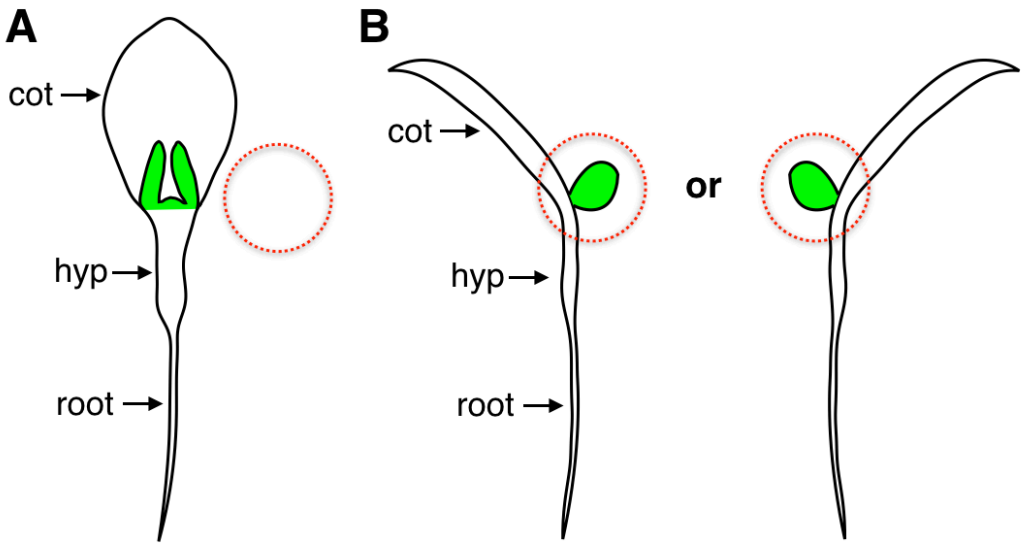

Figure 2.1 Schematic drawing illustrating sample preparation for imaging of leaf ventral side.

(A) Seedling with one of the cotyledons removed. **(B)** Position of the seedling towards right or left. Cot: cotyledon, hyp: hypocotyl, green: first pair of leaves and also meristem region in between in (A). red dashed circle: the hole for positioning the first pair of leaves.

2.6.2 Inflorescence meristem preparation

The apexes of flowering plants were chopped off with a length of 1cm and the big flowers and most of the flower buds were dissected away until the meristem region became visible for imaging. The dissection method was conducted as described (Heisler and Ohno, 2013).

2.7 Confocal Microscopy

Plants were imaged with a Leica SP5 Upright confocal microscope equipped with a water-immersion HCX IRAPO L25×/0.95 W (Leica) objective. Images were captured in 12-bit format in a sequential scan mode and pinhole maximum equivalent to 1.5× the Airy disk diameter, which was adjusted according to different experiment requirement. The argon laser was used to excite CFP, GFP and YPet/VENUS/YFP and the white laser was used to excite tdTomato. Their emissions were detected with Leica HyDs, which are more sensitive than the PMT detectors. Excitation wavelength for CFP is 458 nm, GFP is 488 nm, YFP (Ypet and VENUS) is 514 nm and tdTomato is 561 nm. Emission signal were collected at 460-480 nm for CFP, 490-512 nm for GFP, 516-550 nm for YFP (YPet and VENUS), and 570-620 nm for tdTomato. Excitation of FM4-64 was achieved by using 488 nm laser light and emission was collected at 640-670 nm.

In order to reduce the cross-talk between different fluorescent channels, sequential scanning was accomplished using “between frames” mode in combination with auto-selected notch filters. To obtain a further separation of different fluorescent signals, the resulting z-stacks were processed using the Dye Separation (Channel mode or automatic mode) tool from LAS AF software (Leica).

LAS AF software from Leica and Imaris 8.0.2 by Bitplane were utilized for data analysis. To reduce the background noise of the image, medium Noise Reduction (Median mode) function from the LAS AF program or the smoothing function

(medium filter) from Imaris 8.0.2 by Bitplane were used. “Oblique Slicer” or “Ortho Slicer” tools were used to create the sections of the images.

All the processed images were assembled into figures using Adobe Photoshop CS6.

2.8 Distance measurement of opposite organs

For distance measurements between the oppositely positioned leaves on transgenic plants for inducible KAN1 (*CLV3>>KAN1-2×GFP*) the measurement tool from Imaris 8.0.2 (Bitplane) was used. Untreated seedlings grown on GM+Vit medium (n=10) were compared to seedlings grown on GM+Vit+DEX medium (n=19) at 5 DAS. A t-Test, $p<0.05$ was performed using Excel.

2.9 Cre-lox based mosaic analysis

The T2 inducible transgenic lines were first screened for phenotypes and thirty independent insertion lines showed outgrowth formation in response to clone induction with different frequencies. A particular line that formed outgrowths at a frequency of approximately 53% was chosen for detailed investigation.

Seeds were germinated on GM +Vit medium plates containing 10 μM DEX. Three days after stratification, plates were placed at room temperature for 1h and then heatshocked for 1-2 hours in a 37°C incubator. The plates were then returned to the growth room after cooling to room temperature. Seedlings were dissected one day after heatshock. After removing one cotyledon, the ventral side of the first pair of leaves was imaged at 24h intervals. After each imaging session, seedlings were transferred to a new GM+Vit medium plate without DEX and returned to the growth room.

For analysis of REV sector variability, the ventral leaf surface was subdivided along proximo-distal and medio-lateral axis into six regions: top left, bottom left, top mid-vein, bottom mid-vein, top right and bottom right. The frequency of REV clones in each region was recorded. The outgrowth frequency refers to the percent of sectors that gave rise to localized growth in each domain and the blade outgrowth frequency refers to the frequency of blade shaped outgrowths. The total number of leaves analyzed was 48.

Chapter 3 Results

3.1 Lateral organs form at dorsoventral gene expression boundaries.

The lateral organs of most seed plants are dorsoventrally (top to bottom) flattened and form at the periphery of the shoot apical meristem (SAM). Organ initiation is promoted by high concentrations of the plant hormone auxin which accumulates due to specific patterns of polar auxin transport called convergence patterns (Heisler et al., 2005; Reinhardt et al., 2003). In the SAM, auxin transport is mediated by PIN-FORMED1 (PIN1) (Okada et al., 1991; Reinhardt et al., 2000), which is a membrane-bound auxin efflux carrier. PIN1 is typically localized at the plasma membrane asymmetrically, which in turn confers directionality to cellular auxin efflux.

In the model plant *Arabidopsis thaliana*, dorsoventrality of the leaf is determined by several transcription factors. In this work, I have focused on the dorsally expressed *REVOLUTA* (*REV*) gene, which is a member of class III HD-ZIP family of transcription factors (Emery et al., 2003; Otsuga et al., 2001) and the ventrally expressed *KANADI (KAN)* genes, which belong to the GARP family of transcription factors (Eshed et al., 2001; 2004; Kerstetter et al., 2001).

To understand how organ dorsoventrality is first established in initiating organs a previous PhD student in the Heisler lab, Monica Pia Caggiano, examined the expression patterns of REV and KANADI1 in relation to early patterns of PIN1 polarity and expression at organ initiation using functional fluorescent protein reporters. Monica found that while REV is expressed in the center of the meristem and KAN1 is expressed peripherally, PIN1-CFP expression, which marks positions of organ inception (Heisler et al., 2005; Reinhardt et al., 2003), is centered on the boundary between these domains, where the expression of both markers is weak or absent (Fig. 3.1 A to K). Furthermore, this spatial relationship is maintained during early organ development (Fig. 3.1 C arrowhead). In addition to KAN1, I determined that *KAN2* and *KAN4* are also expressed at the periphery of the meristem, as marked by the expression of *KAN2p::KAN2-2×GFP* (KAN2-2×GFP) and *KAN4p::KAN4-*

2×GFP (KAN4-2×GFP), respectively (Fig. 3.2 A and F and Fig.3.3 A and F). The expression of KAN2-2×GFP appeared to be patchy and present only at the proximal end of the leaf ventral side (Fig.3.2 A to E). KAN4-2×GFP expression was detected throughout the ventral side of the leaf (Fig. 3.3 A to E), similar to that of KAN1-2×GFP (Fig. 3.1 A to D).

All together these data indicate that dorsoventral (D-V) patterning of the leaf corresponds directly with central-peripheral patterning in the shoot, possibly reflecting a causal relationship between D-V patterning and organ positioning.

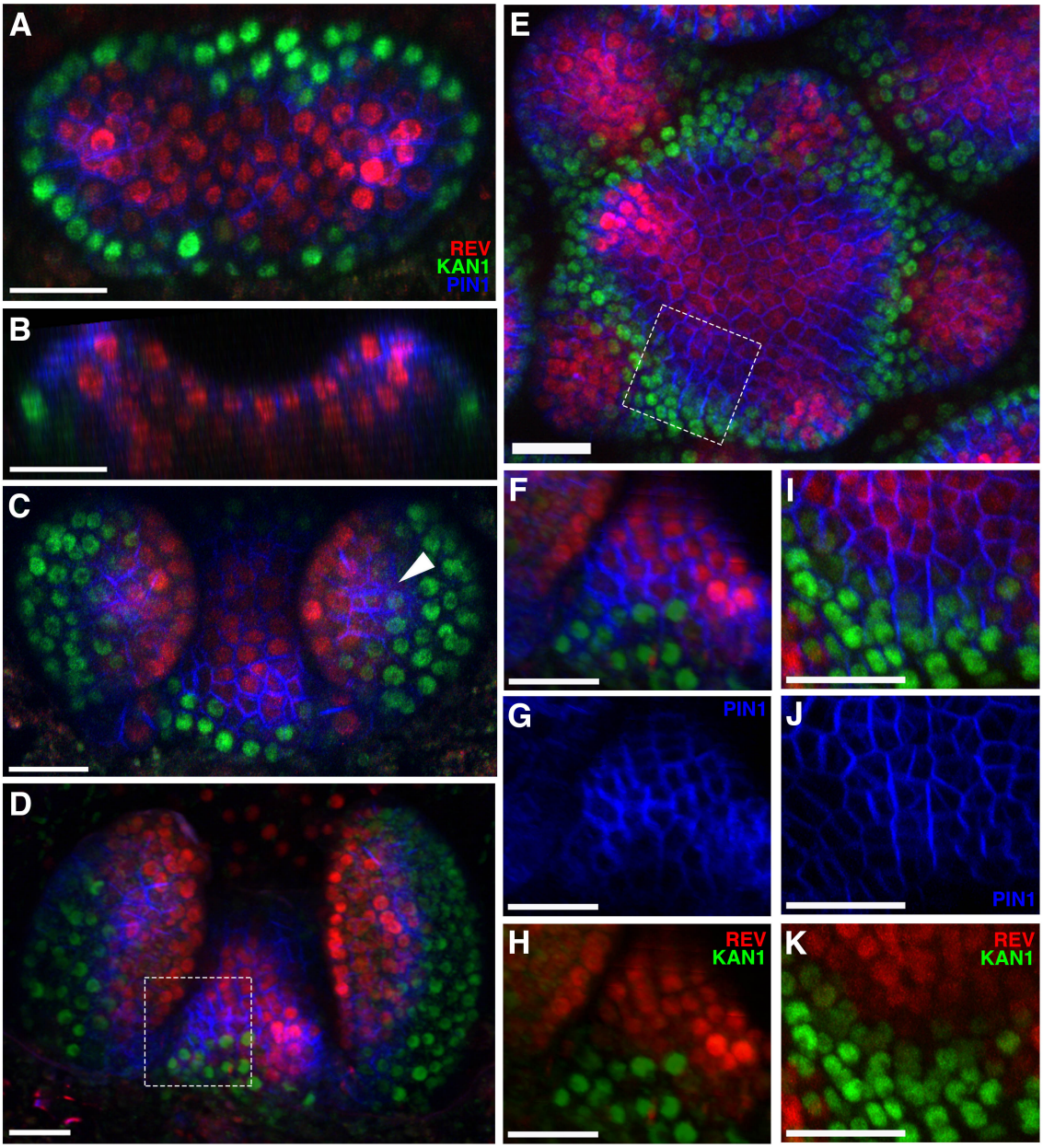

Figure 3.1 Organ initiation marked by PIN1 occurs on dorsal and ventral genes expression boundaries in the shoot meristem.

(A to D) Confocal projections showing REV-2×YPet (red), PIN1-CFP (blue) and KAN1-2×GFP (green) expression patterns in vegetative shoot apical meristem (VM) at 3 days (A), 4 days (C) and 5 days (D) after stratification, respectively. (B) Longitudinal reconstructed section of seedling shown in (A). Magnified views of the dashed box in (D) are shown in (F) to (H). **(E)** Expression pattern of REV-2×YPet, KAN1-2×GFP and PIN1-CFP in an inflorescence meristem (IM). Magnified views of the dashed box are shown in (I) to (K). **(F to K)** High PIN1-CFP expression localizes precisely at the REV-2×YPet /KAN1-2×GFP boundary in both the VM (F) to (H) and IM (I) to (K). Bars = 20 μm. **Note**: Images showed in Panel C and D of this

figure were captured by Monica and also used in her thesis (Fig. 8 A and C) and the original data was re-processed and assembled into this figure.

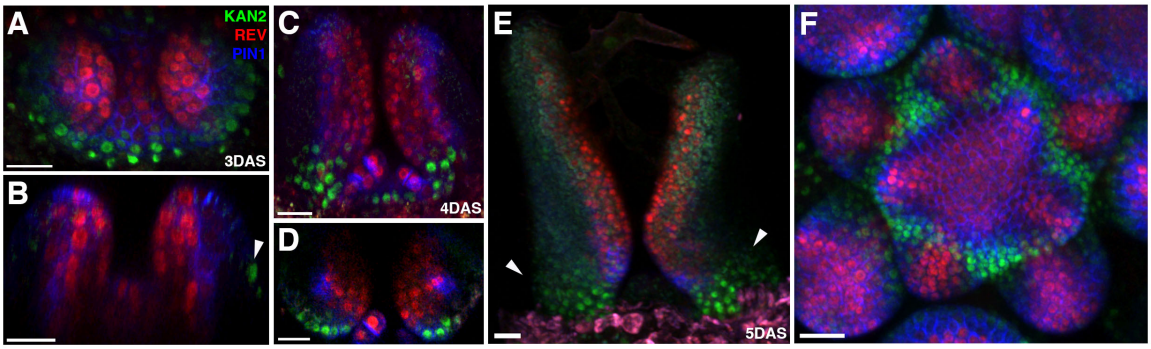

Figure 3.2 Expression pattern of KANADI2.

(A to E) Confocal projections showing REV-2×YPet (red), PIN1-CFP (blue) and KAN2-2×GFP (green) expression in vegetative meristems and leaves at 3 DAS (A), 4DAS (C) and 5DAS (E) respectively. (B) Longitudinal reconstructed section of seedling shown in (A); (D) Cross section of seedling shown in (C), arrowheads indicate KAN2-2GFP expression restricted to the proximal position of the leaves. **(F)** Expression pattern of REV-2×YPet, KAN2-2×GFP and PIN1-CFP in the inflorescence meristem. Scale bars represent 20 µm.

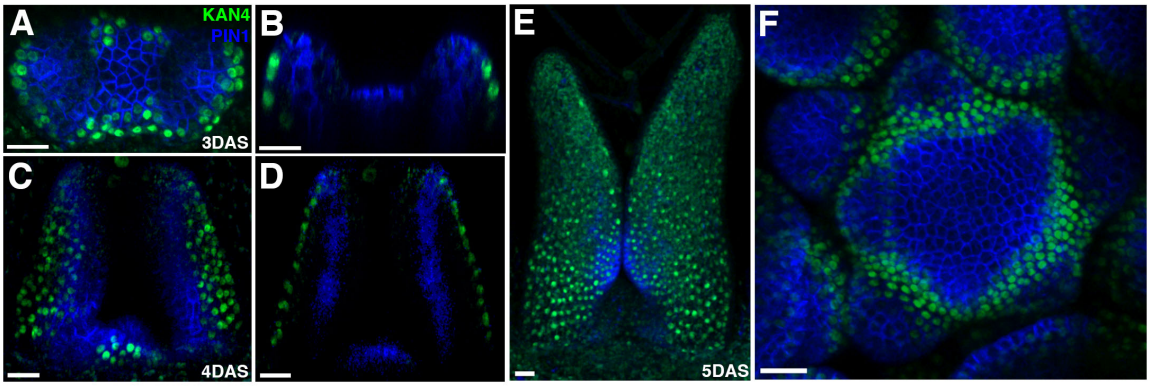

Figure 3.3 Expression pattern of KANADI4.

(A to E) Confocal projections showing PIN1-CFP (blue) and KAN4-2×GFP (green) expression in the vegetative meristem and leaves of 3 DAS (A), 4DAS (C) and 5DAS (E) seedlings respectively. (B and D) Longitudinal reconstructed sections of seedlings shown in (A) and (C). **(F)** Expression pattern of KAN4-2×GFP and PIN1-CFP in the inflorescence meristem. Bar = 20 µm.

3.2 Dorsoventral boundaries in the meristem are necessary for lateral organ formation

To test whether dorsoventral gene expression boundaries in the meristem are

necessary for lateral organ formation, Monica attempted to globally disrupt D-V boundaries by knocking-down or overexpressing D-V genes. She first examined the role of Class III HD-ZIPs post-embryonically by inducing MIR165 in the IM. She found that ectopic organogenesis marked by high expression of PIN1-CFP occurred in the center of the meristem and KAN1-2×GFP expression expanded centrally, which was consistent with previously reported Class III HD-ZIP mutant embryo phenotypes (Izhaki and Bowman, 2007). In contrast, ectopic expression of MIR165/166-resistant *REVr-2×VENUS* driven throughout the epidermis by the *Arabidopsis thaliana Meristem Layer 1* promoter (*AtML1p)* caused an arrest of organogenesis after induction as well as repression of KAN1-2×GFP. Furthermore, I also observed similar results in the vegetative meristem after induction of a short tandem target mimicry construct (*UBQ10>>STTM*) designed to repress MIR165/166 activity (Yan et al., 2012) (Fig. 3.4 A to D) or after epidermal induction of MIR165/166-resistant PHAVOLUTA (*AtML1p>>PHVr*) (Fig. 3.4 E to H).

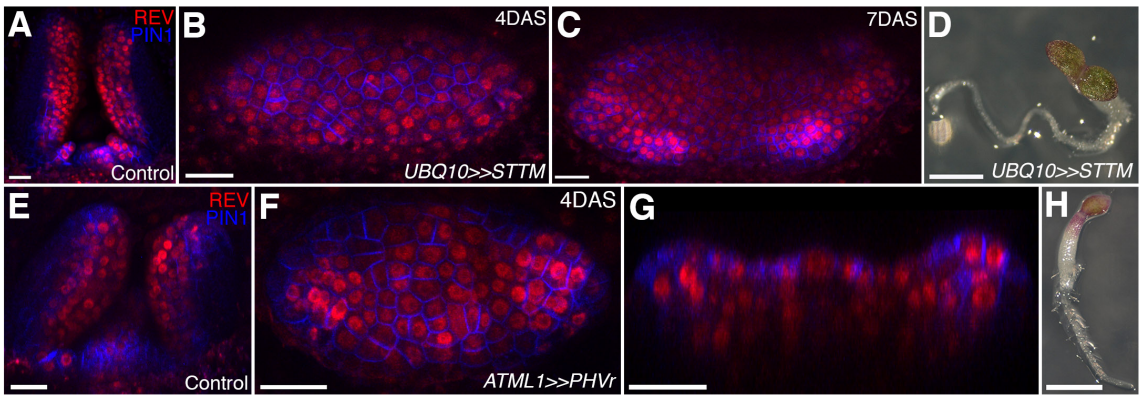

Figure 3.4 Organogenesis is disrupted when MIR165/166 activity is repressed or MIR165/166-resistant PHAVOLUTA is over-expressed in the epidermal layer of the vegetative meristem.

(A) Confocal projection showing PIN1-CFP (blue) and REV-2×YPet (red) expression patterns in wild type control seedling at 4DAS. **(B to C)** Arrest of organogenesis after induction of a short tandem target mimic (STTM) designed to down regulate MIR165/166 activity at 4DAS (B) and 7DAS (C), respectively. **(D)** Macroscopic view of plant in (C). **(E to H)** Ectopic expression of REV-2×YPet (red) and arrest of organogenesis (PIN1-CFP in blue) in 4DAS seedling after induction of MIR165/166 resistant PHAVOLUTA (*AtML1p>>PHVr*). (E) Side view of un-induced control. Top view (F), longitudinal section (G), and macroscopic view (H), of induced seedling showing arrest of organ development. Scale bars represent 20 µm in (A) to (C) and (E) to (G); 1mm in (D) and (H).

Monica also focused on the role of KAN genes. To ectopically express KAN1, she utilized a direct fusion of KAN1 to the glucocorticoid receptor (GR), driven by *AtML1* promoter (*AtML1p::KAN1-GR*) (kindly provided by Prof. John Bowman). Her results showed that although overexpression of KAN1 resulted in the ventralization of initiating leaves, new organs kept forming from the meristem. In contrast, it had been reported previously that over-expression of KAN1 resulted in meristem arrest (Emery et al., 2003; Kerstetter et al., 2001). To further clarify whether KAN1 influences meristem development and organogenesis, I used a pOp6/LhGR, two-component system (Samalova et al., 2005) to induce KAN1-GFP expression ectopically in the epidermal layer of the SAM using *AtML1* promoter driving LhGR (*AtML1p::LhGR_6Op:: KAN1-GFP*). In contrast to Monica's results but similar to the phenotype of ectopic REVr, plants expressing KAN1-GFP ectopically in the epidermis stopped forming organs (Fig. 3.5 A to G) and the inflorescence meristem took on a dome shape before eventually arresting (Fig. 3.5 H to J). I also noted that the expression of PIN1-GFP was repressed in both VM and IM after induction of ectopic KAN1-GFP expression. This observed difference in phenotype is possibly due to the absent expression of *AtML1p::KAN1GR* in the meristem or the level of KAN1 expression induced by directly fusion to GR being much lower than that of *AtML1p::LhGR_6Op:: KAN1-GFP*.

Taken together, our data indicate that restriction of both Class III HD-ZIPs and *KAN1* gene expression in the meristem is required for proper organ formation.

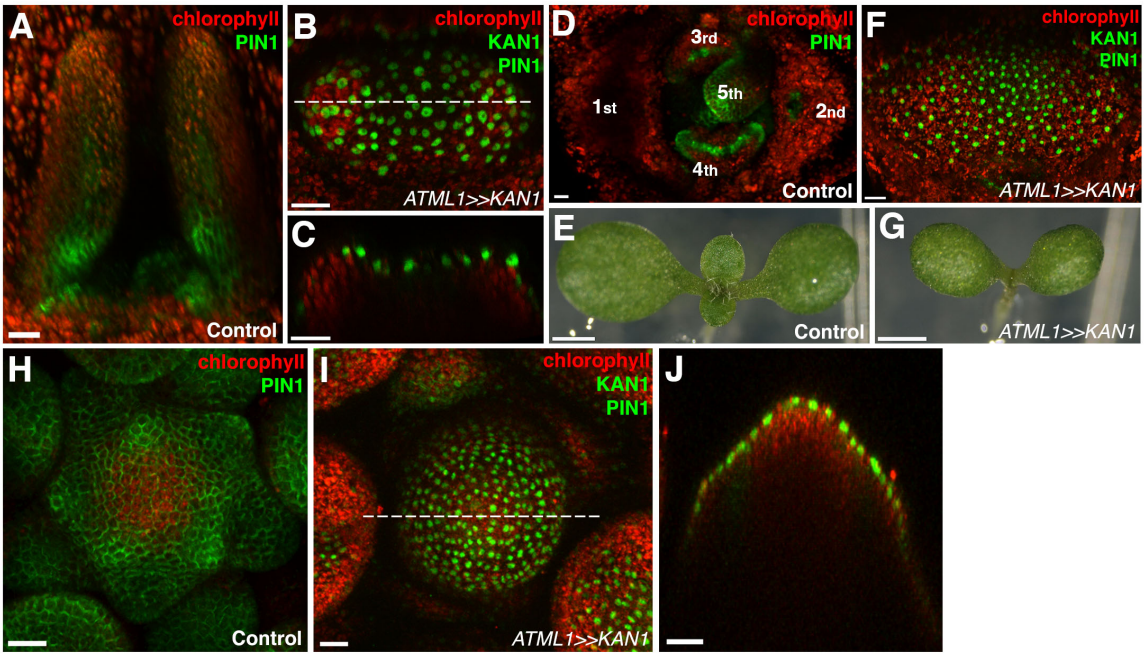

Figure 3.5 Ectopic overexpression of KAN1-GFP blocks organ formation.

(A to C) Arrest of organogenesis after induction of epidermal expression of KAN1-GFP (green nuclei signal) in a seedling at 4DAS germinated on DEX containing medium (B and C) compared to a non-induced control (A), PIN1-GFP (green membrane signal, autofluorescence in red) is down-regulated by overexpression of KAN1-GFP, (C) longitudinal section corresponding to the dashed line in (B). **(D to G)** No leaves have developed in seedlings at 7DAS after induction of KAN1-GFP in epidermis (F and G) compared to the control (D and E). **(H to J)** A dome-shaped IM after 3 DEX treatments over 6 days (I and J) compared to the IM of control (H), (J) longitudinal reconstruction along the dashed line in (I) shows a dome-shaped meristem. Scale bars represent 20 µm in (A) to (D), (F) and (H) to (J), 1mm in (E) and (G).

3.3 Dorsovenrtral patterning in the meristem regulates organ positioning and dorsoventrality.

To directly test whether boundaries between centrally expressed REV-2×YPet and peripherally expressed KAN1-2×GFP in the SAM are instructive in positioning and specifying the dorsoventrality of new organs, I attempted to create a new D-V boundary in the meristem of opposite polarity, with KAN1 expression in the center and REV expression outside. I again used the pOp6/LhGR, two-component system (Samalova et al., 2005) to induce KAN1-2×GFP expression ectopically at the center of the SAM by using the *CLV3* promoter to drive LhGR (*CLV3p::LhGR_6Op::KAN1-2×GFP*). Among 32 independent T2 transgenic plant lines, 10 of them showed

a very mild phenotype that was correlated with very low expression levels of ectopic KAN1-2×GFP. Another 10 lines exhibited complete meristem arrest after production of the first pair of leaves (which had already formed before DEX induction). Interestingly however, the other 12 lines produced several new leaves before the meristem arrested and one line in particular that produced more than two leaves at a frequency of 96.8 % (n=65) was used for further analysis.

Confocal imaging of seedlings 5 days after stratification (DAS) on dexamethasone (DEX) induction medium revealed that new organs, marked by high levels of PIN1-CFP expression, formed ectopically next to an enlarged and irregular central domain of induced KAN1-2×GFP expression (Fig. 3.6 A and B). The positioning of these organs on the new edge of KAN-2xGFP indicates that the boundary of KAN1 expression regulates organ position. Furthermore, within the ectopic KAN1-2×GFP expression domain, REV-2×YPet expression was repressed (Fig. 3.6 B). Although ectopic KAN1-2×GFP was only detected within or bordering organs during their initiation, REV-2×YPet expression was often restricted during later developmental stages, possibly due to the presence of endogenous KAN1 which was not directly monitored (Fig. 3.6 C to H). In general, several classes of aberrant morphology were observed, each correlating with different patterns of REV-2×YPet expression (Fig. 3.6 C to H). In particular, I noted that the morphology of the leaves correlated with REV-2×YPet expression boundaries in the epidermis during early development (arrowheads in Fig. 3.6 D, F and H) and that corresponding morphologies could be observed at maturity (Fig. 3.6 I to M). According to the different expression patterns of REV-2×YPet, the final morphology of the leaves was categorized into four major classes: “class 1” corresponding to a WT leaf (59.7 % of the plants, n = 62) with REV-2×YPet expressing on the dorsal side (Fig. 3.6 A and I); “class 2” corresponding to a cup-shaped leaf (14.5 %) with centrally restricted REV-2×YPet expression (Fig. 3.6 C, D and J); “class 3” corresponding to an inverted leaf (3.2 %) with REV-2×YPet expression in a reversed orientation (Fig. 3.6 E to F and K to L); and “class 4” corresponding to a four-blade leaf (1.6 %) with centrally and laterally expression of REV-2×YPet (Fig. 3.6 G, H and M). The early D-V gene expression patterns corresponding to these four classes are shown in Fig. 3.7 A. Besides these four main classes, I also observed intermediate leaf phenotypes ranging from cup-shaped to a completely radialized morphology, which was associated with the decreasing amount

of dorsal tissue in the leaves (Fig.3.7 C to I). The frequencies of the plants exhibiting different phenotypes are reported in Fig. 3.7 B.

These data, taken together with previous results (Section 3.3 from (Caggiano, Monica Pia 2013), (Izhaki and Bowman, 2007)) suggest a simple model in which both the KAN and Class III HD-ZIP genes repress organogenesis cell autonomously and therefore that organogenesis occurs at DV boundaries because of the low levels of DV gene expression there. The data also imply that when an organ forms, the configuration of the boundary on which it forms dictates how DV gene expression patterns are incorporated into the developing organ, which in turn dictates later organ morphogenesis and cell type patterning.

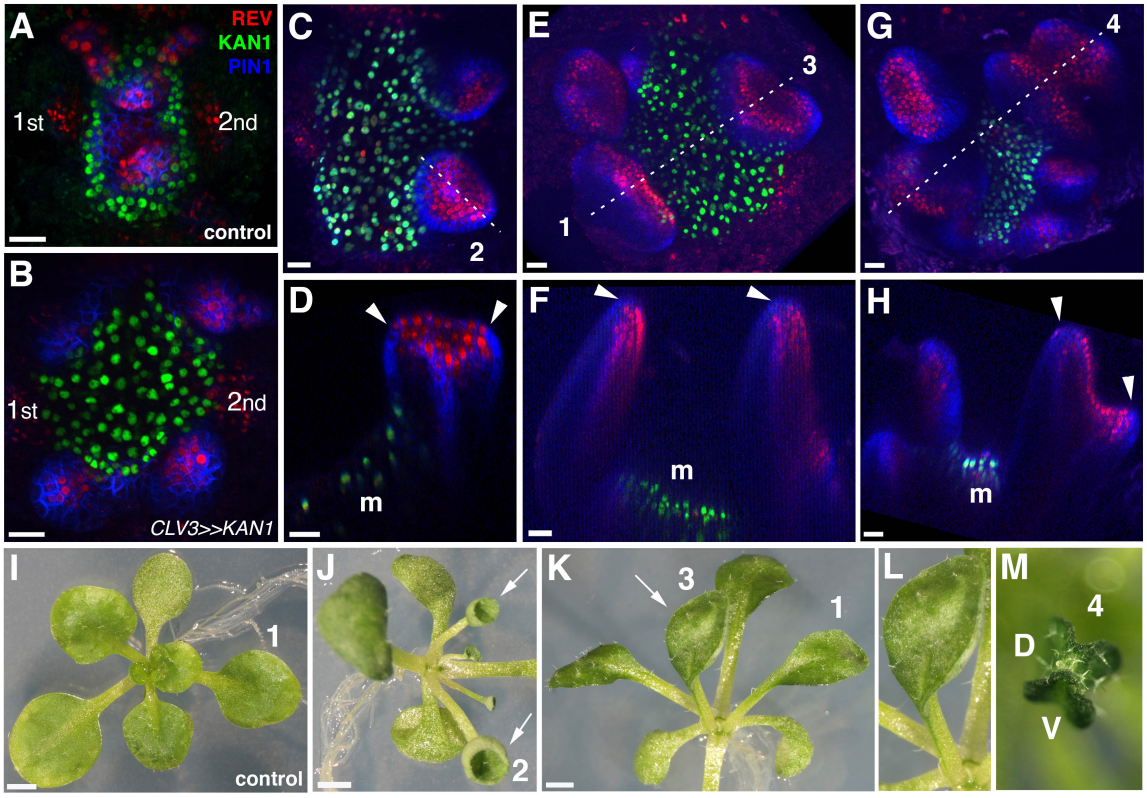

Figure 3.6 D-V boundaries in the shoot specify organ position and dorsoventrality.

(A and B) Confocal projections showing organ initiation marked by REV-2×YPet (red) and PIN1-CFP (blue) at border of *KANp:: KAN1-2×GFP* expression (green) in wild type (A) and after induction of ectopic KAN1-2×GFP (green) using the *CLV3* promoter (*CLV3p>>KAN1-2×GFP*) (B). Distance separating opposite organs was greater for induced (B) compared to control (A) (114.3 ± 3.3 µm, n = 19 vs 54.2 ± 1.0 µm n = 10 (mean±SE, $p < 0.05$, t-test)). **(C to H)** Confocal projections (C, E and G) and longitudinal reconstructions corresponding to dashed lines (D, F and H respectively) showing REV-2×YPet expression (red) after ectopic KAN1-2×GFP induction (green). Four main configurations of REV expression and morphology were observed (labelled 1 to 4). Class 1 organs (E and F) correspond to the wild type, class 2 (C and D) express REV-2×YPet centrally, class 3 (E and F) express REV-2×YPet in a reversed orientation and class 4 (G and H) express REV-2×YPet centrally and laterally only. Correspondence between REV-2×YPet expression boundaries and leaf margins indicated by arrowheads; "m" indicates meristem. Gamma value changed to highlight PIN1-CFP expression (blue). **(I to M)** Mature leaves corresponding to classes 1 to 4. "D" and "V" represent "dorsal" and "ventral" respectively in (M). Scale bar = 20µm in (A) to (H); 1 mm in (I) to (K).

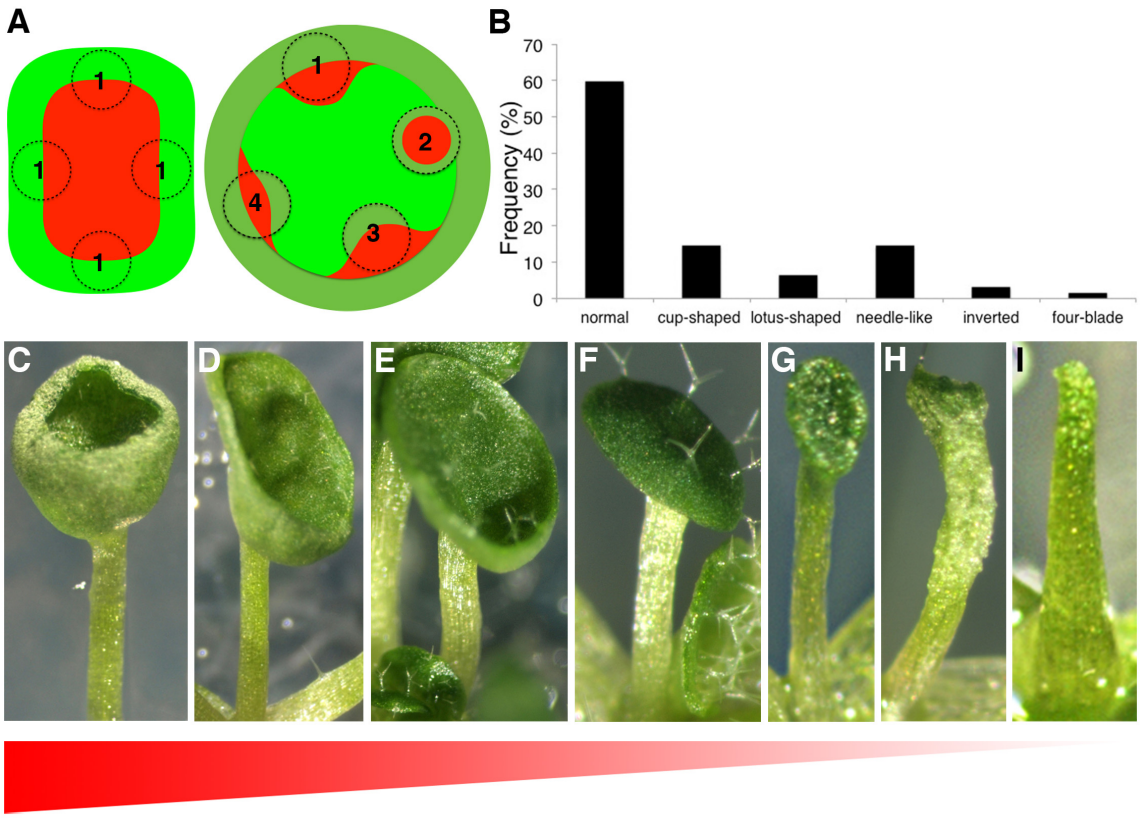

Figure 3.7 Leaves exhibit various degrees of ventralization caused by the ectopic expression of KAN1 in the shoot meristem.

(A) Diagram summarizing the four main configurations of REV-2×YPet (red) and KAN1-2×GFP (light green) expression in leaf primordia (dashed circles labeled 1 to 4) in wild type (left) and after induction of KAN1-2×GFP using the *CLV3* promoter (right). Regions in which neither REV-2×YPet nor KAN1-2×GFP signal was detected (dark green) may potentially express endogenous KAN1, which was not directly monitored. **(B)** Frequency of seedlings exhibiting different leaf morphologies. **(C-D)** Cup-shaped. **(E-G)** Lotus shaped. **(H-I)** Needle-like. Underlying graded red coloring indicates decreasing amount of dorsal tissue remaining.

3.4 Clones expression REV within ventral leaf tissues provoke ectopic laminar outgrowth and pattern tissues non-cell autonomously.

Since the data so far suggest that low levels of both KAN and Class III HD-ZIP expression at D-V boundaries are critical to their function I sought to test this hypothesis and investigate juxtaposition dependent lamina development in general by creating D-V boundaries in which moderate to high levels of REV and KAN expression are immediately juxtaposed without any gap between them. For this purpose I used a CRE- Lox recombination system (Albert et al., 1995; Ow, 1996; Sieburth et al., 1998) to generate DV boundaries *de novo* by inducing clonal sectors of cells expressing miR165/166 resistant REV fused to YPet (REVr-YPet*) within the plant. I reasoned that if REV is unable to downregulate the KAN genes at a distance, there would be no cells separating their expression domains. In order to induce the sectors in different parts of the plant on demand, several promoters were utilized to drive Cre recombinase fused to the glucocorticoid receptor (CRE-GR) for temporal control of localization(Brocard et al., 1998). After an extended period of trouble shooting by the Heisler lab it was found that using the Heatshock promoter(Matsuhara et al., 2000; Takahashi et al., 1992; Yoshida et al., 1995) driving the CRE-GR worked well for tight control of clone induction within leaf tissues. Using the heatshock method (see details in the method section), clones were induced randomly in different parts of the leaf, with variable sizes. I observed that on the ventral sides of leaves outgrowths often appeared with some of outgrowths appearing lamina-like. No changes were observed on the dorsal side. These outgrowths were found to correlate with the induced REV clones, however, the response to clones in terms of growth was very variable. Clones located in proximal positions induced growth and lamina development at higher frequencies compared to clones located distally (Fig. 3.13 I), possibly reflecting the earlier maturation of distal leaf tissues (Nath et al., 2003). I describe these results in detail below.

3.4.1 PIN1 expression and growth is correlated with ectopic REV clones in leaves.

As described in section 3.1, high levels of PIN1 expression occur at D-V gene expression boundaries normally during leaf and meristem development. Therefore, we

first examined whether the expression of PIN1 was also up-regulated along D-V boundaries created *de novo*.

In control seedlings, 4 days after stratification, PIN1-GFP expression was only detected at the tip and in the vasculature tissue of the leaf but not on the ventral side (Fig. 3.8 A to D). In induced leaves however, PIN1-GFP was up-regulated both within and outside the clones of REVr-YPet* expression at 45 hrs after induction (corresponding to 5 DAS) (Fig. 3.8 E to H), indicating both cell and non-cell autonomous up-regulation by REV. Later at 4DAH, PIN1-GFP expression decreased within REVr-YPet* expressing clones, but was maintained in the cells adjacent to the clone (sectors on the left side in Fig. 3.8 I to L). Furthermore, when REVr-YPet* clone was induced in sub-epidermal layers, PIN1-GFP expression was up-regulated in the adjacent cells of the epidermis (clone on the right in Fig. 3.8 G to L), indicating that REV can up-regulate PIN1 non-cell autonomously across cell layers. By visualizing various REVr-YPet* clones induced in different cell layers, I also found that expression of REVr-YPet* only in the epidermis was sufficient to up-regulate PIN1 non-cell autonomously within the same cell layer (Fig. 3.9 A and insertion). Furthermore, the growth occurred within the clone at 3DAH when PIN1-GFP expression was both within and outside the clone (Fig. 3.9 A to C) and later at 4DAH the growth became restricted more towards the edge of the clone, accompanying with the restriction of PIN1-GFP expression partially overlapping with REVr-YPet* expressing cells along the clonal edge (Fig. 3.9 D to F). This close correlation between PIN1-GFP expression and growth patterns was also observed in another example (Fig. 3.9 G to J) and I also observed that the outgrowth formation was associated with the formation of the vasculature (Fig. 3.9 K). Interestingly, when two epidermal REVr-YPet* clones were induced close to each other (Fig. 3.10 A), at 4DAH, PIN1 expression became restricted to the domain between the two clones. Accompanying this, growth occurred in the region between the two clones to form a ridge (Fig. 3.10 B to E). Development of such ridges did not seem to specifically require sub-epidermal clones as I observed the same growth patterns in both cases (Fig. 3.10 F to H, compare H to D). Interestingly, when I examined PIN1-GFP expression closely in the cells adjacent to the clones, I found that PIN1 was localized predominantly on the cell membranes located farthest away from the cells expressing REVr-YPet* suggesting auxin efflux away from the clone and a non-cell autonomous

influence of the clone on PIN1 polarity (Fig. 3.10 I and J). When REVr-YPet* expressing clones were induced throughout the ventral side of the leaf with occasionally small regions without REVr-YPet* expression, PIN1-GFP expression became up-regulated in all cells within the clones initially (Fig. 3.11 A), but later became restricted and highly expressed in the region without REVr-YPet* expression at 4 days after induction (Fig. 3.11 B to D). However, when the distance between the clones was larger at 3DAH (Fig. 3.11 E), PIN1-GFP expression between the clones was not maintained. Instead, PIN1-GFP expression decreased but was maintained at the boundary of each single clone with growth also maximal at the border of the clones rather than in between (Fig. 3.11 F and insertions in E and F).

Overall these results indicate that REV acts non-cell autonomously to influence both PIN1-GFP expression and growth. In both cases there seems to be an early phase of PIN1 expression and anticlinal growth localized to or under the clone respectively. This is then followed by a later phase in which both anticlinal growth and PIN1 are localized adjacent to the clone. When two clones are close to each other their influence on both PIN1 and growth appear to combine in an additive manner that depends on the distance they are apart. The associated polarities of PIN1 towards regions in between clones also suggest the possible accumulation of auxin locally.

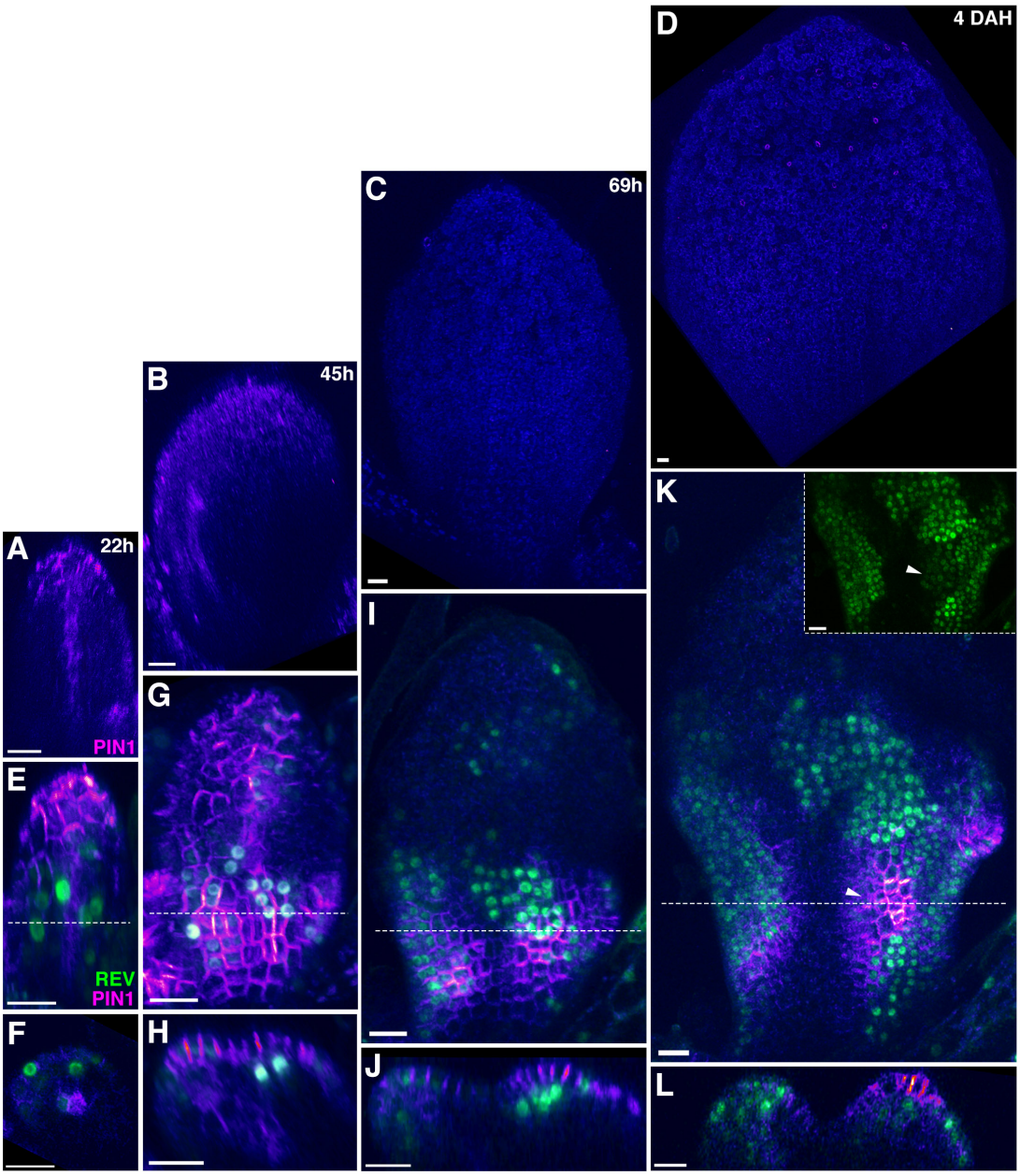

Figure 3.8 Up-regulation of PIN1-GFP by REVr-Ypet* clones on the ventral side of the leaf.

(A to D) Confocal projections showing control images of PIN1-GFP (magenta) expression on the ventral side of a wild type leaf from 1 day after heatshock (DAH) (A) to 4 DAH (D). **(E to L)** Time-lapse projections (E, G, I and K) and cross sections (F, H, J and L) of a developing leaf primordium showing PIN1-GFP expression together with clonally induced REVr-YPet* (green) from 1 day (E and F) until 4 days (K and L) after heat shock. Insert in (K) shows REVr-YPet* expression only. Arrowheads indicate the region in which REVr-YPet* expression in the sub-epidermis while PIN1-GFP expression is induced in the epidermis. Bar = 20 µm.

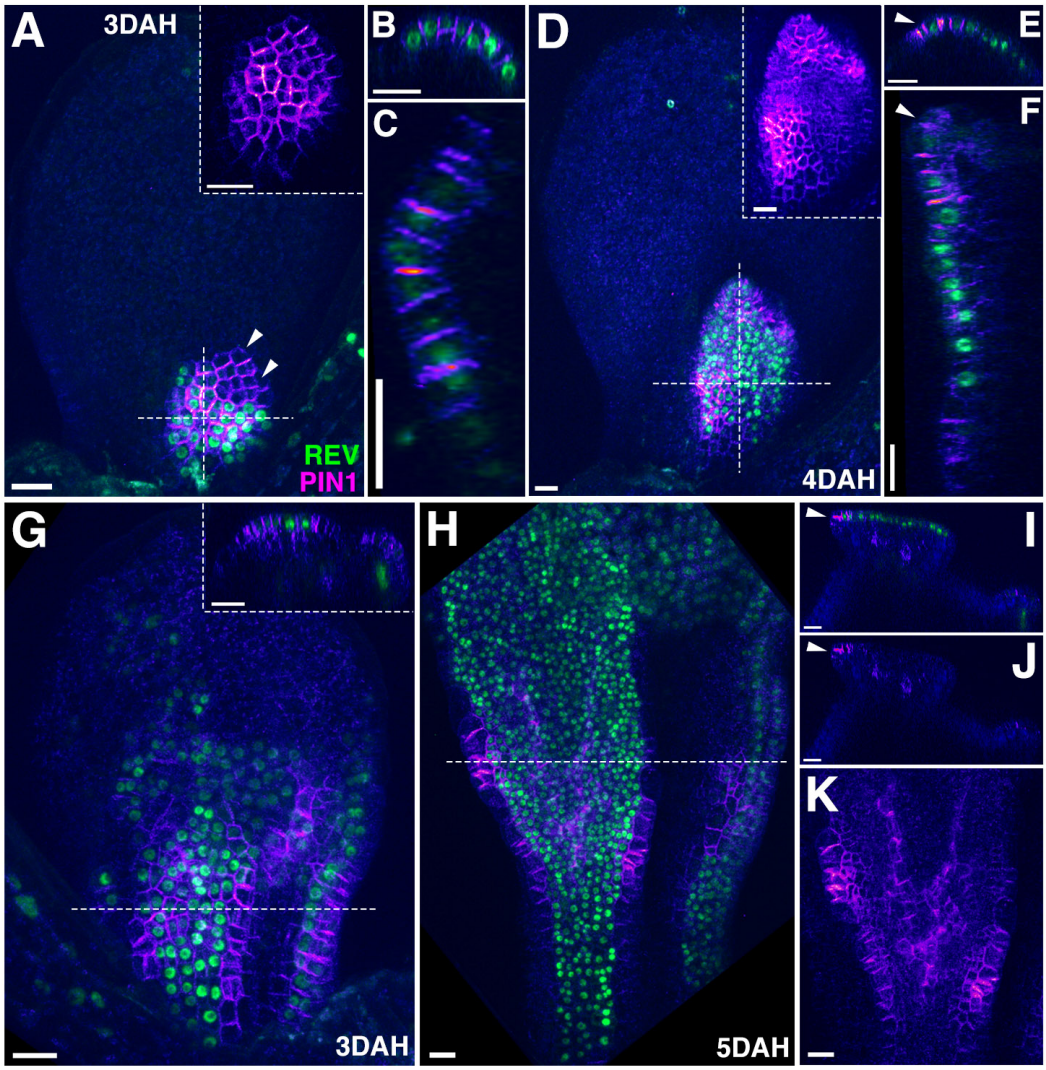

Figure 3.9 Epidermal expression of REVr-YPet* is sufficient to trigger growth within and outside REV clones.

(A to C) An example showing a REVr-YPet* (green) clone in the epidermis is sufficient to up-regulate PIN1-GFP (magenta) within and outside (arrowheads in A) the clone at 3DAH. Growth occurs mainly within the clone initially. Insertion in (A) shows PIN1-GFP expression only. Longitudinal sections correspond to the horizontal and vertical dashed lines in (A) are shown in (B) and (C) respectively. **(D to F)** At 4DAH, PIN1-GFP expression starts to decrease within the REVr-YPet* clone but remains overlapping at the edge of the clone. Growth becomes progressively restricted towards the edge of the clone. (E to F) Sections corresponding to the dashed lines in (D), arrowheads indicate the edge of the clone. **(G to K)** Another example showing growth occurring within the clone at 3DAH (G) but becoming more restricted to the edge of the clone at 5DAH, which correlates with the restriction of PIN1-GFP expression to the clone boundary. (K) Vasculature as marked by PIN1-GFP expression was associated with the formation of the outgrowths triggered by REVr-YPet* expressing clones. Bar = 20 µm.

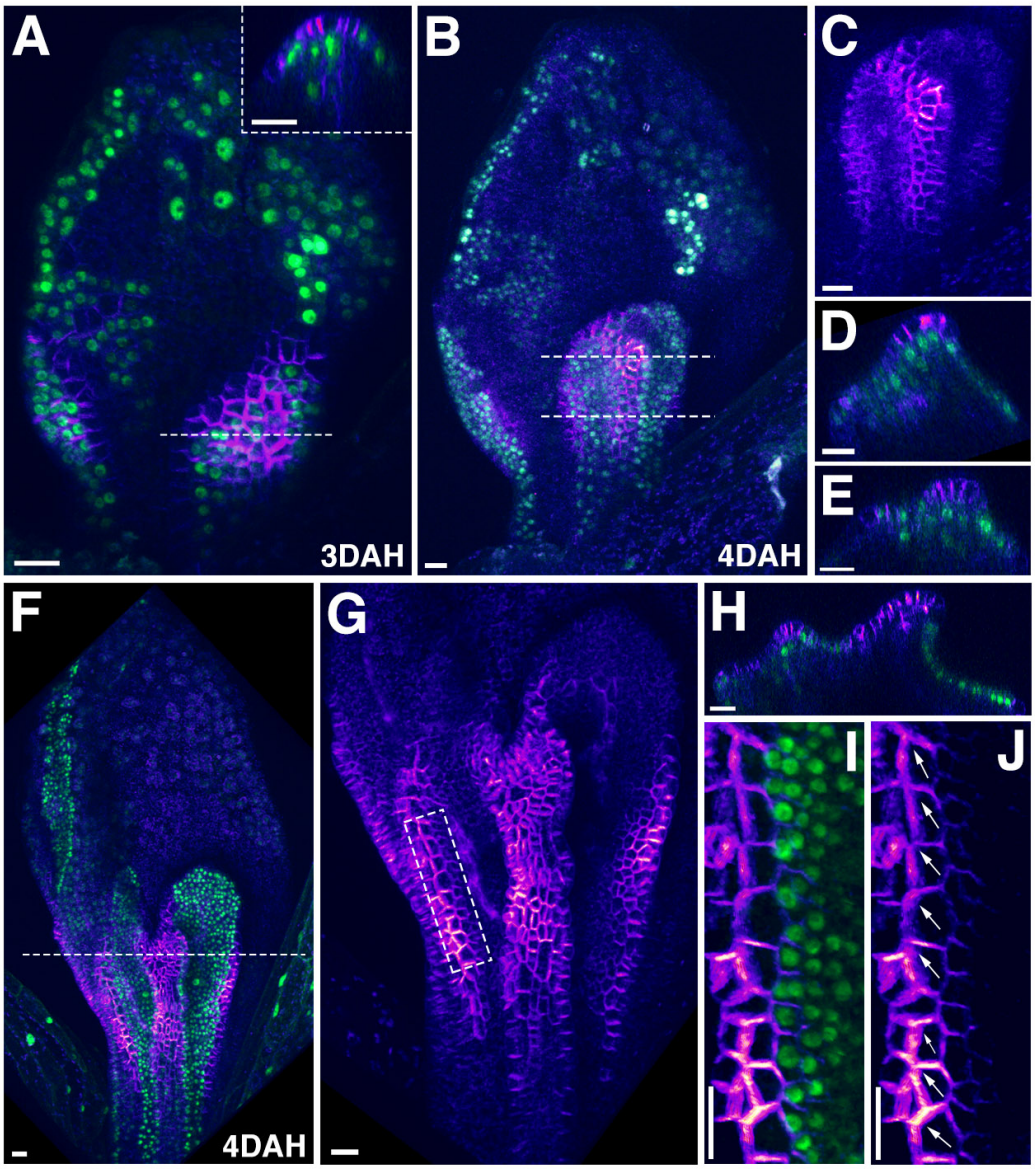

Figure 3.10 The formation of ridges in response to two closely adjacent epidermal REVr-YPet* clones.

(A to E) An example showing PIN1-GFP (magenta) expression throughout the two closely adjacent REVr-YPet* (green) expressing clones and the cells in between at 3DAH (A), while later at 4DAH, PIN1-GFP becomes restricted to the cells between these two clones (B). Note the sub-epidermal REVr-YPet* expression between the two epidermal REVr-YPet* clones. (C) shows PIN1-GFP expression only, (D and E) Longitudinal reconstructions corresponding to the upper and lower dashed lines in (B). **(F to H)** An example showing two adjacent REVr-YPet* (green) clones in the epidermis promote PIN1-GFP expression and growth in between them to form a ridge. A magnified confocal projection with PIN1-GFP expression alone is shown in (G). (H) Longitudinal section corresponding to the dashed line in (F). **(I and J)** Magnified views corresponding to the dashed box in (G) showing PIN1-GFP polarized away from REVr-YPet* expressing cells, indicated by arrows. Bar = 20 µm.

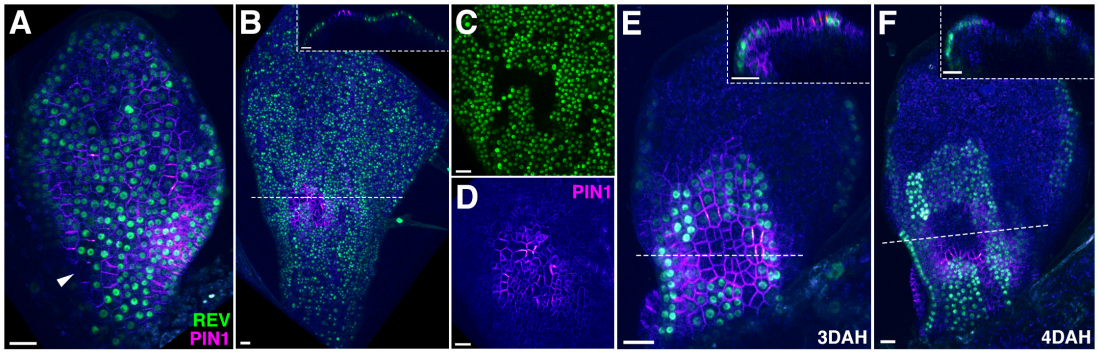

Figure 3.11 PIN1-GFP expression is restricted and highly expressed in the region surrounded by REVr-YPet* expressing cells.

(A to D) An example showing PIN1-GFP (magenta) expression was up-regulated within the induced REVr-YPet* (green) expressing clones almost throughout the ventral side of the leaf at 2 days after induction (A) and later at 4 days after induction, PIN1-GFP became restricted and highly expressed in the region (like a "n" shape) without REVr-YPet* expression (B to D). **(E and F)** Example showing PIN1-GFP expressing was decreased in the region surrounded by REVr-YPet* expression clones at 4 days after induction (F and insert) compared to that at 3 days after induction (E and insert), which might due to the large distance between these clones. Insertions in (E) and (F) showed the longitudinal sections corresponding to the dashed lines. Bar = 20μm.

3.4.2 KAN1 expression and function during *de novo* boundary formation triggered by REV clones.

3.4.2.1 Down-regulation of KAN1 by REV in WT leaves

To address the question of whether a gap between REV and KAN expression accompanies the formation of outgrowths induced by the REV clones I monitored the expression of KAN1-2×GFP together with PIN1-CFP after the induction of REVr-YPet* expression clones by heatshock on the ventral side of the leaves.

In control leaves, KAN1-2×GFP expression was found to decrease from the distal part of the leaf towards the proximal part from 3 days after heathshock (corresponding to 6-day-old seedlings). This turning off of KAN1-2GFP in the cells located in the proximal part of the leaves appeared to occur in a stochastic manner (Fig. 3.12 A to F). However, after induction of REVr-YPet* clones, KAN1-2×GFP was down-regulated within the clones by 24 hrs after heatshock (Fig. 3.12 G and M). Nevertheless, KAN1-2×GFP was still detected in many cells bordering the clones

indicating that REV cannot down regulate KAN1 non-cell autonomously (Fig. 3.12 G to N). In general this meant that the number of cells expressing KAN1 in cells adjacent to REV clones varied amongst experiments. As described below, I noted a correlation in phenotype that correlated with this variation.

At 48 hrs after clone induction, PIN1-CFP was typically up-regulated in the cells within the clones (as describes in the above sections) and the tissue underlying the clones had also started to grow anticlinally causing a local bump to form (Fig. 3.12 H and N). At 3 days after induction, when PIN1-CFP expression was present not only within the REVr-YPEt* clones but also in some cells adjacent to the clones, most prominently where KAN1-2×GFP expression happened to be absent (although not exclusively so) (Fig. 3.12 I and O). As leaf development proceeded, PIN1-CFP expression was found to decrease within the REVr-YPet* clones but remained most strongly expressed in those cells adjacent to the clones where both REV and KAN were absent (Fig. 3.12 J to Q). Finally, lamina-like ridges formed along the boundaries of REVr-YPet* sectors (Fig. 3.12 J to L), indicating that the juxtaposition of DV gene expression is sufficient for triggering specific growth patterns.

Although the size of the induced sectors within the leaf tissues varied, in most cases, the final morphology of the outgrowths strongly correlated with the boundaries of REVr-YPet* sectors (Fig. 3.13 A to H). However, the response to clones in terms of growth was very variable and the frequencies of induced growth and lamina development in different parts of the leaf was reported in a schematic drawing (Fig. 3.13 I). Consistent with the finding that clones located in proximal positions induce growth and lamina development at higher frequencies compared to clones located distally, some examples showed that the up-regulation of PIN1 occurred only within sectors induced proximally rather than that induced distally (Fig.3.13 J). Furthermore, clones induced by heath shock earlier, at one day after stratification, were able to trigger outgrowth formation distally (Fig.3.13 P), indicating outgrowth formation depends on the developmental stage of the tissue. In addition to the position or age dependent up-regulation of PIN1 expression by REV, PIN1 expression also appeared to depend on REV expression levels. When two adjacent epidermal clones with different levels of REVr-YPet* expression were induced, PIN1 was often seen only up-regulated within the clone expressing REVr-YPet* at a lower level (Fig. 3.13 K and insertion), As shown previously, the expression of REVr-YPet* in sub-epidermal

tissues was sufficient to induce PIN1 expression in the epidermis and promote local growth. By monitoring KAN1-2×GFP expression at the same time, I found that PIN1 was co-expressed with KAN1 in the epidermis (Fig. 3.13 L to O), revealing further evidence that an absence of KAN1 expression is not absolutely necessary for the non-cell autonomous up-regulation of PIN1 by REV.

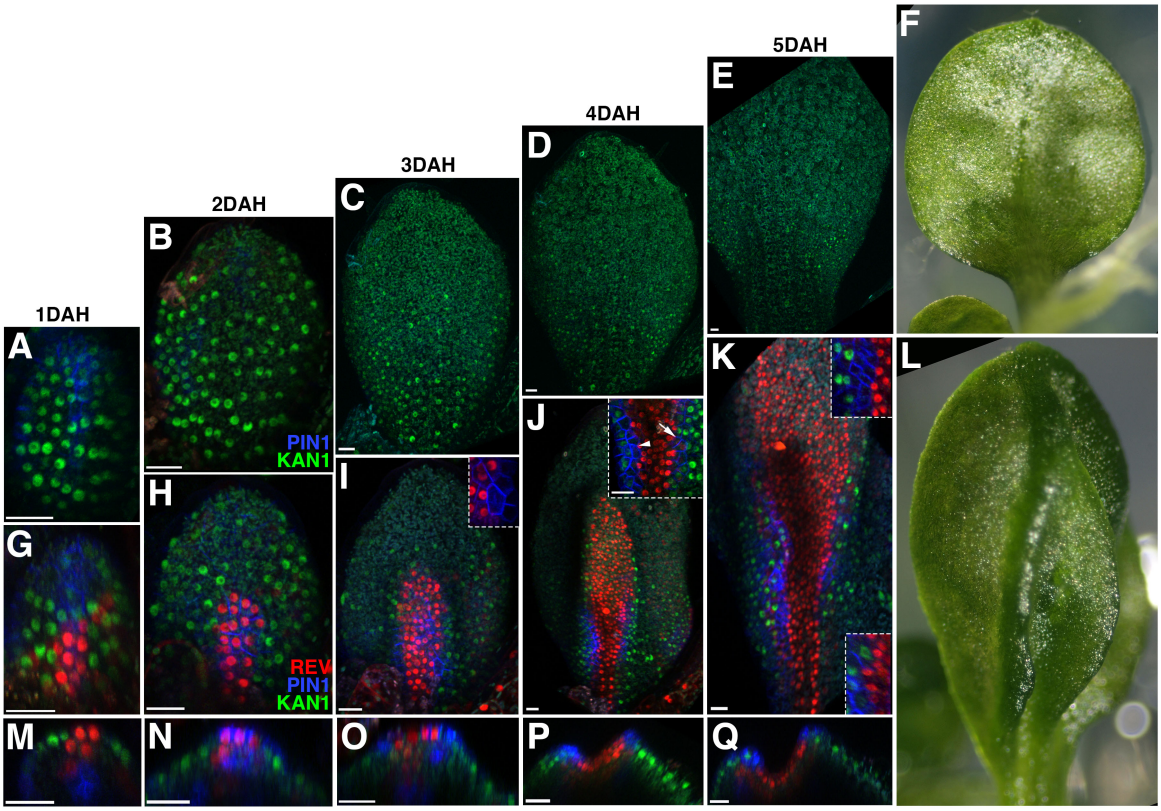

Figure 3.12 REV expression within ventral leaf tissues triggers lamina outgrowth along clonal boundaries.

(A to E) Confocal projections showing control images of KAN1-2×GFP (green) and PIN1-CFP (blue) expression on the ventral side of a wild type leaf from 1 day after heatshock (DAH) (A) to 5 DAH (E). **(F)** Mature leaf morphology. (**G** to **K**) Time-lapse projections of a developing leaf primordium showing the changes of PIN1-CFP and KAN1-2×GFP expression upon clonally induction of REVr-YPet* (red) from 1 DAH (G) to 5DAH (K). Insert in (I) shows non-cell autonomous up-regulation of PIN1-CFP; insert in (J) shows stronger PIN1-CFP expression in the region where there is a gap indicated by arrowhead compare to a much lower PIN1-CFP expression in the region without gap marked by arrow; insert in (K) shows PIN1-CFP expression external to clone in KAN1-2×GFP expression cells, a “gap” without KAN1-2GFP and REVr-YPet* or no “gap” were observed in different regions along the clonal boundaries. **(L)** Final leaf morphology illustrating two ectopic leaf blades. **(M to Q)**

Corresponding transverse views shown in (G to K). Scale bars represent 20 µm in (A) to (E), (G) to (K) and (M) to (Q).

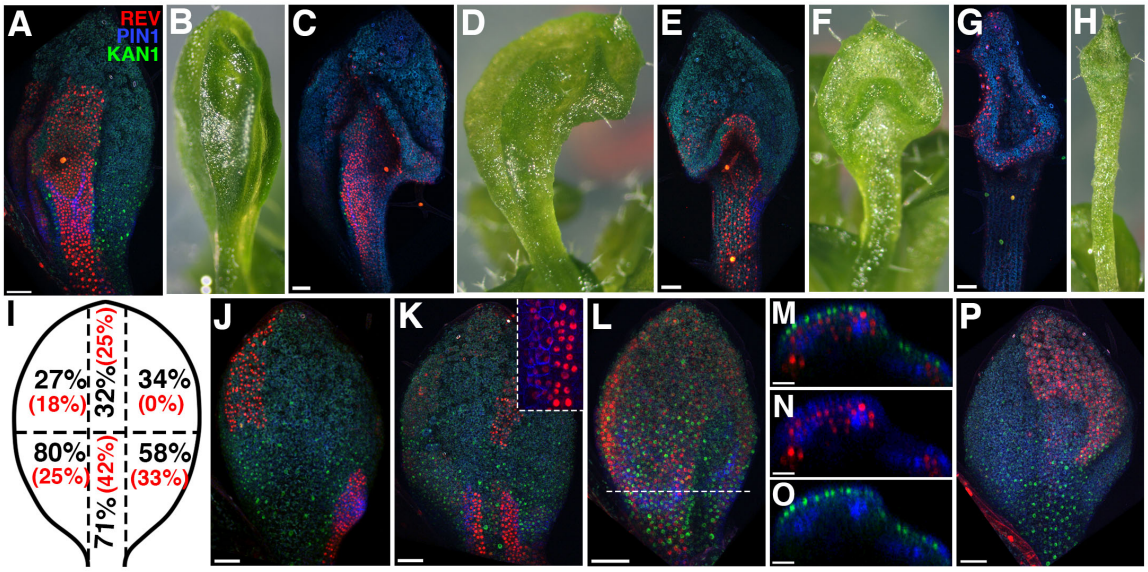

Figure 3.13 Variability of the induced REVr-YPet* clones.

(A to H) Confocal projections showing examples of outgrowth development correlating with the boundary of REVr-YPet* expressing clones during leaf development (A, C, E and G) and at maturity (B, D, F and H). **(I)** Diagram reporting the frequency of sectors that induced localized growth (black) vs ectopic lamina (red) in different regions of leaf primordia, N= 48. **(J)** Confocal projection showing an example of proximal vs distal location bias. PIN1-CFP expression (blue) is only up-regulated by the clone (red) located proximally. **(K)** Confocal projection showing two adjacent epidermal clones expressing REVr-YPet* at different levels. PIN1- CFP (blue) is only up-regulated within the clone expressing REVr-YPet* at a lower level. Close up shown in insert. **(L to O)** Expression of REVr-YPet* (red) in sub-epidermal tissues is sufficient to induce PIN1-CFP expression (blue) in the epidermis where KAN1-2×GFP (green) is co-expressed. Dashed line in (L) shows position of reconstructed sections in (M) to (O). **(P)** Sector induced earlier at 1 DAS triggered localized growth at distal position of the leaf. Bars represent 50 µm in (A), (C), (E), (G), (J) to (L) and (P); 20 µm in (M) to (O);

In addition to the various responses to the induced clones in terms of outgrowth, it was also found that the percentage of lamina development was less than 42% (the percentage varied in different part of the leaf) of the overall growth morphology (Fig. 3.13 I, numbers in red). To further understand the difference between lamina shaped outgrowth and other morphologies like bumps or protrusions. I compared the development of various outgrowth formations in detail. As reported above, KAN1-2×GFP expression was turned off stochastically from 6DAS (correspond to 3DAH) during normal leaf development (Fig. 3.12 C to E). At this stage, when the disappearance of KAN1-2×GFP expression occurred in cells adjacent to REVr-YPet* expression clones, "gap" cells without REV and KAN1 expression can be created. In those cells, growth was most pronounced and often resulted in the formation of a lamina. Interestingly I noted that if heatshock was applied earlier, at 2 days after stratification rather than 3DAS, KAN1-2xGFP expression appeared to be maintained for longer in the vicinity of the clones resulting in fewer or a complete absence of "gap" cells. In these cases confocal images revealed that outgrowth development in response to REV clones always failed to form a lamina shape but instead formed less defined bumps located centrally on REV expressing cells (Fig. 3.14). Based on this observation as well as my data overall, I conclude that the presence of a small "gap" region between the REV and KAN expression domains likely helps to localize PIN1 expression and the growth response to the boundary in order to promote lamina development.

Altogether these data demonstrate that REV does not repress KAN1 expression non-cell autonomously, lamina-like outgrowths can still form in response to REVr-YPet* clones. However whether outgrowths are lamina-like or not correlates with the absence or presence of KAN1-2×GFP expression respectively, which gradually turns off stochastically during early leaf development. Nevertheless, the non-cell autonomous up-regulation of PIN1 and growth response by REVr-YPet* does not absolutely require an absence of KAN1-2xGFP expression. Hence all together these data suggest that while the absence of KAN expression in cells bordering REVr-YPet* probably promotes local PIN1 expression and growth at these boundaries, REV expressing cells also generate a mobile signal that promotes PIN1 and growth non-cell autonomously that can overcome KAN1 to some degree.

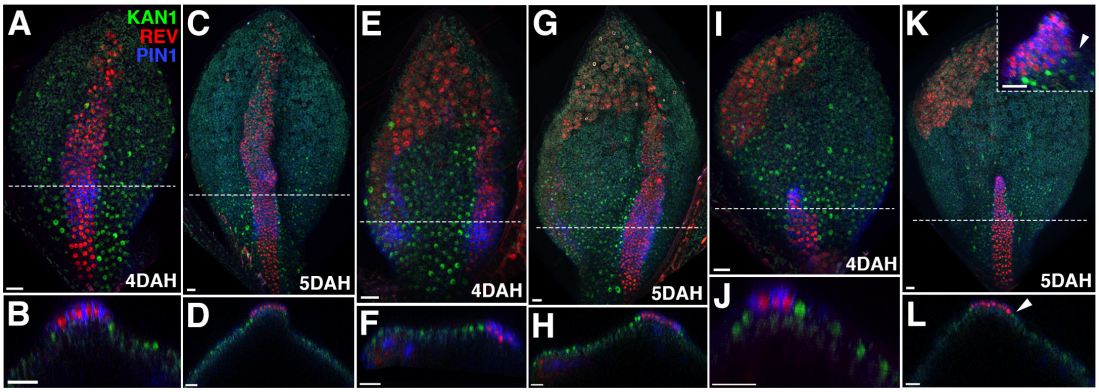

Figure 3.14 Bump formation in response to REVr-YPet* expression clones induced at 2DAS.

(A to L) Confocal projections showing examples of bump development correlating with direct juxtapose of REVr-YPet* (red) and KAN1-2×GFP (green) expressing without any gap in between. Longitudinal reconstructed sections corresponding to the dashed lines in (A, C, E, G, I and K) were showed in (B, D, F, H, J and L). Bar = 20 µm.

3.4.2.2 Down regulation of KAN1 by REV is necessary for lamina formation but not growth per se.

Since the data so far suggest that the maintenance of KAN1 expression in cells neighboring REVr-YPet* sectors inhibits lamina formation but not growth per se, I next tested whether down regulation of KAN1 within REVr-YPet* clones is necessary for growth induction. Towards this end I utilized transgenic plants expressing a direct fusion of KAN1 to GR, driven by the AtML1 (*Arabidopsis thaliana Meristem Layer 1*) promoter in order to initiate epidermal KAN1 expression (*AtML1p::KAN1-GR*) throughout the epidermal layer before and after induction of REV sectors using dexamethasone. In contrast to the completely radialized leaves of KAN1 overexpressing seedlings (grown on DEX induction medium) in the absence of REV clones (Fig. 3.15 A and B), we found that the presence of REV clones induced localized outgrowths. However, similar to the wild type situation when there is no "gap" domain, these outgrowths were not lamina shaped and were centered on the clones (Fig. 3.15 C to F) (data collected by Pierre Le Gars).

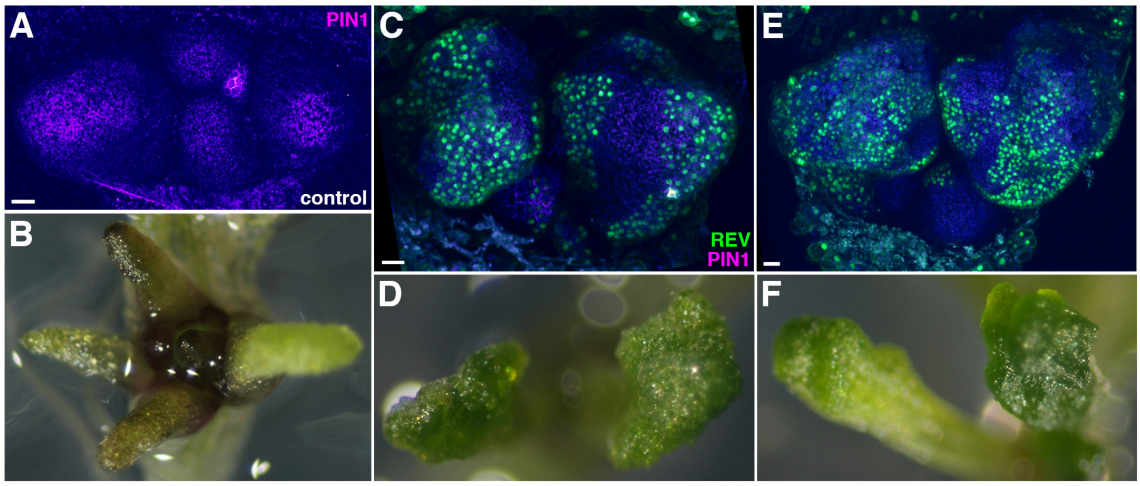

Figure 3.15 Down regulation of KAN1 by REVr-YPet* is necessary for lamina formation.

(A and B) Control plant grown on DEX induction medium with overexpression KAN1 in epidermis showing completely radicalized leaves. **(C to F)** Amorphous and bulging outgrowth formed at positions corresponding to REVr-YPet* expression patches. Bar = 20 µm in (A), (C) and (E). Note: Data was collected by Pierre Le Gars and re-analyzed before assembled in this figure.

However unlike the wild type situation, further time-lapse experiments showed that induction of epidermal REVr-YPet* clones within leaves expressing epidermal KAN1 failed to up-regulate PIN1-GFP expression in the epidermis or induce anticlinal growth under the clone (Fig. 3.16), unlike in the wild type (Fig. 3.9 A to F). Only in cases where sub-epidermal REVr-YPet* clones were present, was PIN1 expression induced in sub-epidermal layers, including non-cell autonomously (Fig. 3.17 A to F, arrowhead in F). In contrast, such clones were unable to induce PIN1 expression in the epidermis (Fig.3.17), unlike in the wild type (Fig. 3.13 L to O). Therefore, this indicates that constitutive expression of KAN1 absolutely inhibits the induction of PIN1 by REVr-YPet*, while endogenous KAN1 or transgenic KAN1 driven by its regular promoter (Fig. 3.13 L to O) does not. This may be due to the stronger expression level of KAN1 driven by the ML1 promoter compared to the endogenous promoter.

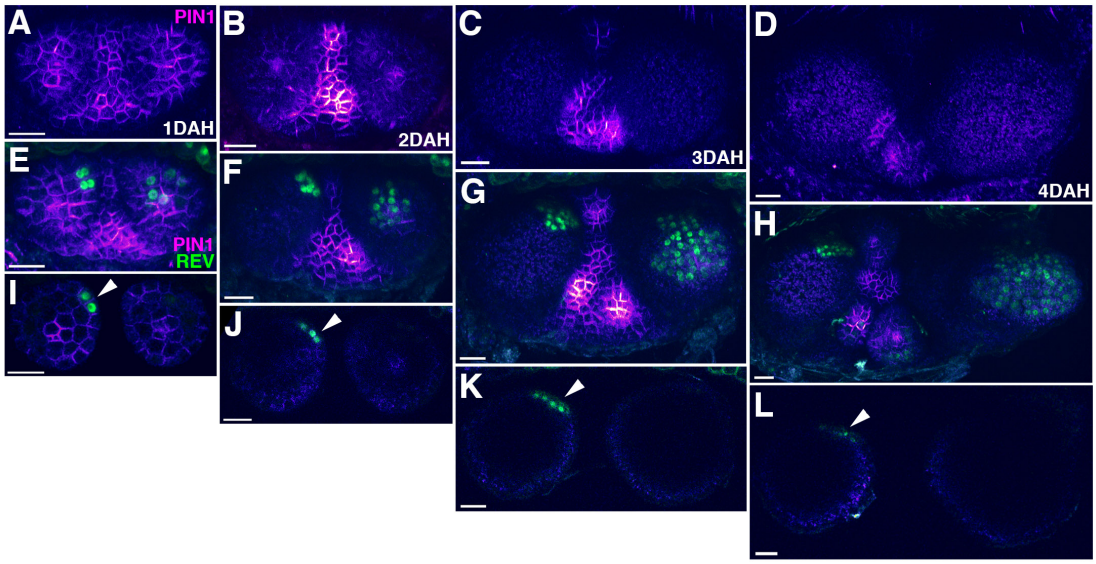

Figure 3.16 No anticlinal growth occurs in response to epidermal REV clones in the presence of KAN1 expression.

(A to D) Time-lapse projections showing control plant with overexpression of KAN1 in the epidermis. **(E to H)** Confocal projections showing epidermal induced REVr-YPet* (green) clones were not able to up-regulate of PIN1-GFP (magenta) expression in the epidermis or induce anticlinal growth. **(I to L)** Cross sections of the leaves shown in (E to H), arrowheads indicate epidermal induced REVr-YPet* expression clones. Bar = 20 µm.

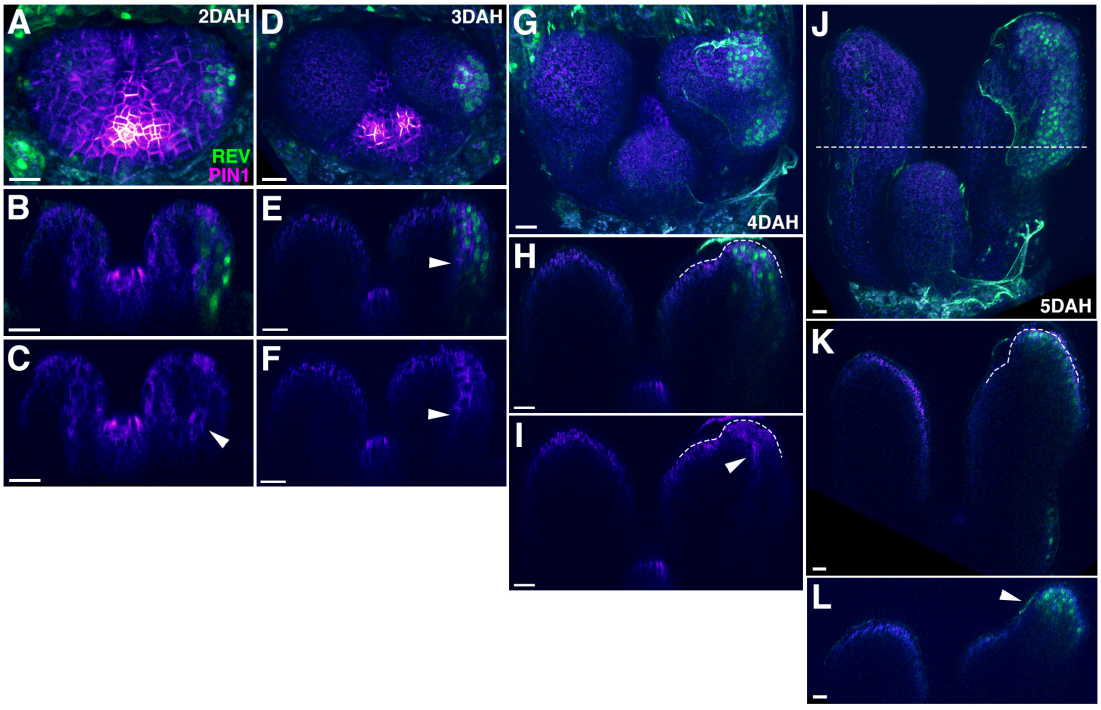

Figure 3.17 Induction of anticlinal growth by sub-epidermal REV but without up-regulation of PIN1 in the epidermis in the presence of epidermal KAN1 expression.

(A to K) Time-lapse projections showing the development of a bulge triggered by REVr-YPet* (green) clones together with overexpression of untagged KAN1 in the epidermis from 2DAH (A) to 5DAH (J). Longitudinal reconstructed sections of (A), (D), (G) and (J) are shown in (B and C), (E and F), (H and I) and (K) respectively. Arrowhead in (C), (F) and (I) indicates induction of PIN1-GFP (magenta, mapped color) expression by REVr-YPet* in sub-epidermal cell layers. Dashed curve in (H), (I) and (K) show the outline of the bulge (compared to the leaf on the left). **(L)** Cross section according to the dashed line in (J) showing the bulge from the side of the leaf corresponding to REVr-YPet* expression cells marked by an arrowhead. Bar = 20 µm.

3.4.2.3 Repression of PIN1 expression by REV in kan1kan2 double mutant.

The data so far suggest a scenario in which REVr-YPet* clones promote localized growth in abaxial leaf tissues by 1) repressing KANADI expression cell-autonomously, 2) by promoting the generation of a mobile signal(s) that acts to promote growth and 3) by repressing growth cell autonomously increasingly over time. An absence of KAN expression in cells bordering REVr-YPet* cells also likely contributes to a focusing of growth at the clonal boundary in order to generate a ridge or leaf-margin like structure. Accordingly, in *kan* mutants one might expect all abaxial tissues to resemble cells within REVr-YPet* clones early after REVr-YPet* induction. Indeed, in *kan1kan2* mutants PIN1 is expressed broadly on the ventral epidermis (Fig. 3.19 A to H) (Abley et al., 2016) where ectopic outgrowths form (Eshed et al., 2001). Imaging data from Dr. Pia Sappl (a former postdoc in the lab) has also shown that expression of REV is not only on the dorsal side of the leaf but also ectopically throughout all sub-epidermal layers of the ventral side, consistent with previous findings that REV transcript are also ectopic in this mutant background (Eshed et al., 2001). My sectoring experiments in WT leaves demonstrate that REVr-YPet* expressing clones in the sub-epidermis can signal across cells layers to up-regulate PIN1 expression in the epidermis. Therefore it seems possible that the outgrowths formed on *kan1kan2* double mutant leaves might be partly the consequence of this ectopic REV expression. Further experiments involving induction of miR165/166 to down regulate Class III HD-ZIPs in the *kan1kan2* double mutant background will help verify this possibility.

What would we expect if clones of cells expressing REVr-YPet* are now induced in the *kan1kan2* ventral epidermis? Since KAN gene function is already reduced and

REV is also expressed sub-epidermally, possibly inducing growth and PIN1 expression non-cell autonomously, I would predict that the main novel phenotype may be cell-autonomous repression of PIN1 and growth.

Indeed, I found that when clones were induced in the *kan1kan2* double mutant, the final morphology of the outgrowths formed on the ventral side of the leaves was dramatically altered (Fig.3.18). In control plants, endogenous REV expression was marked by *REVp::REV-2×VENUS* expression, while in the induced plants, only clonal induced REVr-YPet* expression was monitored. Time-lapse imaging revealed that up to three days after induction, ectopic PIN1-GFP expression appears similar on the ventral side of induced *kan1kan2* leaves compared to *kan1kan2* controls (Fig.3.19 A to D for control and I to L for induced leaf). Later at 4 days after induction, again no changes in PIN1-GFP expression were observed in response to REVr-YPet* sectors induced in the sub-epidermis (Fig.3.19 M to P, sector induced on the left side of the leaf, compared with control shown in E to H). However, PIN1-GFP expression and growth were strikingly decreased within REVr-YPet* expressing clones located in the epidermis compared to adjacent regions and the control (Fig. 3.19 O and P, marked with arrowhead, compared with G and H), confirming a repressive role for REV in regulating PIN1 expression and growth in the absence of KAN1 and KAN2. Furthermore, the down-regulation of PIN1 also correlated with REVr-YPet* expression levels. When two independent clones with different REVr-YPet* expression levels were induced (Fig.3.20 A and F, marked with an arrowhead and an arrow, respectively), weak PIN1 expression could still be detected within the clone with lower REVr-YPet* expression (Fig. 3.20 B and C, magnified view corresponding to the clone indicated by an arrowhead in A), whereas a complete lack of PIN1-GFP expression was observed within the clone expressing REVr-YPet* at a much stronger level (Fig.3.20 D and E). Meanwhile, in the vicinity of REVr-YPet* expressing clones, PIN1 appeared localized on the cell membrane farthest away from the cells expressing REVr-YPet* (Fig.3.20 C and E, cells marked with arrows), suggesting a change in PIN1 polarities similar to that noted in WT leaves with REVr-YPet* clones (Fig. 3.10 I and J). However, it is also possible that these apparent polarity changes do not in fact represent real polarity changes but rather an absence of PIN1 signal in the adjacent cells of the clone. Nevertheless, polarity convergence patterns were clearly visible in between the REV clones (Fig. 3.20 A, F and G).

Figure 3.18 Final morphology of outgrowths formed on the ventral side of leaves after induction of REV clones in the kan1kan2 double mutant.

(A) View of leaf ventral side of a fourteen-day-old WT-like sibling of *kan1kan2*. **(B)** Outgrowth formed on the ventral side of a WT-like sibling after induction of REVr-YPet* clones. **(C to E)** Final morphology of the outgrowths was dramatically altered after induction of REVr-YPet* clones (D and E) compared to the finger-shaped protrusions in un-induced *kan1kan2* double mutant (C).

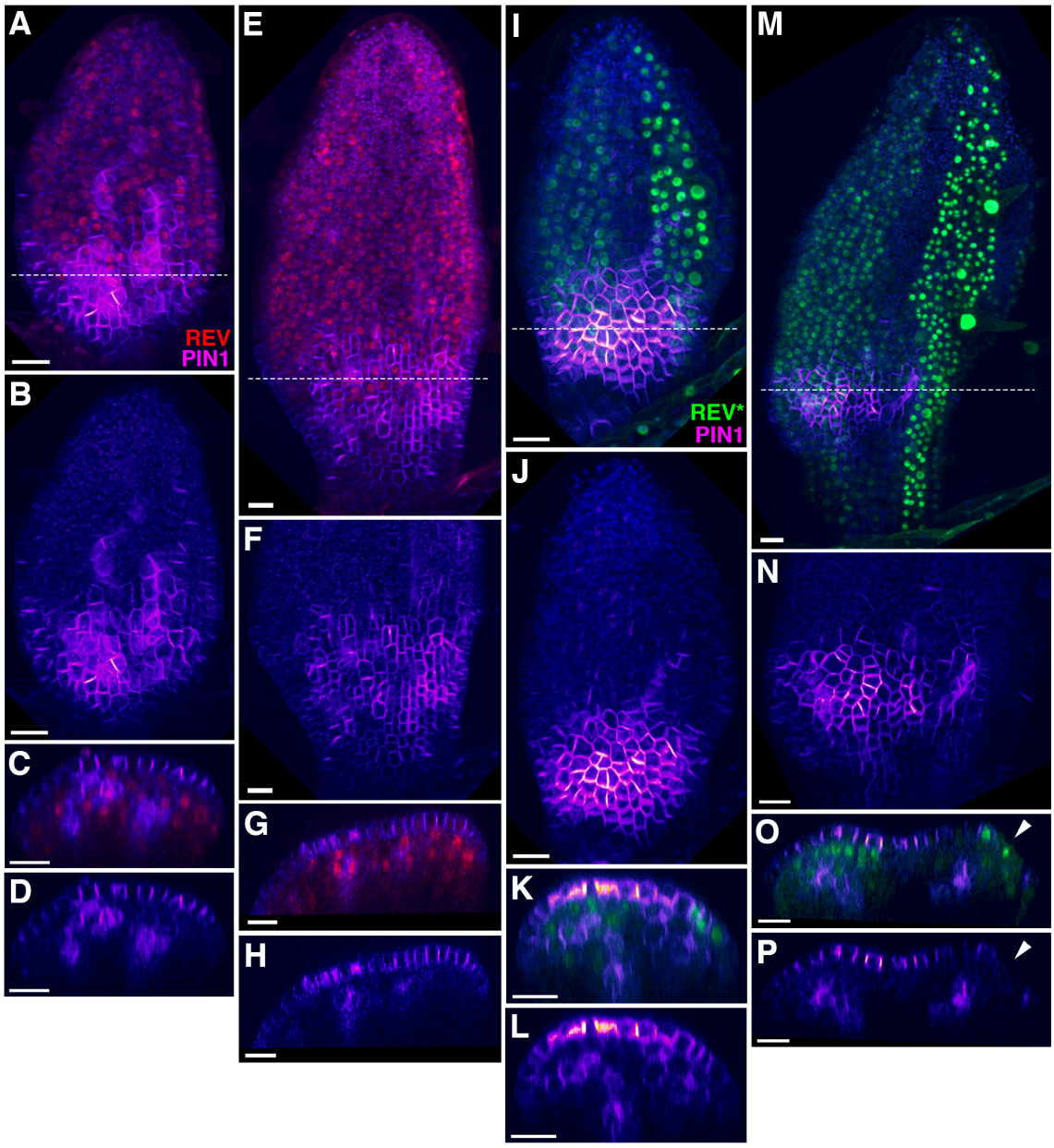

Figure 3.19 REVr-YPet* acts to repress PIN1 expression in the kan1kan2 double mutant.

(A to H) Control plant showing REV-2×YPet (red, driven by native promoter) and PIN1-GFP (magenta, mapped color) expression at 3DAH (A to D) and 4DAH (E to H). Ectopic expression of PIN1-GFP on the ventral side of the leaf is shown in (B) and (F). Cross sections through tissue in (A) and (E) is shown in (C to D) and (G to H), respectively. **(I to L)** Confocal projection and cross sections showing REVr-YPet* (green) expression induced in both sub-epidermis and epidermis layer (K) without any alteration of PIN1-GFP expression (J and L compared to B and D) at 3DAH. **(M to P)** Induction of REVr-YPet* in the epidermis acts to down-regulate PIN1-GFP expression (arrowhead in O and P), while the clones in the sub-epidermis have no effect similar to that in control plant. PIN1-GFP expression is shown separately in (N) and (P). Bar = 20 µm. Note: PIN1-GFP expression levels between control

and induced plants are slightly variable and are not directly quantified in this experiment, therefore it's hard to interpret whether REVr-YPet* expression clones induced in the sub-epidermis act additively to up-regulate PIN1 expression.

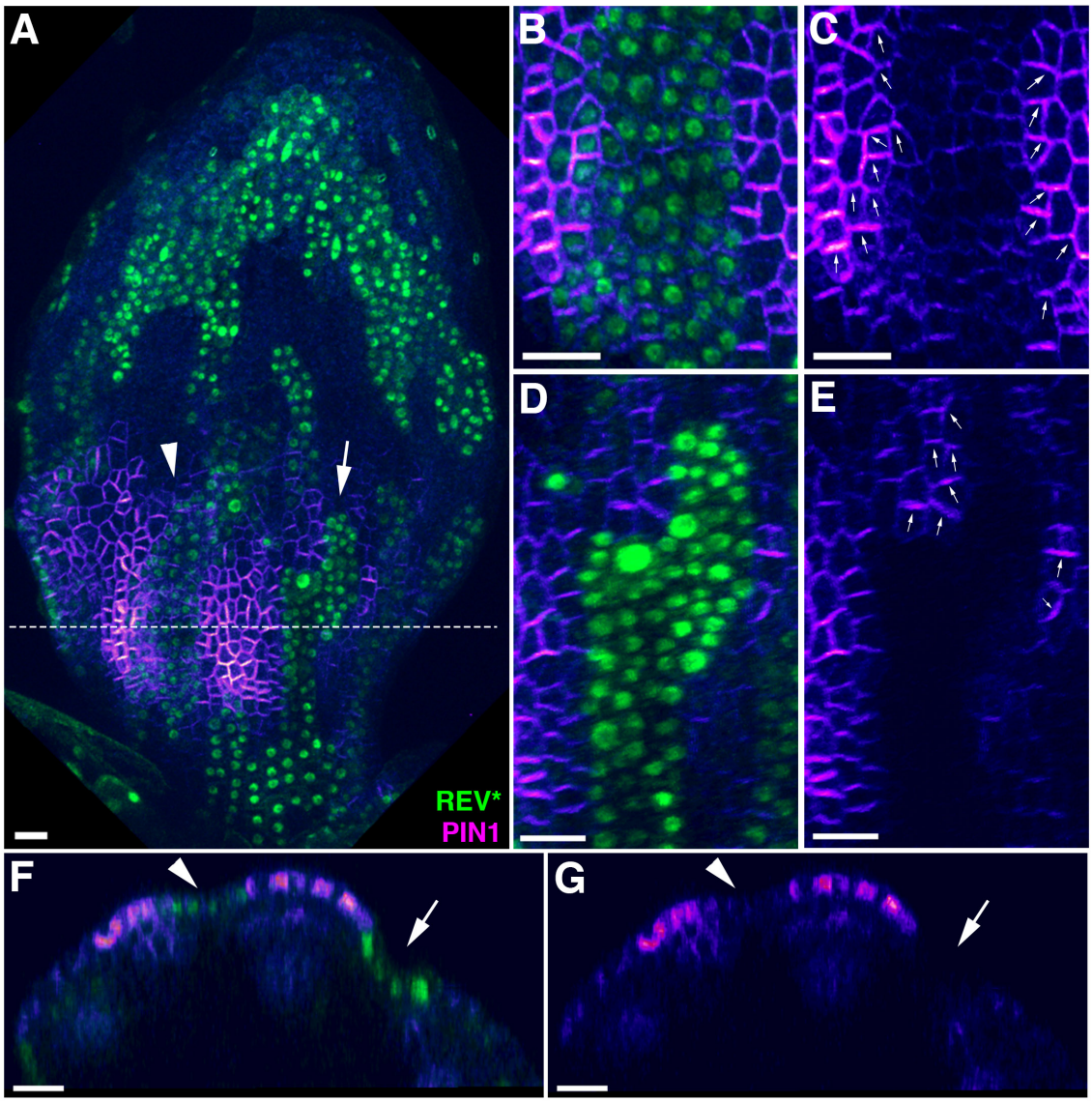

Figure 3.20 REV acts in a dosage-dependent manner to repress PIN1 expression in the kan1kan2 double mutant.

(A) Confocal projection of a leaf ventral side showing PIN1-GFP (magenta, mapped color) expression together with clonally induced REVr-YPet* (green), arrowhead marks a clone with weaker REVr-YPet* expression, whereas the arrow indicates the clone with much stronger expression of REVr-YPet* **(B to C)** Magnified view indicated by the arrowhead in (A) showing decreased expression of PIN1-GFP within REVr-YPet* expressing cells. **(D to E)** Magnified view pointed showing the region marked by the arrow in (A) showing a complete absence of PIN1-GFP expression in the cells with strong REVr-YPet* expression (compare (D) to (B) and (E) to (C)). **(F and G)** Cross section corresponding to the dashed line in (A) showing correlations between PIN1-GFP expression (G) and different levels of REVr-YPet* expression

in epidermal cells (F). Cells marked with arrow in (C) and (E) showing PIN1 localized on the membrane farthest away from REVr-YPet* expressing cells. Scale bars represent 20 µm.

All together these data support the proposal that REVr-YPet* clones regulate growth and PIN1 expression in the absence of KAN function as predicted from observation of REVr-YPet* in the wild type and demonstrate that repression of growth and PIN1 expression do not depend on KAN function.

So far, summarizing all the findings above, I propose that REVr-YPet* clones initiate lamina growth via a four-step process; (i) by switching off KAN1 expression epidermal REVr-YPet* derepresses PIN1 and other potential KAN targets that promote growth. Subsequently (ii) REV induces a mobile signal that up-regulates PIN1 and induces growth both cell and non-cell autonomously; (iii) Epidermal REV starts to suppress PIN1 expression and growth cell autonomously to help focus growth and PIN1 expression external to the clone; (iv) Restriction of PIN1 expression to a narrow linear domain occurs if there is a narrow gap between REVr-YPet* expression and adjacent KAN expression or an adjacent REVr-YPet* expressing clone. Failure in any of the above steps would impede lamina outgrowth formation. For instance, sub-epidermal REVr-YPet* clones promote development of a bulge centered on the clone rather than an external ridge due to a failure in step i, iii and iv. In the case of epidermal REVr-YPet* clones coinciding with constitutive epidermal expression of KAN1, de-repression of PIN1 (step i) and other potential KAN1 targets does not occur, and this again results in the failure to promote growth while sub-epidermal REV in this case promotes local growth centered on the clones thereby creating a bulge. In the *kan1kan2* double mutant, the first two steps have occurred already due to de-repression of KAN targets and ectopic expression of REV throughout the sub-epidermal ventral layers of the leaf. The main influence of REVr-YPet* in this case is growth and PIN1 repression.

As KAN1 is known to repress auxin associated genes including PIN1 (Brandt et al., 2012; Huang et al., 2014; Merelo et al., 2013) and KAN1 acts antagonistically towards activity of the mobile signal induced by REVr-YPet* (which also induces PIN1), an obvious candidate for the REV induced mobile signal is auxin. This will be further discussed below.

3.5 Boundary specification by juxtaposition of DV cell types.

My data reveal that juxtaposition of DV gene expression is sufficient to direct patterning in that clonal boundaries dictate the final morphology of lamina outgrowth. As reported for the D-V (Diaz-Benjumea and Cohen, 1993) and A-P boundaries (Tabata et al., 1995) of the *Drosophila* wing imaginal disk and D-V boundary of the vertebrate limb (Irvine and Rauskolb, 2001; Laufer et al., 1997b; Rodríguez-Esteban et al., 1997; Tanaka et al., 1997), juxtaposition-dependent development is typically associated with boundary localized organizers. As originally proposed by Meinhardt (Meinhardt, 1983), local interactions between adjacent cell types typically result in the formation of specialized boundary cells, which then pattern surrounding tissues through the production of long range diffusible signals. In order to investigate whether/how REVr-YPet* clones in ventral tissues of the leaf also specify boundary cell types, I next examined boundary cell identity and morphology in response to induction of REVr-YPet* expressing clones.

3.5.1 Ectopic lamina resembles WT lamina

To determine whether ectopic lamina is similar to wild type leaves, I first compared cell morphologies along the boundaries of REVr-YPet* clones and WT leaves. Overall the morphology and microtubule orientations of cells along the REVr-YPet* clonal boundaries resemble those of WT leaf margins (Fig. 3.21). In particular, cells located at the tip of WT leaf and ectopic outgrowth are similarly very large in size with randomly oriented microtubules (Fig.3.21 B and F). Cells along the lateral margins of both ectopic lamina and wild type leaves are also similarly long and rectangular in shape with microtubules oriented nearly perpendicular to the long axis of the cells at maturity (Fig. 3.21 D and G).

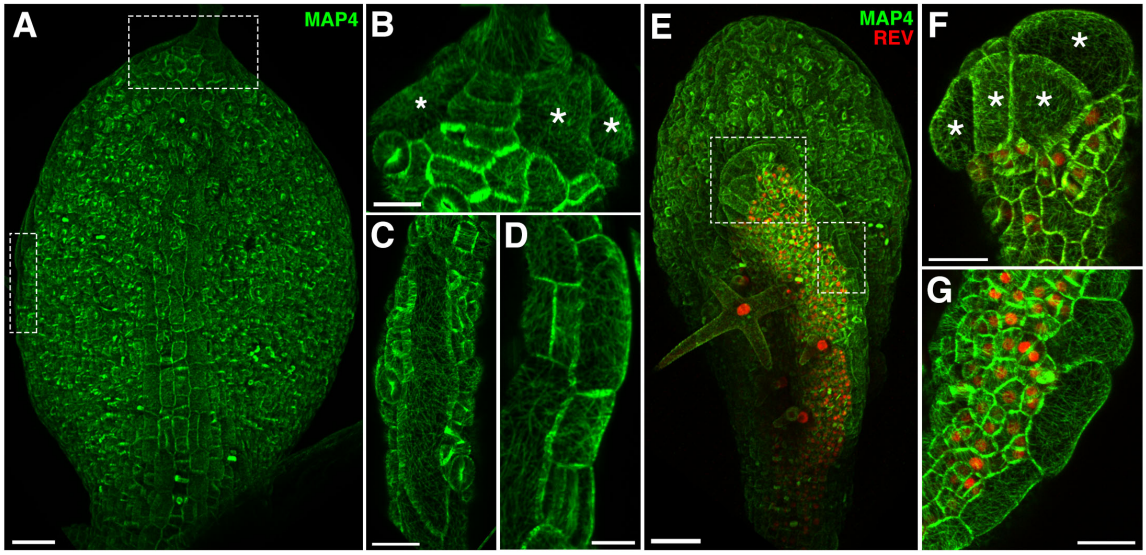

Figure 3.21 Cell shape and microtubule orientation along the margins.

(A) Confocal projection showing MAP4-GFP (green) expression in WT leaves. **(B and C)** Magnified views of boxed regions in (A) showing cell shape and microtubule orientation at the tip (B) and at the margin of the leaf (C). **(D)** An earlier time-point showing cells along the margin of the leaf. **(E to G)** Cell shape and microtubule orientation at the tip of the outgrowth (F) and along the margin (G). Asterisks mark the big cells at the tip of the WT leaf (B) and the outgrowth (F). Bar = 50 µM in (A) and (E), 20 µM in (B) to (D) and (F) to (G).

3.5.2 Boundary-associated genes are up-regulated by the juxtaposition of DV gene expression.

3.5.2.1 Auxin biosynthesis gene TAA1 is turned on by local REV expression.

Since auxin may be involved in the formation of ectopic lamina induced by REVr-YPet* clones and *TRYPTOPHAN AMINOTRANSFERASE OF ARABIDOPSIS 1* (*TAA1*) is an auxin synthesis gene expressed at leaf margins (Stepanova et al., 2008; Tao et al., 2008) which is also a direct REV target (Brandt et al., 2012), I investigated TAA expression in wild type leaves and after induction of REVr-YPet* clones.

At 3 DAS in wild type leaves GFP-TAA1 expression was only detected in the VM (Fig.3.22 A to C), while slightly later at 3.5 DAS, GFP-TAA1 expression was also detected in the dorsal (adaxial) leaf epidermis overlapping with REV-2×YPet, although only at very low levels (Fig. 3.22 D and E). At 4 DAS, GFP-TAA1 becomes highly expressed at the leaf tip and margin (Fig.3.22 F to H). At the same stage, GFP-TAA1 is also detected in the vasculature together with PIN1-CFP and REV-2×YPet,

Interestingly, at the new leaf primordium initiation site (arrowhead in Fig.3.22 F), GFP-TAA1 expression appeared relatively low, indicating possible negative feedback between auxin concentrations and auxin biosynthesis. From 4 DAS onwards, high expression of GFP-TAA1 was maintained along the leaf margins partially overlapping with REV-2×YPet, and the weak expression on the dorsal side of the leaf appeared patchy, which may be due obscuring trichomes (Fig.3.22 I to K).

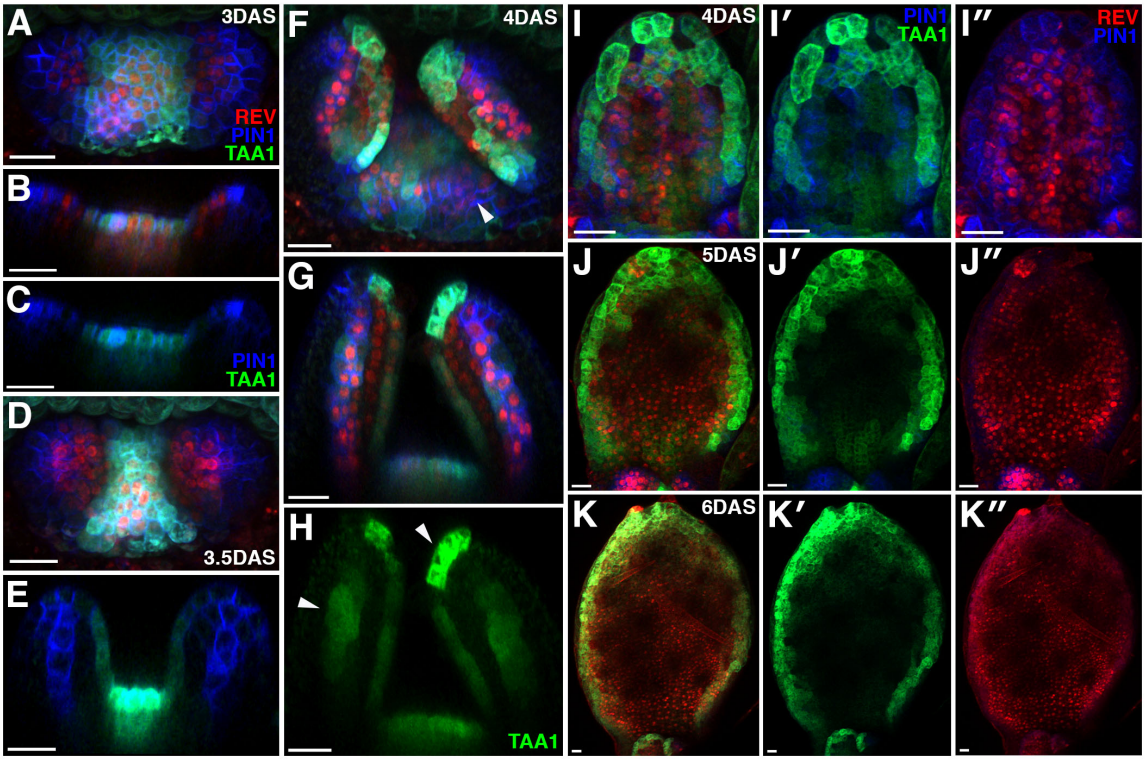

Figure 3.22 Expression pattern of TAA1p:: GFP-TAA1 at the seedling stage.

(A to H) Confocal projections showing REV-2×YPet (red), PIN1-CFP (blue) and GFP-TAA1 (green) expression pattern in the vegetative shoot apical meristem at 3 DAS (A to C), 3.5 DAS (D to E) and 4DAS (F to H), respectively. (B and C) Longitudinal reconstructed sections of seedling shown in (A). (E) Longitudinal section of seedling in (D) showing PIN1-CFP and GFP-TAA1 expression. (G and H) Longitudinal reconstructed sections of seedling in (F) showing the co-expression of GFP-TAA1 with REV and PIN1 in the vasculature, arrowheads in (H) indicated GFP-TAA1 expression in vasculature and at the tip of the leaf. **(I to K)** Confocal projections of leaf dorsal side showing the expression of GFP-TAA1, PIN1-CFP and REV-2×YPet at 4DAS (I to I''), 5DAS (J to J'') and 6DAS (K to K''), respectively. Scale bars = 20 µm.

In heatshock-induced plants, the response of TAA1 to REVr-YPet* expression was variable. In some cases, up-regulation of TAA1 occurred only within the REVr-YPet*

expressing clones (cell-autonomous) from 2 days after heatshock (DAH) and was maintained during outgrowth formation (Fig.3.23 A to D). Occasionally however, the up-regulation of TAA1 could be detected within 24 hrs after heatshock (Fig.3.23 E and F). In other examples, at 2 DAH, TAA1 expression was not only present within the REV clones but also in cells adjacent to the clones (arrow in Fig.3.23 H and insertion), indicating both cell and non-cell autonomous up-regulation by REV. However, the expression level of TAA1 in the cells adjacent to the clones was much stronger compare to that which overlapped with REVr-YPet* clones. During outgrowth development, this pattern was maintained with spots of high TAA1 expression occasionally observed within REV clones. These regions ultimately gave rise to protrusions at maturity (Fig.3.23 J to L, indicated by arrowheads).

Interestingly, by comparing TAA1 expression in different clones expressing REVr-YPet* at different levels, I found TAA1 to be usually expressed more strongly in clones expressing REVr-YPet* at lower levels (Fig.3.24). Thus similar to PIN1, REV appears to regulate TAA1 in a dosage-dependent manner. Strikingly, this pattern was initiated very early upon induction of REV at one day after heatshock, although the expression of TAA1 was very weak (Fig.3.24 A and B, arrowhead). During leaf development, expression of TAA1 became stronger and was maintained in the clones expressing REV at a low level (Fig.3.24 C to K). I also observed the expression of TAA1 in sub-epidermal layers underneath clones expressing REVr-YPet* at both high and low levels (Fig.3.24 F to H and insertions), which possibly was associated with the formation of the vasculature tissue. In more extreme examples, I found that TAA1 expression was induced throughout the leaf seemingly independent of where the clones were located (Fig.3.25 A and B). Most often however, if a linear domain of non-REVr-YPet*-expressing cells was present surrounded by REVr-YPet* expressing cells TAA1 was consistently expressed very strongly in this linear region (Fig.3.25 C and D). Similarly, when the outgrowths were lamina-like TAA1 was, expressed most highly at the blade margins, extending beyond the REV expressing cells (Fig.3.25 E and insert), similar to the pattern observed in wild type leaves (Fig.3.22).

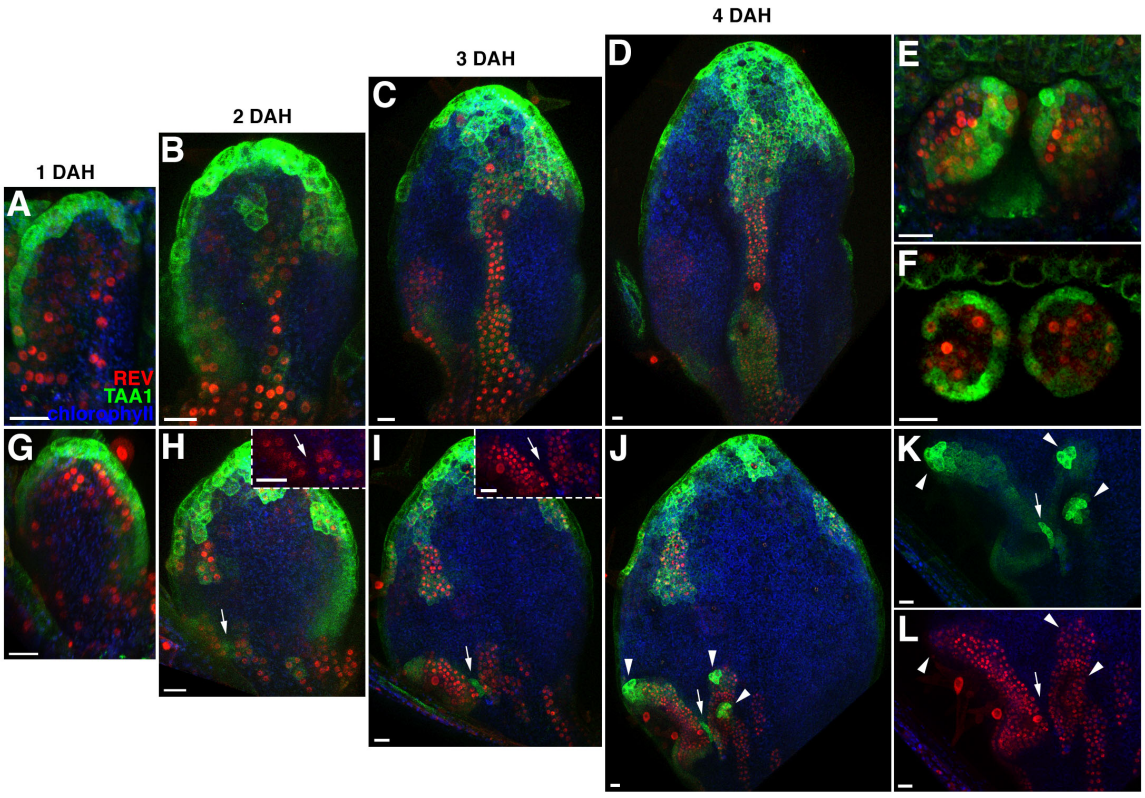

Figure 3.23 Cell and non cell-autonomously up-regulation of GFP-TAA1 by REV.

(A to D) Time-lapse projections of a developing leaf primordium showing GFP-TAA1 (green, autofluorescence in blue) expression and clonally induced REVr-YPet* (red) from 1 DAH (A) to 4DAH (D) with up-regulation of GFP-TAA1 only within the clones (cell-autonomously). **(E to F)** An example showing up-regulation of GFP-TAA1 within 24h after induction of REVr-YPet* clones. **(G to J)** Time-lapse projections of a developing leaf primordium showing up-regulation of GFP-TAA1 non cell-autonomously from 2DAH (H, arrow indicate the region outside the clones with GFP-TAA1 expression) to 4DAH (J), insertion in (H) and (J) showed magnified images with expression of REVr-YPet*, arrows showed the region between two REVr-YPet* clones. **(K to L)** Magnified views of GFP-TAA1 (K) and REVr-YPet* expression, respectively from (J). Arrowheads showing localized high expression of GFP-TAA1 within the clones, while arrow showed the region between the two clones with high levels of GFP-TAA1 expression. Scale bars represent 20 µm.

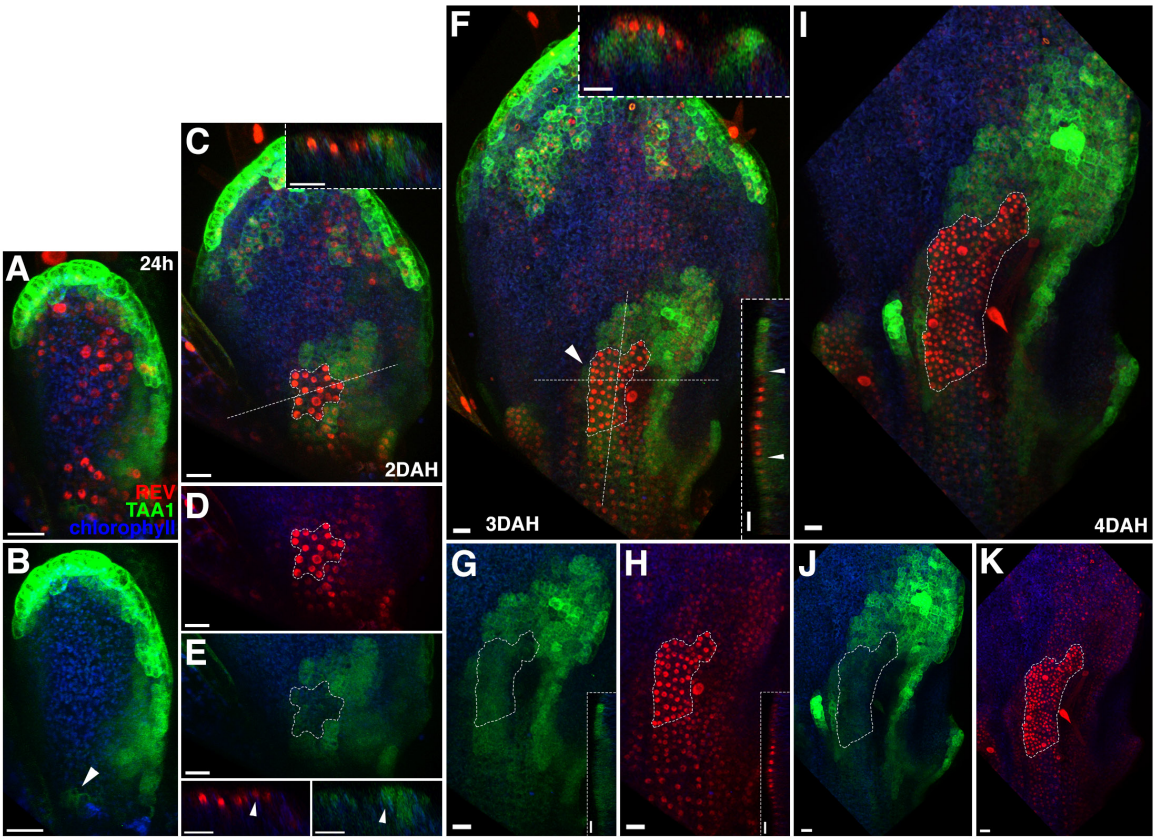

Figure 3.24 REV acts in a dosage-dependent manner to up-regulate TAA1 expression.

(A and B) GFP-TAA1 (green, autofluorescence in blue) was up-regulated in cells with low levels of REVr-YPet* (red), arrowhead in (B) indicated weak GFP-TAA1 expression. **(C to K)** GFP-TAA1 expression increases at 2DAH (C) in the cells with lower REVr-YPet* expression levels and maintained during leaf development (F and I). Magnified views of sector regions from 2 DAH (C), 3DAH (F) and 4DAH (I) are shown with separated channels in (D to E), (G to H) and (J to K) respectively. Longitudinal sections corresponding to the dashed line in (C) are shown as insertions in (C) and (E) and the arrowheads indicate the region where GFP-TAA1 expression overlapps with REVr-YPet* expression at a lower level. Longitudinal reconstructed sections along the dashed lines inserted in (F to H) show GFP-TAA1 is expressed in the sub-epidermis underlying both high and low REVr-YPet* expressing domains. Irregular dashed line indicates the borders of high REVr-YPet* expressing cells. Bar = 20 µm.

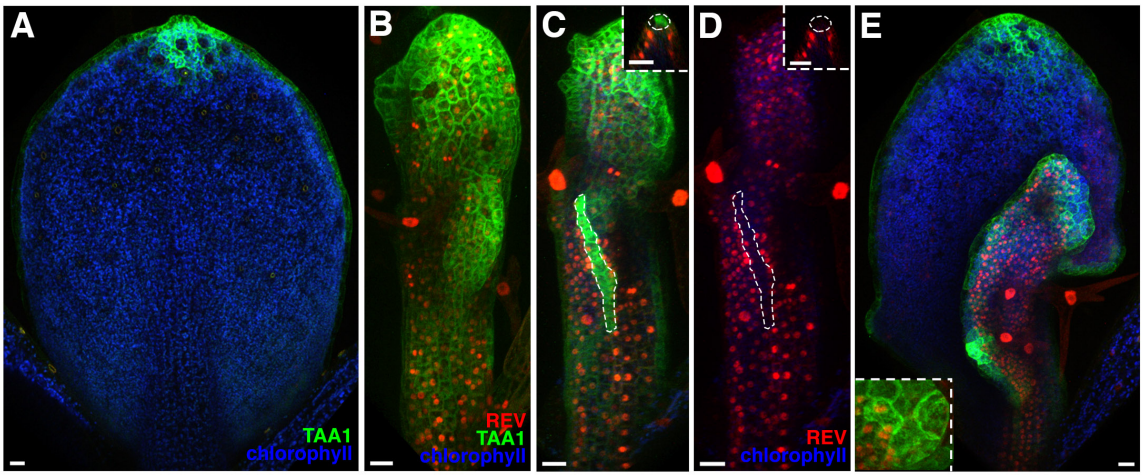

Figure 3.25 More examples of leaf ventral side showing up-regulation of GFP-TAA1.

(A) Ventral side of WT leaf showing GFP-TAA1 (green, autofluorescence in blue) expression along the leaf margins. **(B)** Confocal projection of an example showing up-regulation of GFP-TAA1 throughout the leaf wherever clones (red) are present. **(C and D)** GFP-TAA1 was highly up-regulated at a linear region devoid of REVr-YPet* (red) expression, insertions show cross sections of that region. **(E)** GFP-TAA1 expression along boundaries of REVr-YPet* clones resembling the wild type pattern. Insertion shows close up of TAA1-GFP expression extending beyond REVr-YPet* clonal boundary. Bar = 20 µm.

These data indicate that clones of cells induce REVr-YPet* in a non-cell autonomous manner and that this regulation is established very early and maintained during outgrowth formation.

3.5.2.2 Up-regulation of TAA1 and PIN1 expression does not occur in the same cells.

Since both TAA1 and PIN1 appear to be induced non-cell autonomously in a similar manner by REVr-YPet* clones, I monitored both markers simultaneously after REVr-YPet* clone induction. Interestingly I found that unlike PIN1-CFP, up-regulation of GFP-TAA1 was not dependent on the position of the clone along the proximo-distal axis (Fig.3.26 A to D and I to L). In the proximal region of the leaf, up-regulation of both GFP-TAA1 and PIN1-CFP showed a complementary expression pattern to induced REVr-YPet* clones in a dosage-dependent manner (Fi.3.26 A to D). However, GFP-TAA1 and PIN1-CFP expression were only partially overlapping and often in different cell layers (Fig3.26 E to H). Specifically, while sub-epidermal induced REV sectors up-regulated PIN1-CFP expression in the epidermal layer

(Fig.3.26 E and F) such clones did not induce epidermal GFP-TAA1 expression, indicating difference in the way these two genes are regulated. In particular, REV was not able to induce TAA1 expression across different cell layers (Fig.3.26 F and G). Furthermore, I also observed that GFP-TAA1 expression is absent in regions with very high expression of PIN1-CFP (Fig.3.26 I to P, arrowhead in L), possibly paralleling the situation at organ inception during wild type development as described above (Fig.3.22 F, arrowhead).

To conclude, TAA1 is induced by REV clones in a complex manner that includes cell autonomous, non-cell autonomous and dosage dependent modes of regulation. Nevertheless, overall these findings are consistent with the proposal that the mobile signal induced by REV clones that upregulates PIN1 and growth may correspond to auxin. They also confirm that juxtaposition of REV expression in ventral tissues is sufficient to induce boundary gene expression.

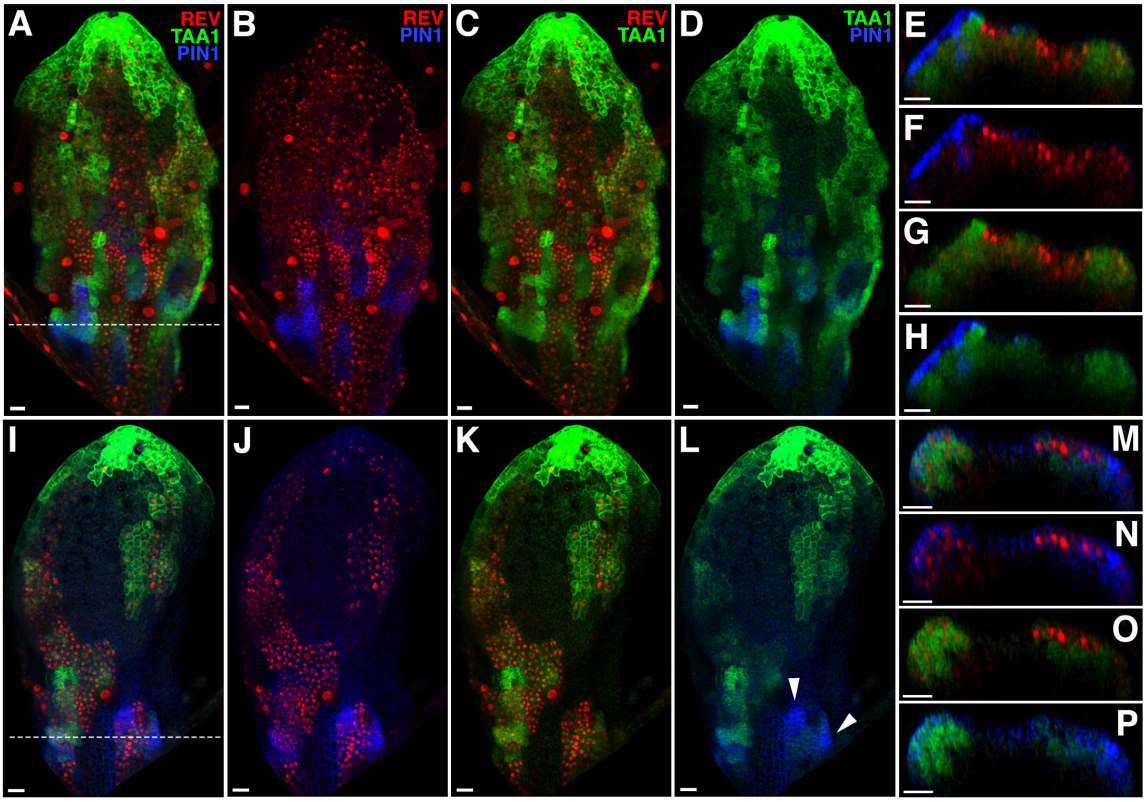

Figure 3.26 TAA1 and PIN1 are up-regulated in a similar manner but in different cell layers.

(A to D) Confocal projections showing complementary expression patterns of GFP-TAA1 (green) and PIN1-CFP (blue) with REVr-YPet* (red) clones on the ventral side of the leaf at 3DAH. **(E to H)** Longitudinal reconstructed sections corresponding to the dashed line in (A)

show that PIN1-CFP and GFP-TAA1 are not expressed in the same layer. **(I to L)** An example showing up-regulation of PIN1-CFP and GFP-TAA1 in response to REVr-YPet* where their response does not completely overlap. **(M to P)** Longitudinal sections along the dashed line in (I) show a negative correlation between GFP-TAA1 expression and high expression levels of PIN-CFP. Bar = 20 µm.

3.5.2.3 WOX1 and PRS are up-regulated by local REV expression but became restricted to the clonal boundary during outgrowth formation.

In plants, several WUSCHEL-RELATED HOMEOBOX (WOX) genes, including PRESSED FLOWER (PRS)/WOX3 and WOX1, are expressed at the leaf D-V boundary where they promote leaf blade outgrowth and margin development (Nakata et al., 2012). To further understand how boundary cell types get specified, the expression patterns of these genes were examined during outgrowth formation triggered by REV clones.

3.5.2.3.1 WOX1 expression pattern in the leaf and the SAM

First of all, the expression pattern of WOX1 during wild type leaf development was examined together with PIN1 expression. Confocal data reveal that expression of 2×GFP-WOX1 at the leaf margin is established early at 3 days after stratification (Fig.3.27 A and B) and is maintained until maturity (Fig.3.27 C to E). In addition, 2×GFP-WOX1 was also expressed in the middle domain of flower sepals, which are leaf-like organs of the flowers (Fig.3.27 insertion in F). However, no expression of WOX1 could be detected either in the VM or the IM (Fig.3.27 A and F).

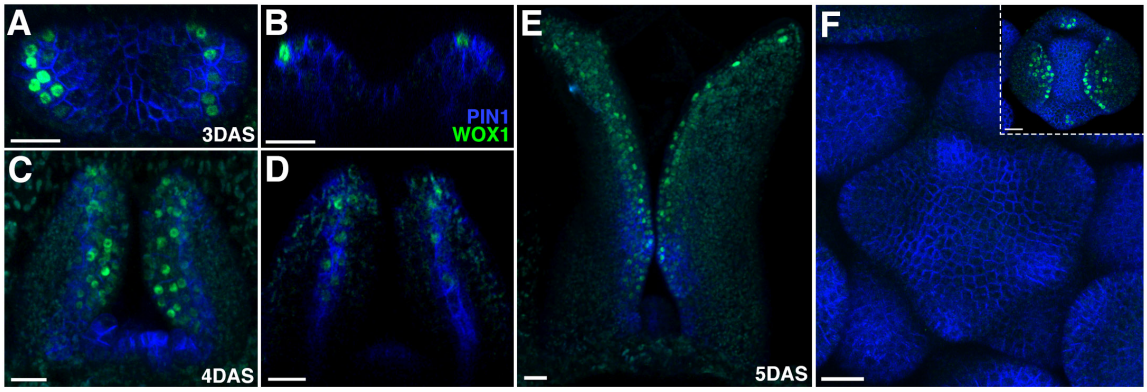

Figure 3.27 Expression pattern of 2×GFP-WOX1.

(A to E) Confocal projections showing PIN1-CFP (blue) and 2×GFP-WOX1 (green) expression pattern in the vegetative meristem and leaves of seedlings at 3 DAS (A), 4DAS

(C) and 5DAS (E), respectively. (B and D) Longitudinal reconstructed sections of seedlings shown in (A) and (C). **(F)** An inflorescence meristem image showing 2×GFP-WOX1 is not expressed in the IM but is expressed in the sepals of the flower (insertion in F). Bar = 20 µm.

3.5.2.3.2 WOX1 expression is up-regulated by REV both cell and non-cell autonomously.

Similar to the up-regulation of GFP-TAA1 by REVr-YPet*, time-lapse experiments revealed that 2×GFP-WOX1 expression is also up-regulated by induction of REVr-YPet* clones both cell and non-cell autonomously and the response is variable (Fig.3.28 and Fig.3.29). For instance in the example shown in Fig. 3.28, up-regulation of 2×GFP-WOX1 occurred only within the REVr-YPet* expressing clones from 3 DAH and was maintained in this manner during outgrowth formation. While in another example, 2×GFP-WOX1 expression was induced in cells located at the edge of the clone either overlapping with REVr-YPet* expressing cells or outside along the clonal boundaries (Fig.3.29 C and D, white arrowhead and pink arrowhead, respectively). During outgrowth formation, 2×GFP-WOX1 became expressed almost all along the clonal boundaries of REVr-YPet* together with PIN1-GFP expression (Fig.3.29 H to J), which is very similar to their expression patterns along WT leaf margins (Fig.3.27 E).

Despite many similarities in the response of GFP-TAA1 and 2×GFP-WOX1 to local REVr-YPet* expression, the up-regulation of 2×GFP-WOX1 occurs from 3DAH (Fig.3.28 C and D, Fig.3.29 C and D), while GFP-TAA1 expression could be detected earlier at one day after heatshock (Fig.3.24 A and B). Since both PIN1 and WOX1 were marked by GFP in this experiment, the apparent late response of 2×GFP-WOX1 may be due to the weak GFP nuclei signal at 2DAH being masked by the strong membrane PIN1-GFP expression (Fig.3.28 A and B, Fig.3.29 A and B). Furthermore, it is not very clear from these results whether 2×GFP-WOX1 is up-regulated only in a few cells at the edge of the clone or in all the cells within the clone 3DAH (Fig.3.29 D). To clarify the timing and extent of up-regulation of 2×GFP-WOX1, future use of the CFP tagged PIN1 would be beneficial.

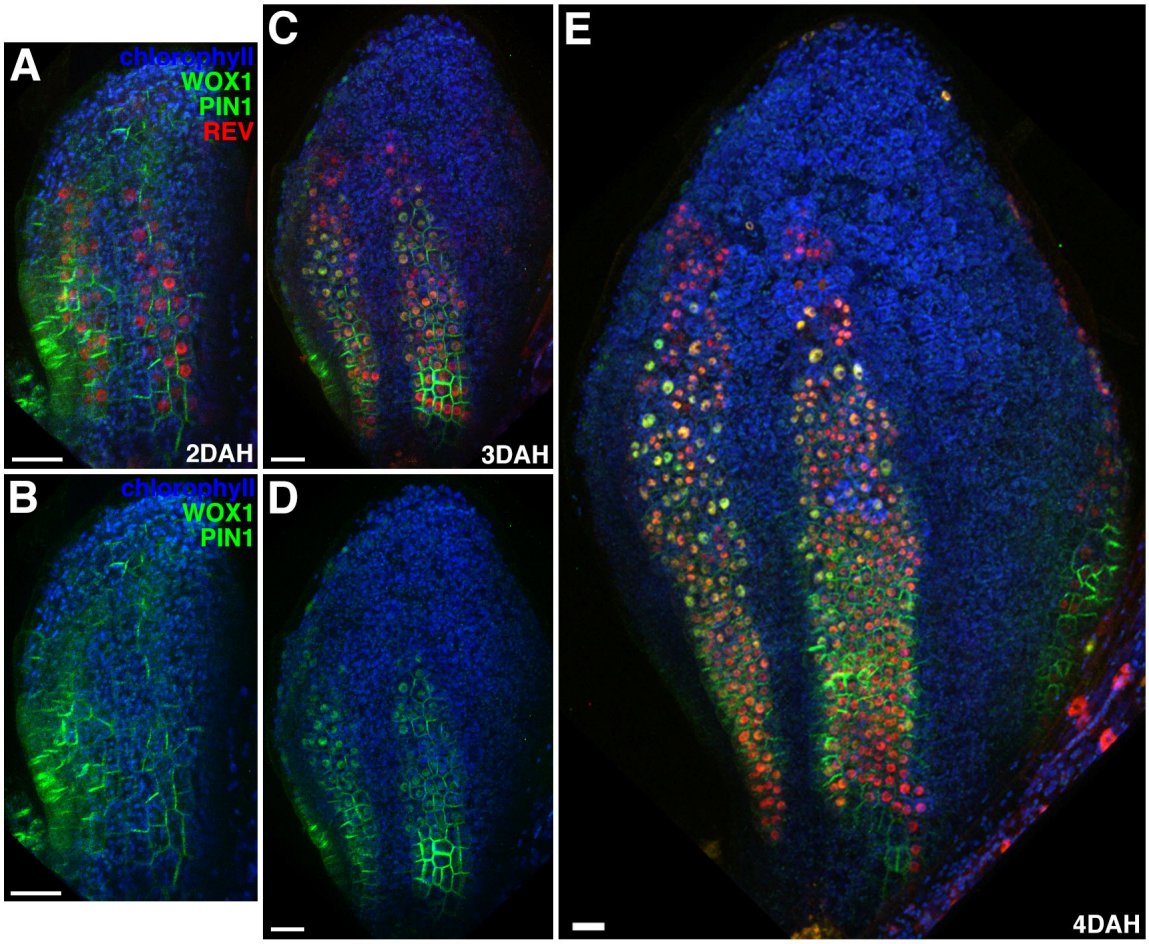

Figure 3.28 Cell autonomous up-regulation of WOX1 by REVr-YPet* clones.

(A and E) Time-lapse projections of a developing leaf primordium showing up-regulation of 2×GFP-WOX1 (green nuclei signal, autofluorescence in blue) from 3DAH (C and D) within a REVr-YPet* (red) clone and the continued overlap with REVr-YPet* during development (E), whereas, PIN1-GFP (green membrane signal) expression is present much earlier within the clone at 2DAH (A and B). Bar = 20 µm.

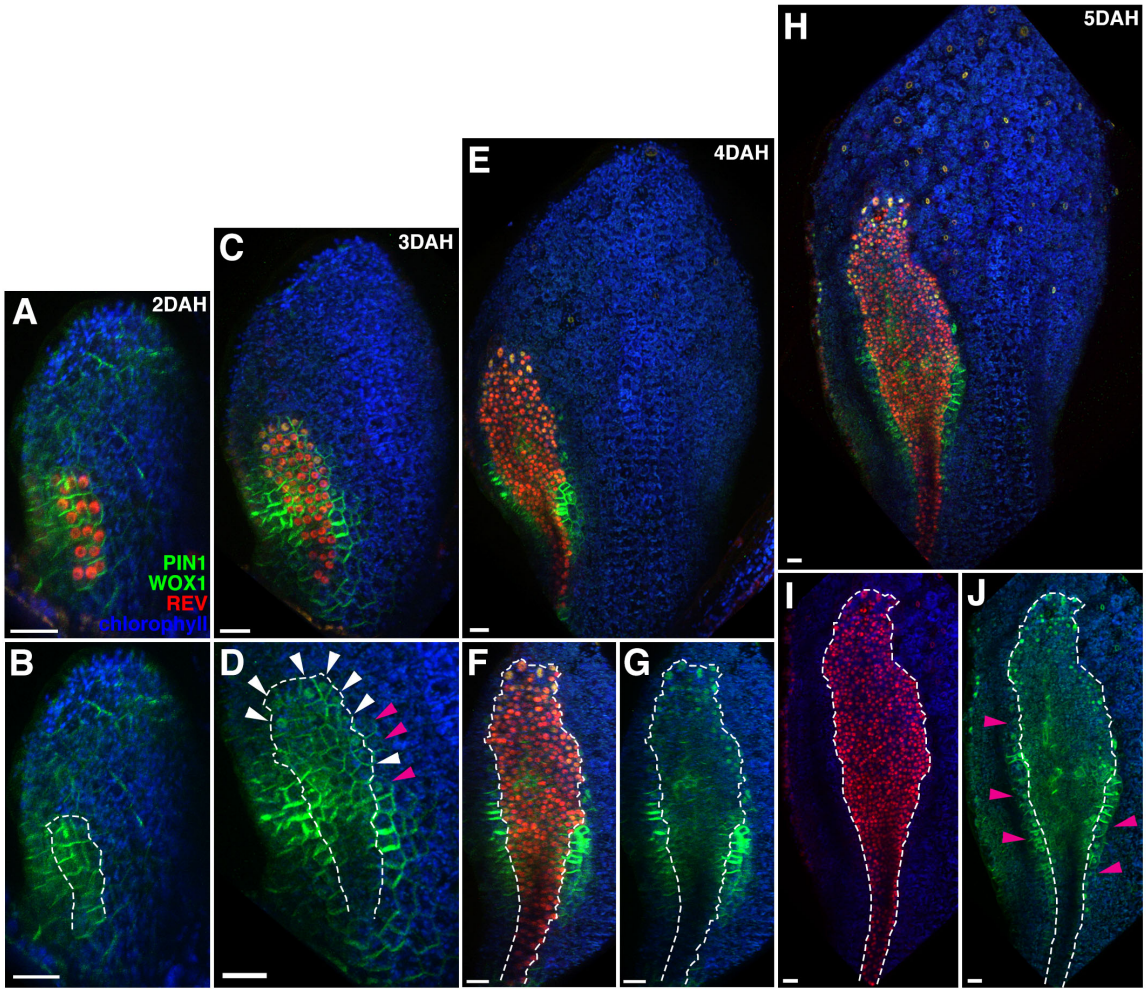

Figure 3.29 WOX1 expression along REVr-YPet* clonal boundaries.

(A and B) Up-regulation of PIN1-GFP (green membrane signal, autofluorescence in blue) by induction of REVr-YPet* (red) expression at 2DAH. **(C and D)** 2×GFP-WOX1 (green nuclei signal) is up-regulated both within (white arrowheads in D) and outside (pink arrowheads in D) the clone. **(E to J)** Confocal projections of the whole leaf (E an H) and magnified view of the outgrowth (F, G, I and J) showing 2×GFP-WOX1 expression along the boundaries of the clone overlapping with PIN1-GFP expressing cells (pink arrowheads in J) during outgrowth development. Irregular dashed line indicates the outline of REVr-YPet* clones. Bar = 20 µm.

3.5.2.3.3 PRS expression is up-regulated and re-patterned by REVr-YPet expression during outgrowth formation.*

As reported, PRS and WOX1 act redundantly to maintain leaf blade growth and are expressed in the middle domain of the leaf (Nakata et al., 2012). To test whether PRS exhibits a similar response to the induction of REVr-YPet* expressing clones, two PRS reporters were used to monitor the activity of PRS upon the induction of REVr-YPet*.

In contrast to the expression pattern of 2×GFP-WOX1 (Fig.3.27), PRS-2×GFP was expressed not only along the margin and in the middle domain of the leaf, but also surrounding the vegetative meristem (VM) (Fig.3.30 A to E). In the IM, however, PRS-2×GFP was only detected at organ inception sites marked by PIN1 expression and polarity (Fig.3.30 I, indicated with arrowhead). Unfortunately, this reporter could not be used in the currently available transgenic plants with inducible REV clones. Instead, another reporter, *PRSp::tdTomato-NLS* was utilized to monitor the expression of PRS together with REVr-YPet* sectors. *PRSp::tdTomato-NLS* showed a similar expression pattern to that of PRS-2×GFP in the IM (Fig.3.30 J, compared with I). However, it appeared that *PRSp::tdTomato-NLS* was initially expressed more broadly throughout young leaves with stronger expression in the middle domain and weak expression on both dorsal and ventral sides until 4DAS (Fig.3.30 F and G, Fig.3.31 A and B). Whether this is because of perdurance of the tdTomato protein remains to be determined. During leaf development, *PRSp::tdTomato-NLS* signal on the ventral side of the leaves decreased until it remained only along the margin and in the leaf middle domain (Fig.3.31 C to H, arrowheads).

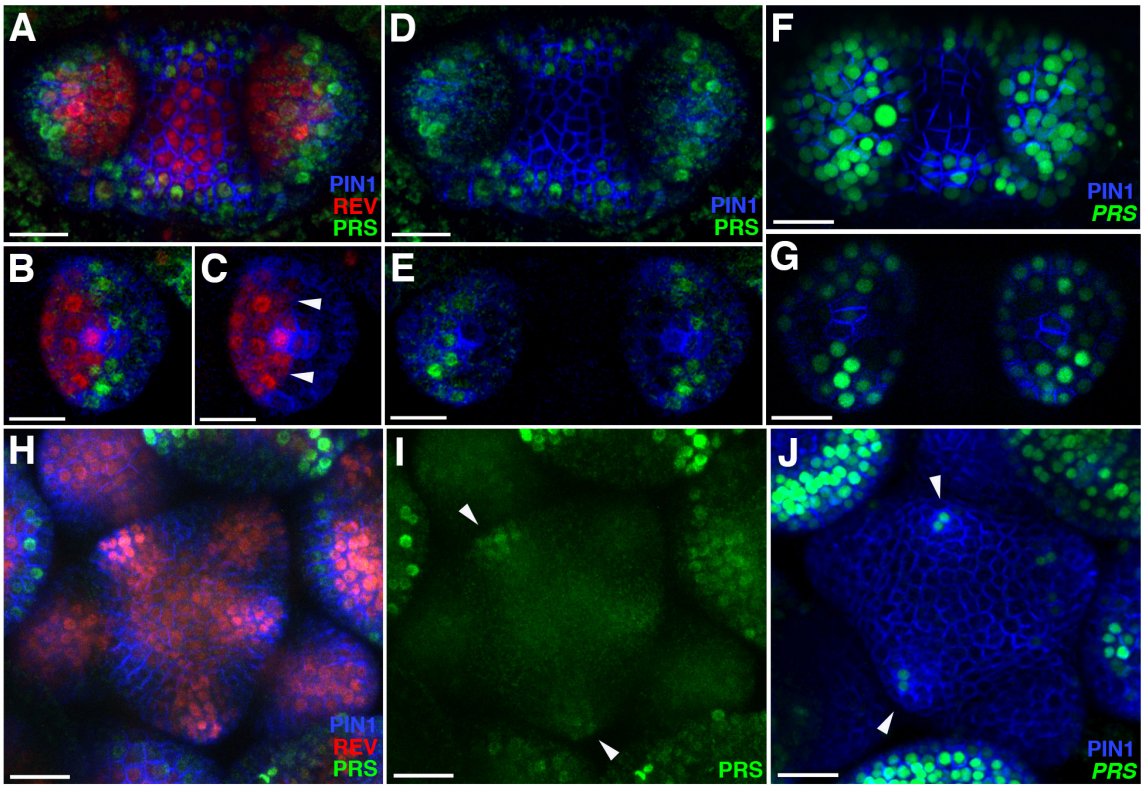

Figure 3.30 Expression pattern of PRSp::PRS-2×GFP and PRSp::tdTomato-NLS.

(A) Confocal projection showing PIN1-CFP (blue), PRS-2×GFP (green) and REV-2×YPet (red) expression in the vegetative meristem and leaves at 3.5 DAS. **(B and C)** Cross sections of leaf on the right side in (A) showing the expression of PRS-2×GFP in the middle domain of the leaf, partially overlapped with REV-2×YPet expressing cells marked with arrowheads. **(D and E)** Confocal projection and cross sections showing PRS-2×GFP is expressed surrounding the VM and in the middle domain of the leaf. **(F and G)** Confocal projection showing expression of *pPRS::tdTomato-NLS* (green) throughout the leaf with high expression in the middle domain and weak expression on both dorsal and ventral sides of the leaves. **(H to J)** *PRSp::tdTomato-NLS* expression in young flower primodia in the IM (J), indicating a similar expression pattern to PRS-2×GFP (H and I). Bar = 20 µm.

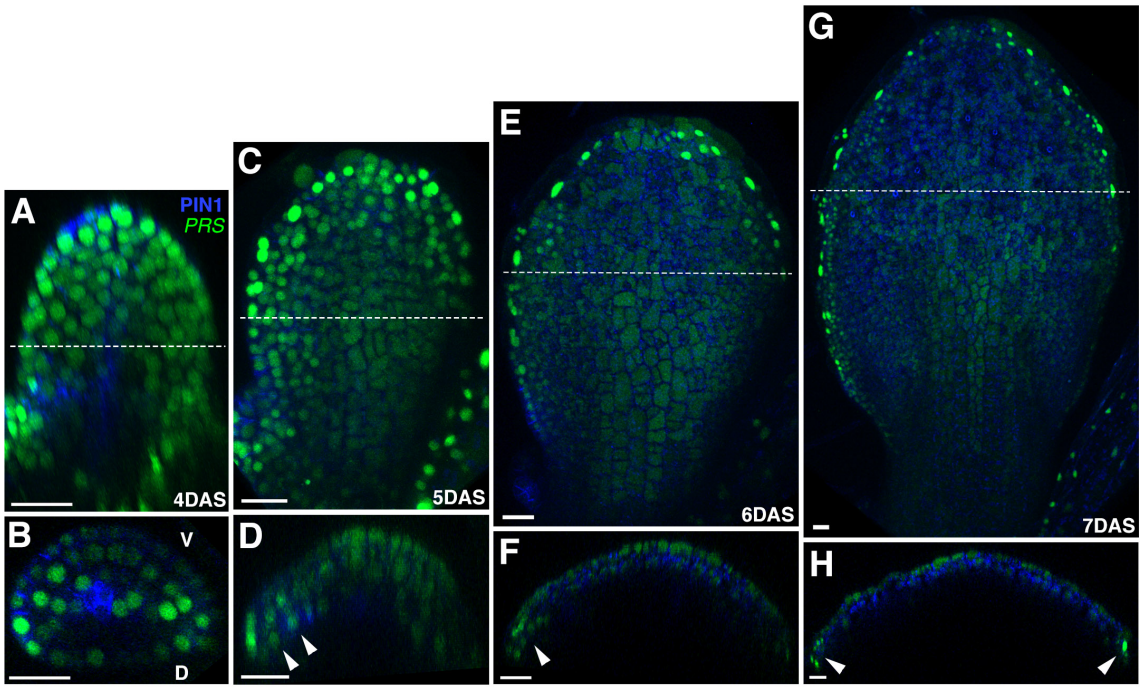

Figure 3.31 Expression pattern of pPRS::tdTomato-NLS on the ventral side of leaves.

(A and B) Confocal projection of the leaf and cross section along the dashed line showing very weak expression of *pPRS::tdTomato-NLS* (green) in the epidermis of the ventral side of the leaf and much stronger expression in the middle domain at 4DAS, vasculature marked by PIN1-CFP (blue). "V" represents "ventral" and "D" represents "dorsal". **(C to G)** *pPRS::tdTomato-NLS* signal decreases from the outmost layer of the leaf but is maintained in the middle region and along the leaf margins (arrowheads in D, F and H) during later leaf development. Note: the fuzzy green signal filling the whole cell corresponds to autofluorescence that overlaps with the tdTomato channel in (C) to (H).

When monitoring the expression pattern of *PRSp::tdTomato-NLS* after induction of REVr-YPet* clones I observed no significant changes at 1 DAH (corresponding to 4 DAS) compared with control leaves (Fig.3.32 A to C, indicated by arrowheads). From 2DAH, both PIN1-GFP and *PRSp::tdTomato-NLS* were up-regulated within the clone (Fig.3.32 D to I). Later, at 3DAH, *PRSp::tdTomato-NLS* expression was present not only within the REVr-YPet* clones but also in cells adjacent to the clones at slightly lower expression levels (Fig.3.32 G to I, irregular dotted circle), indicating non-cell autonomous up-regulation by REV. Starting from 4DAH, *pPRS::tdTomato-NLS* expression decreased dramatically in the epidermis of REVr-YPet* expressing clones but was maintained underneath the clones in the sub-epidermis and at the margin (Fig.3.32 J to Q). The marginal expression of *PRSp::tdTomato-NLS* partially

overlapped the outer clonal cells expressing REV (Fig.3.32 O to Q). Despite the non-lamina nature of the outgrowth, *PRSp::tdTomato-NLS* expression was localized specifically at the margin of REVr-YPet* clone (Fig.3.33 A to F). However, I also found that at the distal end of leaves, *PRSp::tdTomato-NLS* expression typically overlapped REV expressing cells (Fig.3.33 G to L, clones marked with arrow), whereas for proximally localized clones *PRSp::tdTomato-NLS* expression was patterned along the clonal boundaries (Fig.3.33 G to I and M to O, marked with arrowhead), possibly reflecting age dependent regulation of boundary formation.

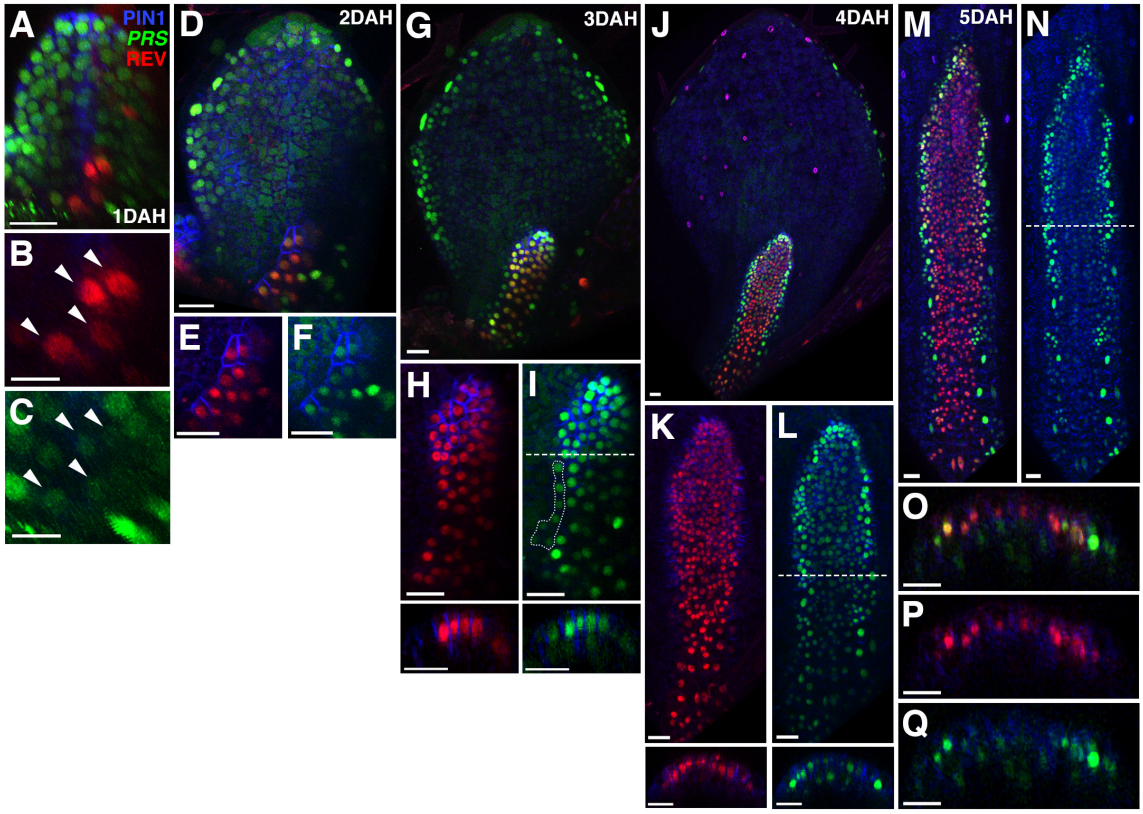

Figure 3.32 Up-regulation of pPRS::tdTomato-NLS by REVr-YPet* in leaves.

(A to C) Confocal projections showing REVr-YPet* (red) induction in the cells with very weak *pPRS::tdTomato-NLS* (green) expression on the ventral side of the leaf at 1DAH (arrowheads in B and C). **(D to I)** Later time-points show up-regulation of PIN1-GFP (blue) and *pPRS::tdTomato-NLS* (green) within the clone at 2DAH (D to F), which is maintained at 3DAH (G to I). Magnified views of the clone with separated channels are showed in (E to F) for 2DAH and (H to I) for 3DAH. **(J to Q)** *pPRS::tdTomato-NLS* signal starts to decrease from the epidermis within the clone at 4DAH (J to L) but is maintained in the sub-epidermis (cross section shown in L) and along the boundaries of the clone at 5DAH (M to Q). Cross sections corresponding to the dashed line in (N) are showed in (O to Q) with different channels. **Note**: compare the magnified view together with the cross sections of the clone (I, L, N and Q) to

observe the graduate change of *pPRS::tdTomato-NLS* expression during outgrowth formation. Scale bars represent 10 µm in (B) and (C); 20 µM in (A) and (D) to (Q).

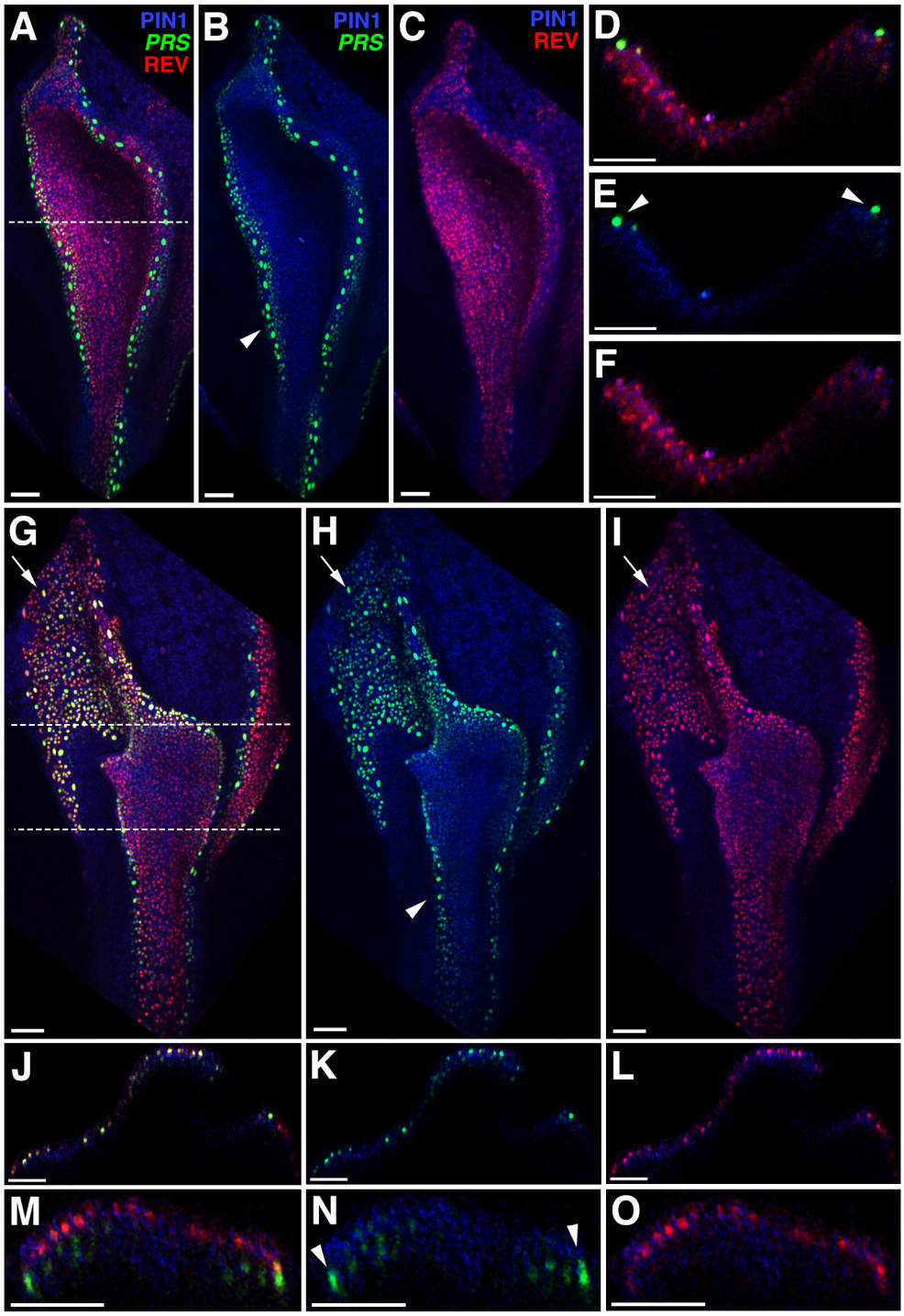

Figure 3.33 The response of pPRS::tdTomato-NLS to REVr-YPet* clones depends on position along the proximdistal axis.

(A to F) Confocal projection and cross sections correspond to the dashed line in (A) showing *pPRS::tdTomato-NLS* (green) expression along the margin of the REVr-YPet* (red) expressing clones. **(G to I)** At the distal part of the leaf, *PRSp::tdTomato-NLS* expression

completely overlaps with REVr-YPet* (marked with arrow), while in the proximal tissues, expression is restricted to the boundaries of REVr-YPet* clones (indicated by arrowhead). **(J to O)** Cross sections correspond to the dashed line across the distal (J to L) and proximal (M to O) regions of the leaf, respectively. Arrowheads in (B, E, H and N) show the clonal boundaries of *PRSp::tdTomato-NLS* (green) expression. Bars = 50μM.

These results indicate that *PRSp::tdTomato-NLS,* like PIN1 and TAA1, is initially expressed within and outside REVr-YPet* expressing clones and only later becomes restricted to the clonal boundaries. However it should be noted that the expression pattern of PRS-2xGFP and *PRSp::tdTomato-NLS* appear different at the early stages of leaf development. The expression of PRS-2×GFP is more restricted to the leaf margin early on at 3.5 DAS, while *PRSp::tdTomato-NLS* expression is still present throughout the leaf (Fig.3.30 D and F). However this could be due to perdurance of the tdTomato-NLS reporter. To investigate this properly, a translational fusion reporter for PRS should be used together with the induction of REV clones. Furthermore in this experiment, I also observed non-cell autonomous up-regulation of *PRSp::tdTomato-NLS* at 3DAH (Fig.3.32 I, irregular dotted line) while later on, the marginal expression of *PRSp::tdTomato-NLS* always appeared to overlap with very weak signal in the REVr-YPet* channel. However this weak signal was possibly due to cross talk between YPet and tdTomato channels, since the tdTomao signal was very strong. This should be clarified in the future.

So far, with respect to the genes that are associated with D-V boundaries that I examined, including PIN1, TAA1, WOX1 and PRS, all were induced in response to juxtaposition of REV expression in ventral tissues. All were initially up-regulated within the clone but over time, became restricted to the boundaries. However their exact boundary expression pattern varied, often along with the variable morphology of the associated ectopic outgrowths. For example when these genes were only up-regulated cell autonomously within REVr-YPet* expressing clones (Fig. 3.14, Fig 3.23 A to D and Fig. 3.28), growth always occurred within the clone which resulted in the formation of a bump. The failure of these genes to be up-regulated outside the clone might be the reason why a lamina morphology did not develop. As described in section 3.4.2, lamina-like development possibly depends on the presence of “gap” cells (without D-V gene expression) between the REV and KAN expression domains. Since it has been reported that KAN1 represses PIN1, TAA1 and perhaps also WOX

genes (Brandt et al., 2012; Huang et al., 2014; Merelo et al., 2013; Nakata et al., 2012), I suspect that the failure of these genes to be up-regulated beyond the clone in many experiments might be due to the presence of KAN expression in the cells directly adjacent to REV expressing clones. Further experiments that include the monitoring these boundary-associated genes together with the KAN1 reporter will be essential to test this hypothesis.

3.6 Induction of KAN1 expressing clones on the dorsal side of the leaf.

As described above, juxtaposition of DV genes generated by induction of REVr-YPet* clones on the ventral side of the leaf is sufficient for outgrowth formation. During outgrowth development, initially REV acts positively to upregulate boundary-associated gene expression both cell and non-cell autonomously and later to repress these genes cell autonomously to restrict further growth to the clonal boundaries. Meanwhile, during this process, the role of KAN was to repress the expression of boundary-associated genes. Therefore, it's of interest to test whether juxtaposition-dependent growth also occurs after inducing KAN1 expressing clones on the dorsal side of the leaf and furthermore and to test whether boundary-associated genes are up-regulated initially within KAN1 clones as they are in REV clones.

For this purpose, I again used the same strategy to induce KAN1-GFP expressing clones within leaf tissues by using the heatshock promoter to drive CRE-GR (*HSp::CREGR_35S::lox-spacer-lox-KAN1-GFP*). In contrast to REVr-YPet* expressing clones, induction of KAN1-GFP clones on the dorsal side of the leaf at 3 DAS by heat shock resulted in a very mild phenotype in the first pair of leaves (Fig. 3.34 B and C). Further live-imaging analysis revealed that down-regulation of REV-2×YPet by KAN1-GFP occurred only gradually during leaf development (Fig. 3.35). This slow down-regulation of REV by KAN1 may be due to low expression levels of the induced KAN1-GFP. I next tried to induce KAN1-GFP clones at different stages after stratification from 1DAS to 7DAS. Interestingly, it was found that seedlings that were heatshocked at 5DAS, 6DAS and 7DAS, developed some outgrowths on leaves numbered 4^{th} to the 7^{th} after germination (Fig. 3.34 D and E), indicating that the KAN1 sector was possibly induced just before or at the time when these leaves were being initiated. However, the outgrowths occurred at a very low frequency (not

directly quantified) and occasionally some plants appeared smaller and yellowish. Very preliminary imaging data of the 5th leaf from plants with KAN1-GFP expression clones induced at 7DAS, showed that PIN1-CFP expression was up-regulated at the boundary between REV-2×YPet and KAN1-GFP expression (Fig. 3.36 A to D and G1 to H4, arrowheads in B and D). Although REV-2×YPet expression still overlapped with KAN1-GFP expression on the left side of the leaf (Fig. 3.36 A), in the region adjacent to PIN1-CFP expression, REV- 2×YPet expression was hardly detected within the KAN1-GFP clones (Fig. 3.36 B and D, indicated by arrowheads, G_2-G_3, H_2 to H_3), which suggests that turning off REV is necessary for up-regulation of PIN1 at the boundaries. Finally, a protrusion formed at the location with high PIN1-CFP expression (Fig.3.36 C to F).

Figure 3.34 Leaf phenotype when KAN1-GFP expressing clones are induced on the dorsal side of the leaf.

(A) Dorsal side view of a leaf from a fourteen-day-old WT seedling. **(B and C)** Phenotypes of the first pair of leaves after induction of KAN1-GFP expressing clones at 3DAS. **(D and E)** Phenotypes of the 5th leaf (D) or 6th leaf (E) when KAN1-GFP clones are induced at 7 DAS, arrowheads in (D) and (E) showing the region with outgrowth.

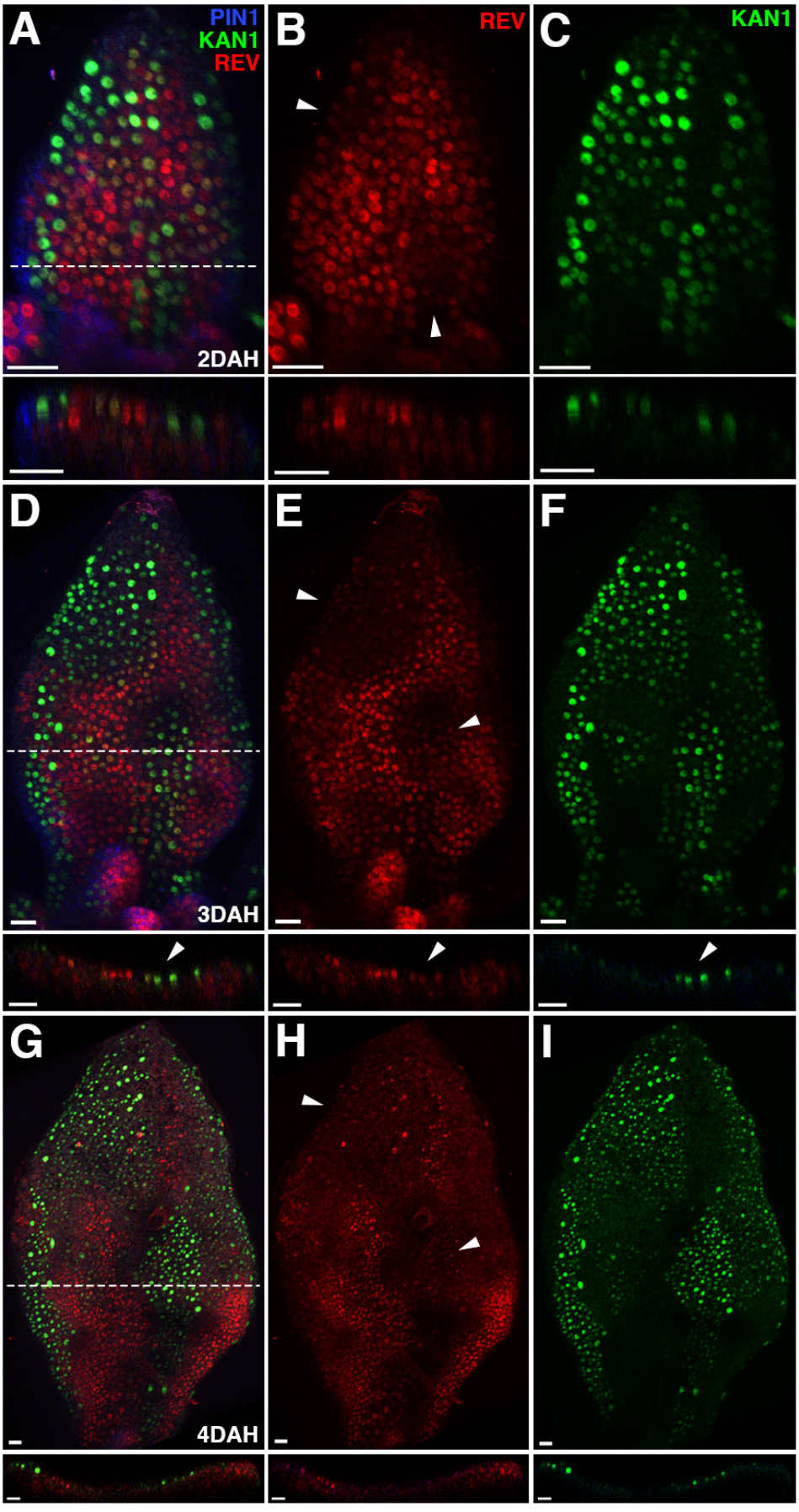
A
PIN1
KAN1
REV
2DAH
B
REV
C
KAN1
D
3DAH
E
F
G
4DAH
H
I

Figure 3.35 Down-regulation of REV by KAN1-GFP clones occurs gradually on the dorsal side of the leaf.

(A to I) Confocal projections and cross sections of one of the first pair of leaves showing REV-2×YPet (red) is down-regulated only gradually by induction of KAN1-GFP (green) expression from 2DAH (A to C) till 4DAH (G to I). Arrowheads in (B), (E) and (H) indicate the region where REV-2×YPet is down-regulated by KAN1. Bar = 20 µm.

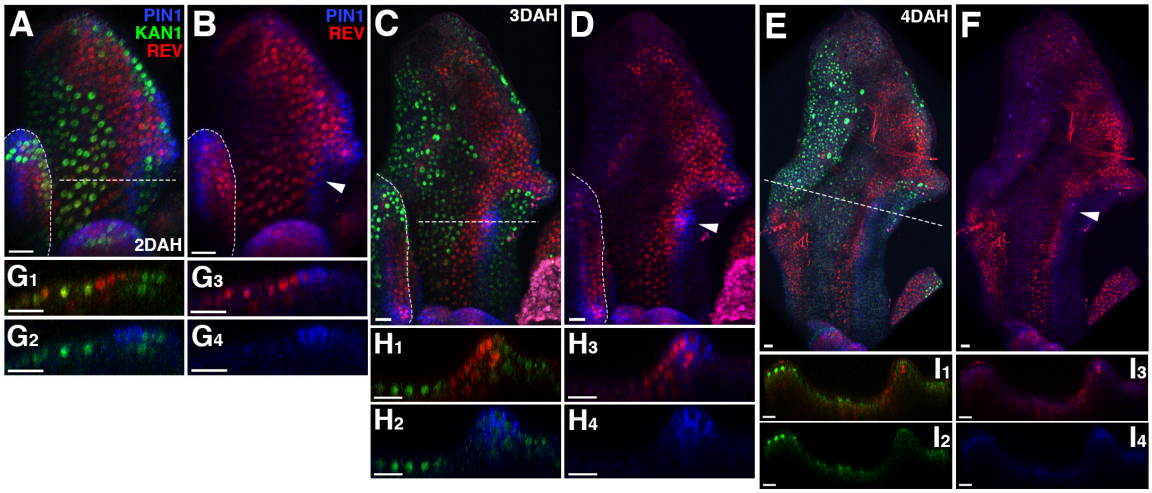

Figure 3.36 PIN1 is up-regulated at the boundary of the REV and KAN1 expression domains.

(A and F) Time-lapse projections of the 5th leaf showing up-regulation of PIN1-CFP (blue) occurring at the boundary of REV-2×YPet (red) and KAN1-GFP expression (green), indicated by the arrowheads. **(G to I)** Cross sections corresponding to the dashed lines shown in (A), (C) and (E), respectively. Dotted lines on the bottom left in (A to D) show the 7th leaf instead of part of the 5th leaf. Bar = 20 µm.

Taken together, these data indicate that juxtaposition dependent growth also occurs after induction of KAN1-GFP clones on the dorsal side of the leaf, but depends on the complete down-regulation of REV within the KAN1 clones. However, the frequency of growth and laminar development in response to such clone is very low. One reason for the low frequency and speed of response could be the absence of ETT and ARF4 in dorsal tissues. These factors are known to physically interact with KAN1 and are necessary for KAN function (Pekker et al., 2005). Since it has been reported that *ARF3/ETT* and *ARF4* are targets of ta-siRNAs, which are in turn dependent on AGO7 (Allen et al., 2005; Hunter et al., 2006; Williams et al., 2005), further experiments inducing KAN1 clones in an ago7 mutant background may lead to more dramatic responses.

3.7 Summary

Previous observations from the Heisler lab indicate that in the SAM, organ positions are centered on a region of cells located between centrally expressed REV and peripherally expressed KAN1, indicating a possible causal relationship between dorsal-ventral patterning in the SAM and organ positioning and subsequent development. My imaging and perturbation experiments (in collaboration with Dr. Monica Pia Caggiano) show that disruption of D-V patterning in the SAM not only influences leaf initiation, but also leaf dorsoventrality and subsequent morphogenesis. Taken together, these results strongly support a model in which genes involved in promoting dorsal or ventral cell fate also function to repress auxin signaling and therefore that dorsoventral boundaries pattern morphogenesis due to the presence of cells located at these boundaries in which neither Class HD-ZIP or KAN genes are expressed.

To test this model and investigate juxtaposition dependent morphogenesis in general, I analyzed mosaic plants in which clones of cells expressing REV were induced and followed by live-imaging in ventral leaf tissues. I found that although direct juxtaposition of Class III HD-ZIPs and KANADI gene expression was sufficient to induce ectopic outgrowth at clonal boundaries, lamina growth in particular correlated with the presence of "gap" cells located between the REV clones and cells expressing KAN1, supporting the model described above that depends on local "de-repression" of auxin response by the local absence of D-V gene activity. However my experiments also revealed that REV clones act non-cell autonomously to promote boundary gene expression even when no "gap" happens to be present between the REV and KAN expression domains. This suggests a more complex model based not only on cell autonomous repression of auxin activity by D-V genes but also on non-cell autonomous activation of auxin activity by REV expressing cells.

Chapter 4 Discussion and future plans

A fundamental question in plant development is how leaves are positioned and obtain a laminar shape. In this thesis I have addressed these questions by focusing on the role genes expressed along the leaf dorsal-ventral (adaxial-abaxial) axis. In animals, cells located in boundary regions between cell types often act as long-range organizers of tissue patterning (Dahmann et al., 2011; Lawrence and Struhl, 1996; Meinhardt, 1983). Strikingly, my results support the proposal that a similar tissue patterning strategy seems to be utilized in plants (Waites and Hudson, 1995), despite multicellularity in plants having involved independently. In the sections below, I will discuss my findings in detail.

4.1 Dorsoventrality of the leaves corresponds to a pre-pattern in the SAM.

The question of how leaf dorsoventrality is initially established has long interested plant biologists. Early microsurgical experiments by Ian Sussex suggested that a meristem-derived signal is required for the specification of dorsal cell fate, although the nature of this signal is still uncertain. So far, several potential candidates for "the Sussex signal" have been proposed and the relevance of these candidates may vary between species. For instance, tasiR-ARFs are candidates in maize and rice, whereas, auxin is proposed as a "reverse Sussex signal" in *Arabidopsis* and tomato. Furthermore, a lipophilic molecule is considered as an attractive candidate based on its potential to bind the START domain of Class III HD-ZIPs (reviewed by (Kuhlemeier and Timmermans, 2016)). Recent genetic studies have revealed a large number of genes that contribute to leaf dorsoventrality and most of these genes are expressed in a polar fashion within leaves. As leaves form at the periphery of the meristem, Dr. Monica Pia Caggiano decided to investigate the establishment of dorsoventral patterning by examining how genes involved in this process are patterned within the meristem. Monica found that dorsoventral gene expression patterns within developing leaves could be traced directly back to concentric patterns of gene expression within the shoot. Specifically, expression and polarity of the auxin

efflux carrier PIN1 marked the initiation of new organs within a narrow region of cells located between the expression domains of key factors such as REV, KAN1 and *MIR165/166* (Caggiano, Monica Pia 2013). Furthermore, as organs start to grow, *KAN1* expression was found to remain in the same cells or their progeny, indicating that ventral gene expression is incorporated into developing organs directly from precursor tissues (Caggiano, Monica Pia 2013).

4.2 An instructive role for D-V boundary in the shoot apical meristem (SAM)

Although previous experiments by Monica revealed a distinct correlation between organ positioning and patterns of REV and KAN1 expression, the question of whether this correlation represents a causal relationship was only partially addressed by her subsequent experiments involving global perturbations of REV and KAN expression. To show that boundaries between REV and KAN expression domains play an instructive role in positioning new leaves and determining their subsequent patterns of morphogenesis I reversed the orientation of the REV/KAN boundary by inducing the expression KAN1 centrally within the meristem using the *CLV3* promoter. I found that this not only altered the orientation and morphology of newly developing organs but also their position, which correlated with the new boundary of KAN expression that I had induced. Hence these findings not only demonstrate that leaf orientation is defined by the polarity of D-V gene expression domains within the meristem but also, that D-V boundaries play a specific role in organ positioning.

These findings also suggest a simple model to account for how D-V genes pattern morphogenesis. As localized auxin signaling via MONOPTEROS polarizes surrounding cells and induces organ growth (Bhatia et al. 2016) it should be sufficient to account for DV boundary function in organ positioning if DV boundaries simply acted to restrict or localize MP-induced signaling. Considering the observation that PIN1 localizes its expression and polarity initially between the REV and KAN expression domains, and, that ectopic REV or KAN expression blocks organ formation (Caggiano, Monica Pia, 2013), it seems likely that localized auxin signaling is achieved via cell autonomous repression of signaling by REV and KAN combined with the specific creation of a boundary domain that lacks REV and KAN expression. Furthermore, such a restriction of auxin signaling may not only account for organ

positioning in the SAM periphery but also the way in which D-V boundaries are thought to pattern leaf morphogenesis, as discussed further towards the end of this discussion.

4.3 Juxtaposition-dependent growth

Boundary localized organizers have been found to play essential roles in tissue patterning during the development in both insects and vertebrates. A hallmark of these organizers is juxtaposition dependent growth. Specifically, when two distinct cell types are juxtaposed, a developmental program is induced that can trigger the formation of ectopic organs (Diaz-Benjumea and Cohen, 1993; Tanaka et al., 1997). Strikingly, my mosaic experiments with induction of REVr-YPet* expressing clones on the ventral side of leaves demonstrate a similar phenomenon, in which ectopic leaf lamina are often induced. This observation confirms the proposal by Waites and Hudson over twenty years ago that juxtaposition of dorsal and ventral cell types may not only be required for lamina development but also sufficient to trigger *de novo* outgrowth formation (Waites and Hudson, 1995). Most importantly, these experiments provide critical insights into how these boundaries actually control plant tissue growth.

4.3.1 Down-regulation of KAN1 is essential for juxtaposition-dependent lamina growth

My mosaic data reveal that upon the induction of REVr-YPet* expressing clones, several phases of response can be distinguished. E.g.

1. KAN1 is downregulated by REV cell-autonomously.
2. D-V boundary-associated genes including PIN1, TAA1, WOX1 and PRS are up-regulated both within and outside the clone, although the up-regulation outside the clone varies.
3. Over time, the expression of boundary genes becomes restricted to cells beyond the clone but adjacent to REV expressing cells.

4. Accompanying step 3, lamina-like ridges sometimes formed along the clonal boundaries or alternatively growth was more centered on the clone resulting in more of a "bump" forming.

In regard to the variation in outgrowth morphology, the presence of KAN1 directly adjacent to REV expression cells always resulted in the formation of less defined bumps located centrally on REV expressing cells rather than a lamina shaped outgrowths centred at the clone boundary. In contrast, the occurrence of "gap" cells (without REV and KAN1 expression) adjacent to REV clones, due to the stochastic disappearance of KAN1 expression, was often associated with higher expression levels of PIN1 and more lamina-like growth. Furthermore, I also suspect that the failure of boundary-associated genes to be up-regulated beyond the clone in many experiments is due to the presence of KAN expression in these cells, especially since it has been reported that KAN1 represses PIN1, TAA1 and the WOX genes (Brandt et al., 2012; Huang et al., 2014; Merelo et al., 2013; Nakata et al., 2012).

To further understand the functional significance of step 1 above, involving down-regulation of KAN1, I tried two variations of the clone induction experiment. The first was to induce REV clones in plants constitutively expressing KAN1 in the epidermis while the second was to induce REV clones in *kan1kan2* mutants. Through these experiments I found that KAN1 in epidermal cells expressing REV could completely block REV in terms of having any influence at all on morphogenesis. This implies that REV and KAN compete for some of the same target genes and regulate them in an opposite manner, as also indicated by previous target gene analyses (Brandt et al., 2012; Huang et al., 2014; Reinhart et al., 2013).

Interestingly, when REV clones were induced in the *kan1kan2* mutant, the most obvious phenotype was repression of growth and PIN1 expression. In contrast to these experiments in the wild type background, no obvious positive regulation of PIN1 or growth was noted. There are two possible explanations for this. Firstly, the positive regulation of growth and PIN1 expression seen in the wild type could be the result of inhibition of KAN function. Thus *kan1kan2* would be expected to be epistatic to the positive influence of REV clones on growth and boundary gene induction. This is consistent with the cell-autonomous down-regulation of KAN1 by REV and in fact may also explain the non-cell autonomous regulation of PIN1 by REV, as discussed

further below. The other alternative is that the positive role of REV in promoting growth and PIN1 expression is already being carried out by endogenous Class III HD-ZIP expression non-cell autonomously in the *kan1kan2* mutant. This is supported by the finding that REV is expressed within *kan1kan2* ventral sub-epidermal cells adjacent to the ventral epidermis where PIN1 is ectopically expressed and outgrowths occur. My experiments with REV clones in the wild type indicate that such localized expression would be expected to up-regulate PIN1 in the epidermis regardless of whether KAN1 is present there or not (see Fig 3.13 L to O). Hence the ectopic outgrowth and PIN1 expression associated with *kan1kan2* mutant leaves may entirely be due to miss-regulation of the Class III HD-ZIPs. Testing this hypothesis will require an in-depth evaluation of Class III HD-ZIP function in contributing to the *kan1kan2* phenotype.

4.3.2 The establishment of boundaries between dorsal and ventral cell types

As described above, one interesting observation I noted was that induction of REV clones in the sub-epidermal layer can up-regulate PIN1 expression in the epidermis where KAN1 is co-expressed. Also, low levels of PIN1 expression can often be detected in KAN1 expressing cells directly adjacent to epidermal REV clones. Since KAN1 is known to directly repress PIN1 (Merelo et al., 2013), these observations suggest that KAN1 function may be blocked by REV non-cell autonomously. If true, this could also account for induction of other boundary markers outside REV clones including PRS, WOX and TAA1 since these are all KAN targets also (Brandt et al., 2012; Huang et al., 2014; Nakata et al., 2012).

In opposition to this proposal is the observation that when KAN1 expression was made constitutive throughout the epidermal layer, the induction of PIN1 by REVr-YPet* was inhibited (see Fig. 3.16 and Fig. 3.17). However possibly this difference may be due to the stronger expression level of KAN1 driven by the two-component system under the control of the ML1 promoter compared to that driven by its endogenous promoter.

What could mediate non-cell autonomous inhibition of KAN1 by REV? What possible short-range signal could be produced by REV expressing cells that can

diffuse to block or out compete KAN1 activity? In addition, how could a "gap" region (a region without REV and KAN1 expression) in wild type leaves be generated? Below I propose hypotheses to address these questions and suggest experiments to further test them.

4.3.2.1 Auxin- a potential short-range signal from the dorsal side

As shown from my mosaic experiments, boundary-associated genes such as PIN1, TAA1, WOX1 and PRS are upregulated both cell and non-cell autonomously upon the induction of REV clones. At least for PIN1, this occurs even in the presence of KAN1 co-expression. Growth also appears to be triggered by REV expressing clones in a non-cell autonomous manner. The plant hormone auxin is an obvious candidate signal that could be produced by REV expressing cells to achieve at least some of this signalling. For instance PIN1 expression is known to be upregulated by auxin (Heisler et al., 2005). In addition, preliminary data from the Heisler lab also shows that PRS expression can be up-regulated by auxin (WOX1 hasn't been tested yet but it seems likely), indicating that boundary genes in general may all be induced by auxin. Although KAN1 is known to repress these genes, including PIN1 (Brandt et al., 2012; Huang et al., 2014; Merelo et al., 2013) and WOX1/PRS (Nakata et al., 2012), high levels of auxin adjacent to REV clones may potentially overcome this repression - hence giving rise to localized boundary gene expression adjacent to the clones where auxin concentrations may be highest. Consistent with the proposal, my results demonstrate that REV expression is sufficient to induce expression of the auxin synthesis enzyme TAA1 ectopically and it has been reported that REV regulates both *YUC5* and *TAA1* directly (Brandt et al., 2012). To account for the absence of boundary-gene expression within REV clones, this hypothesis needs to also incorporate the assumption that over time, REV activity also represses auxin signalling cell autonomously, similarly to KAN.

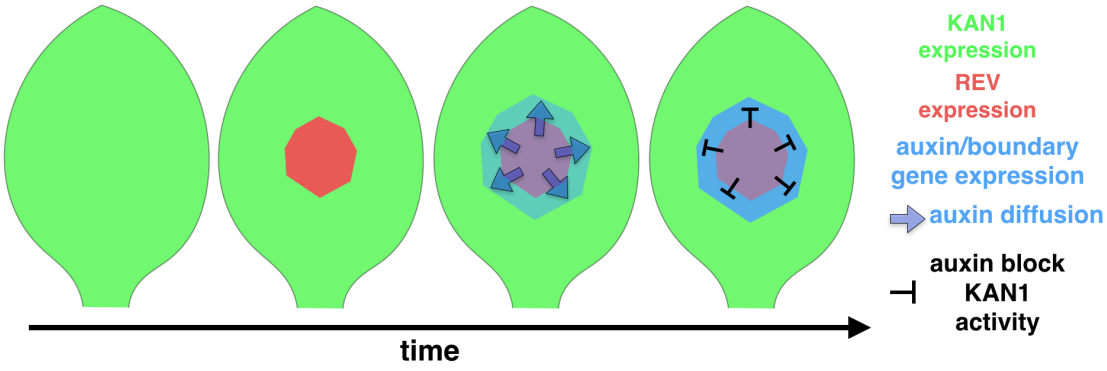

Figure 4.1 Auxin as a putative short-range signal.

Schematic drawing showing how the onset of REV could induce auxin production that promotes boundary gene expressing by diffusing outside the clone. Overtime REV also is assumed to represses auxin signaling cell autonomously. At the clonal boundary auxin may potentially overcome the repression of target genes by KAN, giving rise to localized boundary gene expression adjacent to the clones where auxin concentrations are highest.

A relatively simple test of this hypothesis would be to monitor auxin levels spatially using the ratio-metric intracellular auxin sensor R2D2 (Liao et al., 2015). The above proposal would predict that auxin concentrations should be highest within the clones but also be relatively high in cells immediately adjacent to them.

4.3.2.2 The role of tasiR-ARFs in boundary specification.

Rather than overcoming or out-competing KAN mediated repression via auxin itself, REV clones may produce short-range signals that upregulate auxin signalling by blocking KAN function. It is now well known that small, mobile RNAs called tasiR-ARFs are produced in dorsal tissues, which appear to form a gradient of activity that decreases toward the dorsal side (Chitwood et al., 2009). As elaborated in Chapter 1, these small RNAs act to repress expression of ETT/ARF4 (Chitwood et al., 2009). Since KAN function requires ETT/ARF4 activity, these tasiR-ARFs also seem ideal candidates for short range signals, produced by REV expressing cells, which may promote auxin signalling locally to promote boundary gene expression.

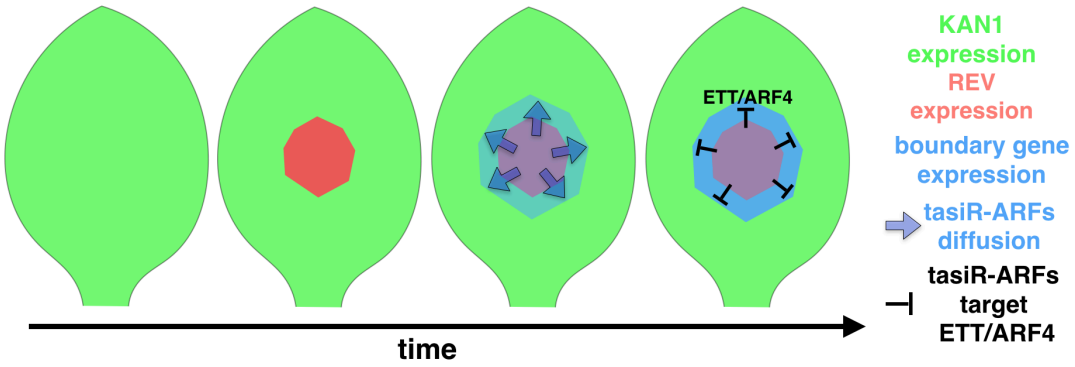

Figure 4.2 tasiR-ARFs as a diffused signal for boundary specification.

Schematic drawing shows that tasiR-ARFs are produced within REV expression clones that act as a mobile signal to repress the expression of ETT/ARF4, such that blocking KAN1 activity. As a consequence, boundary genes are up-regulated by the removal of KAN1 repression.

To test whether tasiR-ARFs are indeed produced upon the induction of REV, one would need to monitor a tasiR-ARF biosensor as well as *ETT* expression in response to REVr-YPet* clone induction. In this case, if the tasiR-ARFs are produced, I would predict that a sensor or ETT expression should be downregulated at a distance from the REV clones. To further investigate the relevance of the tasiR-ARFs, REVr-YPet* expressing clones could be induced in the *ago7* mutant, in which tasiR-ARFs production is defective (Hunter et al., 2006) and PIN1 or PRS monitored to assess whether these genes are still induced non-cell autonomously or not. As in the auxin production hypothesis above, this model also assumes that auxin response is gradually blocked in REV expressing cells, as it is in KAN expressing cells but that this repression does not require ETT/ARF4.

4.3.2.3 The role of miR165/166 in boundary specification.

As mentioned above, my mosaic experiments indicate that stronger PIN1 expression is present in regions where there is a gap between REV and KAN expressing cells (see Fig 3.12 J insertion). Furthermore, in such cases growth is more lamina-like. These observations indicate that in addition to any non-cell autonomous inhibition of KAN1 function or local auxin production by REV clones, the absence of both Class III HD-ZIP and KAN gene activities in boundary regions contributes substantially to boundary function. Other evidence supporting this proposal includes the observation

that at least PIN1 and TAA1 respond to REV clones in a dose-dependent manner (PRS and WOX were not adequately investigated to make any conclusions in terms of their dose dependent response). For instance, when adjacent clones express REV at different levels (presumably due to differences in the number of transgene copies knocked in), both PIN1 and TAA1 are consistently more highly expressed in the clones where REV expression is lower. Hence during normal development, these genes are expected to be expressed most highly in boundary regions where REV expression is relatively low.

How could a gap between KAN1 and REV expression be formed during normal development? As the Class III HD-ZIPs are regulated by miR165/166 and miR165/166 are known to be mobile signals (Carlsbecker et al., 2010), I propose that miR165/166 likely acts from the ventral side to down-regulate REV in cells adjacent to KAN. To test this proposal, one possible strategy would be to try to substitute miR165/166 sensitive REV for insensitive REV in our sectoring experiments. If driven by a strong enough promoter it may be possible to switch fates despite repression of REV by miR165/166. The finding that REV directly represses miR165/166 (Merelo et al., 2016) further suggests that a cell fate switch may be possible. If this worked, then as the clone grows, a gradient of REV expression may form in response to miR165/166 expression outside the clone in contrast to my current experiments with miR165/166 resistant REV. The prediction from this hypothesis would be that boundary genes become induced in the cells towards the clone edge where a gap may have formed. An alternative approach would be to use Cre-lox to knock in miR165/166 in dorsal tissues. Since miR165/166 moves cell-to-cell, we would expect a gradient of REV expression to form (in an opposite orientation with respect to the clone compared to the previous experiment) and as a result, induction of boundary-associated genes may occur again in the predicted "gap". Lastly, if miR166 is directly induced by KAN1 as previously reported (Merelo et al., 2013), induction of KAN1 expressing clones on the dorsal side of the leaf could possibly have a similar effect. Although my data indicate that induction of KAN1-GFP clones on the dorsal side of the leaf triggers outgrowth only very rarely, this frequency would be predicted to increase if ETT/ARF4 were also present in dorsal tissues, such as in *ago7* mutants. Hence it would be a good idea to try to induce KAN1 expressing clones in an *ago7* mutant background. By monitoring a

miR165/166 reporter together with REV expression, we would be able to assess whether miR165/166 might act as a short-range signal downstream of KAN1 to create a local absence of both REV and KAN expression.

Taken together, an attractive hypothesis is that the initial formation of D-V boundaries involves short-range signals corresponding to both miR165/166 and tasiR-ARFs. In particular, the activity of miR165/166 might be to create a region with low or a complete absence of Class III HD-ZIP expression, while the activity of tasiR-ARFs may act to enhance boundary function by blocking KAN function locally via regulation of ETT/ARF4. Notably, I suspect that miR165/166 is more important in this process since the knock down of miR165/166 activity by STTM from our work and others results in a complete loss of laminar development, which resembles a HD-ZIP III overexpression phenotype (Yan et al., 2012). In contrast, mutants defective in tasiR-ARF production show no strong leaf polarity changes, possibly indicating that miR165/166 activity may fully compensate in maintaining boundary function. A final test of the importance of both miR165/166 and tasiR-ARFs in juxtaposition dependent lamina development, would be to disrupt both of them by inducing KAN1 expressing clones in an *ago7* mutant together with miR165/166 resistant REV driven by its endogenous promoter. The prediction would be that no outgrowth or PIN1 induction occurs in contrast to a similar experiment with miR165/166 sensitive REV.

4.3.3 How dorsal-ventral boundaries organize morphogenesis

4.3.3.1 D-V boundaries act to localize auxin response

Regardless of the underlying mechanisms, there are several lines of evidence indicating that D-V boundaries act generally to localize auxin response. When auxin is applied to *pin1* mutant or NPA pins, localized growth only occurs at a fixed position (corresponding to a D-V boundary) no matter where auxin is applied (Reinhardt et al., 2000; 2003). Also, KAN1 is known to repress auxin associated genes including PIN1 (Brandt et al., 2012; Huang et al., 2014; Merelo et al., 2013), indicating a role of KAN1 in repression auxin-induced growth. Although there is no direct evidence from the literature that REV represses auxin response, our data indicate such a role. Firstly, data from Dr. Monica Pia Caggiano shows that auxin-induced organ formation is completely blocked when miR165/166 resistant REV is

induced throughout the L1 during either the vegetative or reproductive stage (Caggiano, Monica Pia 2013), similar to that of overexpression of KAN1. Secondly, my mosaic data in both wild type and *kan1kan2* double mutant plants indicate a gradual repression of auxin associated boundary genes by REV. Although initially PIN1 is up-regulated in REV expressing cells, this expression is ultimately repressed cell-autonomously by REV such that PIN1 is localized adjacent to the clone. Growth in response to REV clones follows a similar pattern. This is perhaps most obvious when REV is expressed at high levels within ventral clones in the *kan12* mutant, where PIN1 expression is switched off completely within the clones in contrast to the surrounding cells (Fig. 3.20 C and E). Lastly, during wild type leaf development, auxin response marked by *DR5v2* reporter is also localized at D-V boundaries along the margin of the leaf (Liao et al., 2015). Below I discuss how such a localized auxin response might relate to long-range signalling and lamina formation.

4.3.3.2 How do D-V boundaries organize surrounding tissues?

So far, I have discussed evidence that dorsal-ventral boundaries localize auxin signalling. How does this relate to the role of the boundary in organizing growth of the surrounding tissues?

Recently, work from Neha Bhatia in the Heisler lab (Bhatia et al., 2016) has demonstrated that localized auxin signaling, via the auxin response factor MONOPTEROS (MP) or ARF5, not only promotes localized growth but also orients cell polarity non-cell autonomously. This polarity influence involves both PIN1 polarities as well as microtubule orientations such that polarity is directed towards cells with high auxin signaling. Hence this relationship promotes a positive feedback loop between auxin concentrations and polar auxin transport via auxin-regulated transcription and is expected to also orient growth directions towards high auxin signaling regions via non-cell autonomous control over interphase microtubule cytoskeletons (Bhatia et al., 2016).

Therefore, a plausible hypothesis is that dorsal-ventral boundaries regulate morphogenesis and long-range patterning through this influence of localizing auxin signaling, i.e. in effect creating restricted zones of MP or auxin induced signaling that then not only promote growth but also orient this growth and potentially lead to

positive feedback that maintains high auxin signaling in boundary regions. At the shoot meristem the circumferential boundary between Class III HD-ZIP and KAN expression would enable the MP-cell polarity feedback loop to create organs periodically within this zone. When this boundary becomes incorporated into developing organs localized auxin signaling could still function similarly by acting to promote growth and by orienting this growth toward the boundary. In Arabidopsis, auxin signaling is not so obviously periodic along leaf margins suggesting that although auxin signaling is high, part of the feedback loop with auxin transport is not functional (Bilsborough et al., 2011). Nevertheless, local auxin signaling would be expected to help orient growth towards the boundary and therefore help promote lamina morphogenesis. In other plant species that produce complex leaves, incorporation of the meristem boundary into leaves would also enable the MP-cell polarity feedback loop to create periodic leaflets. Notably, this process would also involve propagation of the DV boundary from the primary leaf into these leaflets potentiating further rounds of subsequent leaflet formation. In such a way highly complex leaves may result. Despite ever increasing levels of complexity, such leaves would be lamina like because auxin signaling, which orients growth, is always restricted to the boundary.

To directly test this proposal one could test whether localized auxin signaling is sufficient to trigger lamina formation without manipulation of D-V genes. For instance by using heat-shock to induce linear clones of constitutively active MP in *mp* mutant leaves, it could be tested whether this is sufficient to induce ectopoic lamina growth and boundary gene expression. Preliminary results from the Heisler lab look very promising in that ubiquitous induction of constitutively active MP has been found to result in isotropic leaf growth and a loss of final lamina shape, indicating at least that localized auxin signaling is required to restrict leaf growth patterns.

To identify the actual boundary-localized intercellular signal that patterns growth and polarity downstream of auxin signaling, the identification of MP targets that regulate growth and polarity is required. However, based on earlier work (Heisler et al 2010), Bahtia et al (2016) propose that MP influences polarity via changing mechanical stress. Therefore cell wall loosening caused by auxin signalling at the boundary may be what mediates polarization of adjacent cells, including both PIN1 and microtubules.

4.3.3.3 Summary of putative molecular mechanism underling leaf tissue patterning

i) The boundary region between dorsal and ventral cell types is established by the activities of auxin, tasiR-ARFs and miR165/166.

ii) High auxin signalling/activity is restricted at the boundary region by the repression of HD-ZIPIII and KAN gene from both sides of the leaf.

iii) Putative cell wall loosening caused by auxin signalling at the boundary may mediate polarization of adjacent cells, such that oriented growth occurs towards the boundary, thereby promoting lamina morphogenesis.

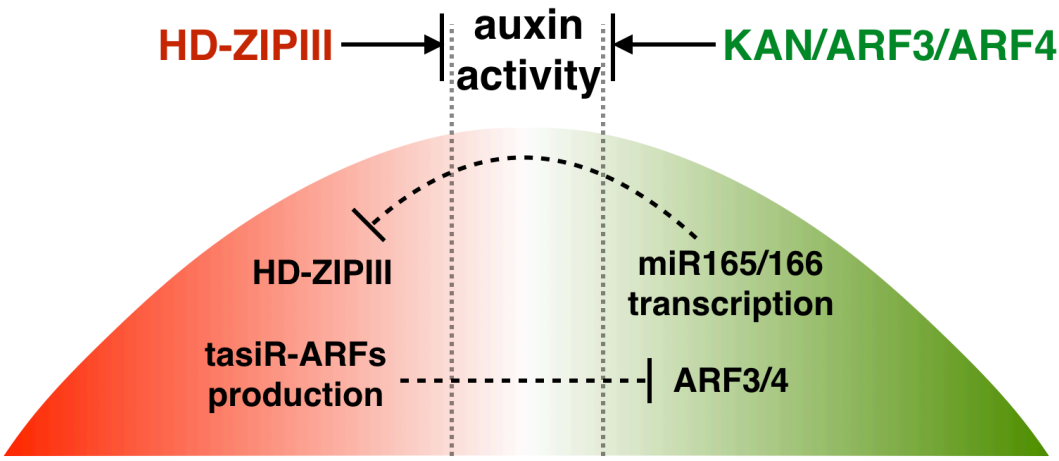

Figure 4.3 Putative molecule mechanism underling leaf development.

Schematic drawing illustrates how the boundary region is established by putative mobile signals and act to localize auxin signalling/activity.

4.3.4 Boundary localized organizers – common feature across Kingdoms

Considering the independent evolution of multicellularity in plants and animals, my results indicate striking similarities and also differences in developmental strategies. In both Kingdoms, cell type boundaries are used as positional signals for generating specialized cells that pattern surrounding tissues. Below I will compare the putative molecular mechanism in plants, based on my work, to the common characteristics of such systems in animals.

Compartment boundaries are established by the activity of selector genes in both invertebrate and vertebrate, which determine cell identity and fate within their expression domains (Dahmann et al., 2011). In the *Drosophila* wing imaginal disc, *engrailed-invected* and *apterous* (*ap*) act as selector genes to specify posterior and dorsal cell fate, respectively (Coleman et al., 1987; Kornberg et al., 1985). While in the vertebrate limb, the expression of the transcription factor *Engrailed1* (*En1*) in the ventral ectoderm is very important for ventral limb patterning (Loomis et al., 1996). Although in plants a larger number of genes/gene families act redundantly in determining the dorsal or ventral cell fate of leaves, some key factors resemble these selector genes. For instance, the expression of HD-ZIPIII genes specify dorsal cell fate in leaves, since gain or loss of function results in cell identity alterations associated with a loss of domain territory (dorsalized or ventralized) (Emery et al., 2003; McConnell and Barton, 1998; McConnell et al., 2001). Therefore, in both Kingdoms, cell autonomous specification of cell identity by selector genes seems to be a common characteristic.

The boundary-localized organizers so far discussed are located at compartment boundaries, i.e. cell lineage restrictions. In the *Drosophila* wing imaginal disk this boundary appears without any obvious morphological features distinguishing it within the epithelial sheet (Blair, 2003). The dorsal-ventral compartment restriction in the vertebrate limb is likely similar to that of the *Drosophila* compartments (Blair, 2003). However, in vertebrate limbs this lineage restriction also occurs within mesenchymal cells which together form a three-dimensional structure, such that the boundary appears as a plane rather than a line (Arques et al., 2007). Unlike these examples, in the SAM of plants, cells cross the boundary between Class III HD-ZIP and KAN expression domains constantly in regions where organs do not get specified. Hence this boundary is certainly not analogous to a compartment boundary in animals in its association with lineage restriction. However whether this is also true within developing leaves is not clear from the literature. Unpublished imaging data from the Heisler lab indicates that while most cells and their progeny retain their initial identity during the early stages of leaf initiation near the D-V boundary, some cells do not. This would suggest that there is a weaker restriction on cell fate based on lineage compared to the situation in animals. Such a conclusion is supported by other cell fate studies in plants that indicate that the clonal restriction of fate mostly arises due to

stereotypic cell division and growth patterns and that cell identity in plants depends more on spatial signals (Bossinger and Smyth, 1996). Hence while my data supports the proposal that Class III HD-ZIP / KAN expression boundaries act as organizers of plant development, these boundaries do not necessarily separate cell lineages.

The establishment of boundaries in animals is dependent on short-range signals such as Hh and Notch signalling. Instead of secreted peptides or cell surface receptors and ligands, I have proposed that small RNAs, e.g. tasiR-ARFs and miR165/166 play a similar role for the establishment of D-V boundary cell types in plants. In fact several cases are known for which small RNAs act as mobile signals in plants (ref), although there is no reason why similar types of molecules could not play a similar role. Therefore, although the molecular mechanisms may be distinct, the strategy for establishing boundary cell types seems to be similar. However, further work is required to validate this proposal.

4.3.4.1 The role of the boundaries

A common feature of the compartments in both invertebrate and vertebrate is the association with signalling centres at the compartment boundaries, which localize long-range signals for tissue patterning (Blair, 2003). In *Drosophila* wing imaginal disc, A-P and D-V boundary cells produces Decapentaplegic (Dpp) and Wingless (Wg), respectively. The secretion of these proteins facilitates their function as morphogens that can diffuse at a long-range to pattern surrounding tissues (Hamaratoglu et al., 2014; Swarup and Verheyen, 2012). Similarly, in the vertebrate limb, fibroblast growth factors (FGFs) are produced by the D-V boundary localized AER, which play an instructive role in limb development (Fallon et al., 1994; Niswander et al., 1993). Among the phytohormones, perhaps auxin is the best potential candidate for a morphogen (Benková et al., 2009), However based on my results, boundary regions act to localized auxin response. Thus I propose that long-range signaling occurs downstream of auxin signaling. In particular I have proposed that cell wall loosening caused by auxin signalling at the boundary may cause the polarization of adjacent cells, such that growth is oriented towards the boundary. Therefore, in the plant case mechanical stress may act as the main signal that acts to pattern leaf morphogenesis rather than a morphogen gradient, although mechanics is

now also thought to play an important role in the development of both the Drosophila wing (Aigouy et al., 2010) and vertebrate limb bud (Lau et al., 2015).

To summarize, although plants evolved independent of animals, my data indicates both Kingdoms utilize the juxtaposition of cell types as a spatial signal to localize organizer activity. The convergent evolution of this developmental strategy may reflect its simplicity and utility as a pattern generator, especially for the formation of flattened, bilaterally symmetric structures since such organizers are often linear.

References

Abley, K., Sauret-Güeto, S., Marée, A.F., Coen, E., and Hardtke, C.S. (2016). Formation of polarity convergences underlying shoot outgrowths. eLife Sciences *5*, e18165.

Ahn, K., Mishina, Y., Hanks, M.C., Behringer, R.R., and Crenshaw, E.B. (2001). BMPR-IA signaling is required for the formation of the apical ectodermal ridge and dorsal-ventral patterning of the limb. Development *128*, 4449–4461.

Aigouy, B., Farhadifar, R., Staple, D.B., Sagner, A., Röper, J.-C., Jülicher, F., and Eaton, S. (2010). Cell Flow Reorients the Axis of Planar Polarity in the Wing Epithelium of Drosophila. Cell *142*, 773–786.

Albert, H., Dale, E.C., Lee, E., and Ow, D.W. (1995). Site-specific integration of DNA into wild-type and mutant lox sites placed in the plant genome. The Plant Journal *7*, 649–659.

Allen, E., Xie, Z., Gustafson, A.M., and Carrington, J.C. (2005). microRNA-Directed Phasing during Trans-Acting siRNA Biogenesis in Plants. Cell *121*, 207–221.

Arques, C.G., Doohan, R., Sharpe, J., and Torres, M. (2007). Cell tracing reveals a dorsoventral lineage restriction plane in the mouse limb bud mesenchyme. Development *134*, 3713–3722.

Benková, E., Ivanchenko, M.G., Friml, J., Shishkova, S., and Dubrovsky, J.G. (2009). A morphogenetic trigger: is there an emerging concept in plant developmental biology? Trends in Plant Science *14*, 189–193.

Benková, E., Michniewicz, M., Sauer, M., Teichmann, T., Seifertová, D., Jürgens, G., and Friml, J. (2003). Local, Efflux-Dependent Auxin Gradients as a Common Module for Plant Organ Formation. Cell *115*, 591–602.

Besnard, F., Refahi, Y., Morin, V., Marteaux, B., Brunoud, G., Chambrier, P., Rozier, F., Mirabet, V., Legrand, J., Lainé, S., et al. (2014). Cytokinin signalling inhibitory fields provide robustness to phyllotaxis. Nature *505*, 417–421.

Bilsborough, G.D., Runions, A., Barkoulas, M., Jenkins, H.W., Hasson, A., Galinha, C., Laufs, P., Hay, A., Prusinkiewicz, P., and Tsiantis, M. (2011). Model for the regulation of Arabidopsis thaliana leaf margin development. Proc. Natl. Acad. Sci. U.S.a. *108*, 3424–3429.

Blair, S.S. (2003). Lineage compartments in Drosophila. Current Biology *13*, R548–R551.

Bossinger, G., and Smyth, D.R. (1996). Initiation patterns of flower and floral organ development in Arabidopsis thaliana. Development *122*, 1093–1102.

Bowman, J.L., and Smyth, D.R. (1999). CRABS CLAW, a gene that regulates carpel and nectary development in Arabidopsis, encodes a novel protein with zinc finger and helix-loop-helix domains. Development *126*, 2387–2396.

Bowman, J.L., and Floyd, S.K. (2008). Patterning and Polarity in Seed Plant Shoots. Annu. Rev. Plant Biol. *59*, 67–88.

Brandt, R., Salla Martret, M., Bou Torrent, J., Musielak, T., Stahl, M., Lanz, C., Ott, F., Schmid, M., Greb, T., Schwarz, M., et al. (2012). Genome-wide binding-site analysis of REVOLUTA reveals a link between leaf patterning and light-mediated growth responses. The Plant Journal *72*, 31–42.

Brocard, J., Feil, R., Chambon, P., and Metzger, D. (1998). A chimeric Cre recombinase inducible by synthetic,but not by natural ligands of the glucocorticoid receptor. Nucl. Acids Res. *26*, 4086–4090.

Brückner, K., Perez, L., Clausen, H., and Cohen, S. (2000). Glycosyltransferase activity of Fringe modulates Notch–Delta interactions. Nature *406*, 411–415.

Byrne, M.E., Barley, R., Curtis, M., Arroyo, J.M., Dunham, M., Hudson, A., and Martienssen, R.A. (2000). Asymmetric leaves1 mediates leaf patterning and stem cell function in Arabidopsis. Nature *408*, 967–971.

Carlsbecker, A., Lee, J.-Y., Roberts, C.J., Dettmer, J., Lehesranta, S., Zhou, J., Lindgren, O., Moreno-Risueno, M.A., Vatén, A., Thitamadee, S., et al. (2010). Cell signalling by microRNA165/6 directs gene dose-dependent root cell fate. Nature *465*, 316–321.

Chapman, E.J., and Carrington, J.C. (2007). Specialization and evolution of endogenous small RNA pathways. Nature Reviews Genetics *8*, 884–896.

Chitwood, D.H., Nogueira, F.T.S., Howell, M.D., Montgomery, T.A., Carrington, J.C., and Timmermans, M.C.P. (2009). Pattern formation via small RNA mobility. Genes Dev. *23*, 549–554.

Clough, S.J., and Bent, A.F. (1998). Floral dip: a simplified method forAgrobacterium-mediated transformation ofArabidopsis thaliana. The Plant Journal *16*, 735–743.

Coleman, K.G., Poole, S.J., Weir, M.P., Soeller, W.C., and Kornberg, T. (1987). The invected gene of Drosophila: sequence analysis and expression studies reveal a close kinship to the engrailed gene. Genes Dev. *1*, 19–28.

Dahmann, C., Oates, A.C., and Brand, M. (2011). Boundary formation and maintenance in tissue development. Nature Reviews Genetics *12*, 43–55.

Dealy, C.N., Roth, A., Ferrari, D., Brown, A.M.C., and Kosher, R.A. (1993). Wnt-5a and Wnt-7a are expressed in the developing chick limb bud in a manner suggesting roles in pattern formation along the proximodistal and dorsoventral axes. Mechanisms of Development *43*, 175–186.

Diaz-Benjumea, F.J., and Cohen, S.M. (1993). Interaction between dorsal and ventral cells in the imaginal disc directs wing development in Drosophila. Cell *75*, 741–752.

Doherty, D., Feger, G., Younger-Shepherd, S., Jan, L.Y., and Jan, Y.N. (1996). Delta is a ventral to dorsal signal complementary to Serrate, another Notch ligand, in Drosophila wing formation. Genes Dev. *10*, 421–434.

Emery, J.F., Floyd, S.K., Alvarez, J., Eshed, Y., Hawker, N.P., Izhaki, A., Baum, S.F., and Bowman, J.L. (2003). Radial Patterning of Arabidopsis Shoots by Class III HD-ZIP and KANADI Genes. Current Biology *13*, 1768–1774.

Eshed, Y., Baum, S.F., Perea, J.V., and Bowman, J.L. (2001). Establishment of polarity in lateral organs of plants. Current Biology *11*, 1251–1260.

Eshed, Y., Izhaki, A., Baum, S.F., Floyd, S.K., and Bowman, J.L. (2004). Asymmetric leaf development and blade expansion in Arabidopsis are mediated by KANADI and YABBY activities. Development *131*, 2997–3006.

Fallon, J.F., Lopez, A., Ros, M.A., Savage, M.P., Olwin, B.B., and Simandl, B.K. (1994). FGF-2: apical ectodermal ridge growth signal for chick limb development. Science *264*, 104–107.

Gaillochet, C., and Lohmann, J.U. (2015). The never-ending story: from pluripotency to plant developmental plasticity. Development *142*, 2237–2249.

Garcia, D., Collier, S.A., Byrne, M.E., and Martienssen, R.A. (2006). Specification of Leaf Polarity in Arabidopsis via the trans-Acting siRNA Pathway. Current Biology *16*, 933–938.

García-Bellido, A., and Santamaría, P. (1972). Developmental analysis of the wing disc in the mutant engrailed of Drosophila melanogaster. Genetics *72*, 87–104.

García-Bellido, A., Ripoll, P., and Morata, G. (1973). Developmental Compartmentalisation of the Wing Disk of Drosophila. Nature *245*, 251–253.

García-Bellido, A., Ripoll, P., and Morata, G. (1976). Developmental compartmentalization in the dorsal mesothoracic disc of Drosophila. Developmental Biology *48*, 132–147.

Gälweiler, L., Guan, C., Müller, A., Wisman, E., Mendgen, K., Yephremov, A., and Palme, K. (1998). Regulation of Polar Auxin Transport by AtPIN1 in Arabidopsis Vascular Tissue. Science *282*, 2226–2230.

Haecker, A., Groß-Hardt, R., Geiges, B., Sarkar, A., Breuninger, H., Herrmann, M., and Laux, T. (2004). Expression dynamics of WOX genes mark cell fate decisions during early embryonic patterning in Arabidopsis thaliana. Development *131*, 657–668.

Hamaratoglu, F., Affolter, M., and Pyrowolakis, G. (2014). Dpp/BMP signaling in flies: From molecules to biology. Seminars in Cell & Developmental Biology *32*, 128–136.

Heisler, M.G., and Ohno, C. (2013). Live-Imaging of the Arabidopsis Inflorescence Meristem. In Plant Developmental Biology, L. Hennig, and C. Köhler, eds. (New York, NY: Springer New York), pp. 431–440.

Heisler, M.G., Ohno, C., Das, P., Sieber, P., Reddy, G.V., Long, J.A., and Meyerowitz, E.M. (2005). Patterns of Auxin Transport and Gene Expression during Primordium Development Revealed by Live Imaging of the Arabidopsis Inflorescence Meristem. Current Biology *15*, 1899–1911.

Huang, T., Harrar, Y., Lin, C., Reinhart, B., Newell, N.R., Talavera-Rauh, F., Hokin, S.A., Barton, M.K., and Kerstetter, R.A. (2014). Arabidopsis KANADI1 acts as a transcriptional repressor by interacting with a specific cis-element and regulates auxin biosynthesis, transport, and signaling in opposition to HD-ZIPIII factors. Plant Cell *26*, 246–262.

Hudson, A. (2005). Plant Meristems: Mobile Mediators of Cell Fate. Current Biology *15*, R803–R805.

Hunter, C., Willmann, M.R., Wu, G., Yoshikawa, M., la Luz Gutiérrez-Nava, de, M., and Poethig, S.R. (2006). Trans-acting siRNA-mediated repression of ETTIN and ARF4 regulates heteroblasty in Arabidopsis. Development *133*, 2973–2981.

Irvine, K.D., and Rauskolb, C. (2001). Boundaries in development: formation and function. Annual Review of Cell and ….

Ishibashi, N., Kanamaru, K., Ueno, Y., Kojima, S., Kobayashi, T., Machida, C., and Machida, Y. (2012). ASYMMETRIC-LEAVES2 and an ortholog of eukaryotic NudC domain proteins repress expression of AUXIN-RESPONSE-FACTOR and class 1 KNOX homeobox genes for development of flat symmetric leaves in Arabidopsis. Biology Open *1*, 197–207.

Iwakawa, H., Ueno, Y., Semiarti, E., Onouchi, H., Kojima, S., Tsukaya, H., Hasebe, M., Soma, T., Ikezaki, M., Machida, C., et al. (2002). The ASYMMETRIC LEAVES2 gene of Arabidopsis thaliana, required for formation of a symmetric flat leaf lamina, encodes a member of a novel family of proteins characterized by cysteine repeats and a leucine zipper. Plant Cell Physiol *43*, 467–478.

Iwasaki, M., Takahashi, H., Iwakawa, H., Nakagawa, A., Ishikawa, T., Tanaka, H., Matsumura, Y., Pekker, I., Eshed, Y., Vial-Pradel, S., et al. (2013). Dual regulation of ETTIN (ARF3) gene expression by AS1-AS2, which maintains the DNA methylation level, is involved in stabilization of leaf adaxial-abaxial partitioning in Arabidopsis. Development *140*, 1958–1969.

Izhaki, A., and Bowman, J.L. (2007). KANADI and Class III HD-Zip Gene Families Regulate Embryo Patterning and Modulate Auxin Flow during Embryogenesis in Arabidopsis. The Plant Cell Online *19*, 495–508.

Jenik, P.D., and Barton, M.K. (2005). Surge and destroy: the role of auxin in plant embryogenesis. Development *132*, 3577–3585.

Kawakami, Y., Capdevila, J., Büscher, D., Itoh, T., Rodríguez-Esteban, C., and Izpisúa Belmonte, J.C. (2001). WNT signals control FGF-dependent limb initiation

and AER induction in the chick embryo. Cell *104*, 891–900.

Kelley, D.R., Arreola, A., Gallagher, T.L., and Gasser, C.S. (2012). ETTIN (ARF3) physically interacts with KANADI proteins to form a functional complex essential for integument development and polarity determination in Arabidopsis. Development *139*, 1105–1109.

Kerstetter, R.A., Bollman, K., Taylor, R.A., Bomblies, K., and Poethig, R.S. (2001). KANADI regulates organ polarity in Arabidopsis. Nature *411*, 706–709.

Kidner, C.A., and Timmermans, M.C.P. (2010). Signaling sides adaxial-abaxial patterning in leaves. Curr. Top. Dev. Biol. *91*, 141–168.

Kiecker, C., and Lumsden, A. (2005). Compartments and their boundaries in vertebrate brain development. Nature Reviews Neuroscience *6*, 553–564.

Kim, J., Irvine, K.D., and Carroll, S.B. (1995). Cell recognition, signal induction, and symmetrical gene activation at the dorsal-ventral boundary of the developing drosophila wing. Cell *82*, 795–802.

Kimmel, R.A., Turnbull, D.H., Blanquet, V., Wurst, W., Loomis, C.A., and Joyner, A.L. (2000). Two lineage boundaries coordinate vertebrate apical ectodermal ridge formation. Genes Dev. *14*, 1377–1389.

Kornberg, T., Sidén, I., O'Farrell, P., and Simon, M. (1985). The engrailed locus of drosophila: In situ localization of transcripts reveals compartment-specific expression. Cell *40*, 45–53.

Kuhlemeier, C., and Timmermans, M.C.P. (2016). The Sussex signal: insights into leaf dorsiventrality. Development *143*, 3230–3237.

Kumaran, M.K., Bowman, J.L., and Sundaresan, V. (2002). YABBY polarity genes mediate the repression of KNOX homeobox genes in Arabidopsis. The Plant Cell Online *14*, 2761–2770.

Lau, K., Tao, H., Liu, H., Wen, J., Sturgeon, K., Sorfazlian, N., Lazic, S., Burrows, J.T.A., Wong, M.D., Li, D., et al. (2015). Anisotropic stress orients remodelling of mammalian limb bud ectoderm. Nature Cell Biology *17*, 569–579.

Laufer, E., Dahn, R., Orozco, O.E., Yeo, C.Y., and Pisenti, J. (1997a). Expression of Radical fringe in limb-bud ectoderm regulates apical ectodermal ridge formation. Nature.

Laufer, E., Dahn, R., Orozco, O.E., Yeo, C.Y., and Pisenti, J. (1997b). Expression of Radical fringe in limb-bud ectoderm regulates apical ectodermal ridge formation. Nature.

Lawrence, P.A., and Struhl, G. (1996). Morphogens, compartments, and pattern: lessons from drosophila? Cell.

Lecuit, T., Brook, W.J., Ng, M., Calleja, M., Sun, H., and Cohen, S.M. (1996). Two distinct mechanisms for long-range patterning by Decapentaplegic in the Drosophila

wing. Nature *381*, 387–393.

Liao, C.-Y., Smet, W., Brunoud, G., Yoshida, S., Vernoux, T., and Weijers, D. (2015). Reporters for sensitive and quantitative measurement of auxin response. Nat Meth *12*, 207–210.

Lin, W.-C., Shuai, B., and Springer, P.S. (2003). The Arabidopsis LATERAL ORGAN BOUNDARIES-domain gene ASYMMETRIC LEAVES2 functions in the repression of KNOX gene expression and in adaxial-abaxial patterning. The Plant Cell Online *15*, 2241–2252.

Loomis, C.A., Harris, E., Michaud, J., Wurst, W., and Hanks, M. (1996). The mouse Engrailed-1 gene and ventral limb patterning. Nature.

Matsuhara, S., Jingu, F., Takahashi, T., and Komeda, Y. (2000). Heat-shock tagging: a simple method for expression and isolation of plant genome DNA flanked by T-DNA insertions. The Plant Journal *22*, 79–86.

Matsumoto, N., and Okada, K. (2001). A homeobox gene, PRESSED FLOWER, regulates lateral axis-dependent development of Arabidopsis flowers. Genes Dev. *15*, 3355–3364.

McAbee, J.M., Hill, T.A., Skinner, D.J., Izhaki, A., Hauser, B.A., Meister, R.J., Venugopala Reddy, G., Meyerowitz, E.M., Bowman, J.L., and Gasser, C.S. (2006). ABERRANT TESTA SHAPEencodes a KANADI family member, linking polarity determination to separation and growth of Arabidopsis ovule integuments. The Plant Journal *46*, 522–531.

McConnell, J.R., and Barton, M.K. (1998). Leaf polarity and meristem formation in Arabidopsis. Development *125*, 2935–2942.

McConnell, J.R., Emery, J., Eshed, Y., Bao, N., Bowman, J., and Barton, M.K. (2001). Role of PHABULOSA and PHAVOLUTA in determining radial patterning in shoots. Nature *411*, 709–713.

Meinhardt, H. (1983). Cell determination boundaries as organizing regions for secondary embryonic fields. Developmental Biology *96*, 375–385.

Merelo, P., Ram, H., Pia Caggiano, M., Ohno, C., Ott, F., Straub, D., Graeff, M., Cho, S.K., Yang, S.W., Wenkel, S., et al. (2016). Regulation of MIR165/166 by class II and class III homeodomain leucine zipper proteins establishes leaf polarity. Proc. Natl. Acad. Sci. U.S.a. 201516110.

Merelo, P., Xie, Y., Brand, L., Ott, F., Weigel, D., Bowman, J.L., Heisler, M.G., and Wenkel, S. (2013). Genome-Wide Identification of KANADI1 Target Genes. Plos One *8*, e77341.

Meyerowitz, E.M. (1997). Genetic Control of Cell Division Patterns in Developing Plants. Cell *88*, 299–308.

Montgomery, T.A., Howell, M.D., Cuperus, J.T., Li, D., Hansen, J.E., Alexander, A.L., Chapman, E.J., Fahlgren, N., Allen, E., and Carrington, J.C. (2008). Specificity

of ARGONAUTE7-miR390 Interaction and Dual Functionality in TAS3 Trans-Acting siRNA Formation. Cell *133*, 128–141.

Caggiano, Monica Pia, Dorso-ventral patterning and lateral organ positioning in Arabidopsis thaliana / presented by Monica Pia Caggiano. - 2013. - 147 S. : Ill., graph. Darst

Nagasaki, H., Itoh, J.-I., Hayashi, K., Hibara, K.-I., Satoh-Nagasawa, N., Nosaka, M., Mukouhata, M., Ashikari, M., Kitano, H., Matsuoka, M., et al. (2007). The small interfering RNA production pathway is required for shoot meristem initiation in rice. Proc Natl Acad Sci USA *104*, 14867–14871.

Nakata, M., and Okada, K. (2012). The three-domain model: a new model for the early development of leaves in Arabidopsis thaliana. Plant Signaling & Behavior *7*, 1423–1427.

Nakata, M., Matsumoto, N., Tsugeki, R., Rikirsch, E., Laux, T., and Okada, K. (2012). Roles of the middle domain-specific WUSCHEL-RELATED HOMEOBOX genes in early development of leaves in Arabidopsis. Plant Cell *24*, 519–535.

Nath, U., Crawford, B.C.W., Carpenter, R., and Coen, E. (2003). Genetic Control of Surface Curvature. Science *299*, 1404–1407.

Neumann, C.J., and Cohen, S.M. (1997). Long-range action of Wingless organizes the dorsal-ventral axis of the Drosophila wing. Development *124*, 871–880.

Bhatia, N., Bozorg, B., Larsson, A., Ohno, C., Jönsson, H., and Heisler, M. G. (2016) Auxin acts through MONOPTEROS to regulate plant cell polarity and pattern phyllotaxis. Curr Bio (in press)

Niswander, L. (2003). Pattern formation: old models out on a limb. Nature Reviews Genetics *4*, 133–143.

Niswander, L., Tickle, C., Vogel, A., Booth, I., and Martin, G.R. (1993). FGF-4 replaces the apical ectodermal ridge and directs outgrowth and patterning of the limb. Cell *75*, 579–587.

Nogueira, F., and Timmermans, M. (2007). An interplay between small regulatory RNAs patterns leaves. Plant Signaling & Behavior.

Okada, K., Ueda, J., Komaki, M.K., Bell, C.J., and Shimura, Y. (1991). Requirement of the Auxin Polar Transport System in Early Stages of Arabidopsis Floral Bud Formation. Plant Cell *3*, 677–684.

Ori, N., Eshed, Y., Chuck, G., Bowman, J.L., and Hake, S. (2000). Mechanisms that control knox gene expression in the Arabidopsis shoot. Development *127*, 5523–5532.

Otsuga, D., DeGuzman, B., Prigge, M.J., Drews, G.N., and Clark, S.E. (2001). REVOLUTA regulates meristem initiation at lateral positions. The Plant Journal *25*, 223–236.

Ow, D.W. (1996). Recombinase-directed chromosome engineering in plants. Current Opinion in Biotechnology *7*, 181–186.

Panin, V.M., Papayannopoulos, V., Wilson, R., and Irvine, K.D. (1997). Fringe modulates Notch-ligand interactions. Nature.

Parr, B.A., Shea, M.J., Vassileva, G., and McMahon, A.P. (1993). Mouse Wnt genes exhibit discrete domains of expression in the early embryonic CNS and limb buds. Development *119*, 247–261.

Pekker, I., Alvarez, J.P., and Eshed, Y. (2005). Auxin Response Factors Mediate Arabidopsis Organ Asymmetry via Modulation of KANADI Activity. Plant Cell *17*, 2899–2910.

Pizette, S., Abate-Shen, C., and Niswander, L. (2001). BMP controls proximodistal outgrowth, via induction of the apical ectodermal ridge, and dorsoventral patterning in the vertebrate limb. Development *128*, 4463–4474.

Ponting, C.P., and Aravind, L. (1999). START: a lipid-binding domain in StAR, HD-ZIP and signalling proteins. Trends in Biochemical Sciences *24*, 130–132.

Reinhardt, D. (2004). Microsurgical and laser ablation analysis of leaf positioning and dorsoventral patterning in tomato. Development *132*, 15–26.

Reinhardt, D., Mandel, T., and Kuhlemeier, C. (2000). Auxin regulates the initiation and radial position of plant lateral organs. The Plant Cell Online *12*, 507–518.

Reinhardt, D., Pesce, E.-R., Stieger, P., Mandel, T., Baltensperger, K., Bennett, M., Traas, J., rcaron, J., Friml, Í., and Kuhlemeier, C. (2003). Regulation of phyllotaxis by polar auxin transport. Nature *426*, 255–260.

Reinhart, B.J., Liu, T., Newell, N.R., Magnani, E., Huang, T., Kerstetter, R., Michaels, S., and Barton, M.K. (2013). Establishing a framework for the Ad/abaxial regulatory network of Arabidopsis: ascertaining targets of class III homeodomain leucine zipper and KANADI regulation. Plant Cell *25*, 3228–3249.

Reinhart, B.J., Weinstein, E.G., Rhoades, M.W., Bartel, B., and Bartel, D.P. (2002). MicroRNAs in plants. Genes Dev. *16*, 1616–1626.

Rhoades, M.W., Reinhart, B.J., Lim, L.P., Burge, C.B., Bartel, B., and Bartel, D.P. (2002). Prediction of Plant MicroRNA Targets. Cell *110*, 513–520.

Riddle, R.D., Ensini, M., Nelson, C., Tsuchida, T., Jessell, T.M., and Tabin, C. (1995). Induction of the LIM homeobox gene Lmx1 by WNT6a establishes dorsoventral pattern in the vertebrate limb. Cell *83*, 631–640.

Rodríguez-Esteban, C., Schwabe, J., and Pena, J. (1997). Radical fringe positions the apical ectodermal ridge at the dorsoventral boundary of the vertebrate limb. Nature.

Samalova, M., Brzobohaty, B., and Moore, I. (2005). pOp6/LhGR: a stringently regulated and highly responsive dexamethasone-inducible gene expression system for tobacco. The Plant Journal *41*, 919–935.

Sarojam, R., Sappl, P.G., Goldshmidt, A., Efroni, I., Floyd, S.K., Eshed, Y., and Bowman, J.L. (2010). Differentiating Arabidopsis shoots from leaves by combined YABBY activities. Plant Cell *22*, 2113–2130.

Saunders, J.W. (1948). The proximo-distal sequence of origin of the parts of the chick wing and the role of the ectoderm. Journal of Experimental Zoology Part a: Ecological Genetics and Physiology *108*, 363–403.

Sawa, S., Watanabe, K., Goto, K., Liu, Y.G., Shibata, D., Kanaya, E., Morita, E.H., and Okada, K. (1999). FILAMENTOUS FLOWER, a meristem and organ identity gene of Arabidopsis, encodes a protein with a zinc finger and HMG-related domains. Genes Dev. *13*, 1079–1088.

Schwartz, C., Locke, J., Nishida, C., and Kornberg, T.B. (1995). Analysis of cubitus interruptus regulation in Drosophila embryos and imaginal disks. Development *121*, 1625–1635.

Semiarti, E., Ueno, Y., Iwakawa, H., Tsukaya, H., Machida, C., and Machida, Y. (2001). The Asymmetric Leaves2 (AS2) Gene of Arabidopsis Thaliana Regulates Lamina Formation and is Required for Patterning of Leaf Venation (Elsevier).

Sessa, G., Steindler, C., Morelli, G., and Ruberti, I. (1998). The Arabidopsis Athb-8, -9 and genes are members of a small gene family coding for highly related HD-ZIP proteins. Plant Mol Biol *38*, 609–622.

Sieburth, L.E., Drews, G.N., and Meyerowitz, E.M. (1998). Non-autonomy of AGAMOUS function in flower development: use of a Cre/loxP method for mosaic analysis in Arabidopsis. Development *125*, 4303–4312.

Siegfried, K.R., Eshed, Y., Baum, S.F., Otsuga, D., Drews, G.N., and Bowman, J.L. (1999). Members of the YABBY gene family specify abaxial cell fate in Arabidopsis. Development *126*, 4117–4128.

Stahle, M.I., Kuehlich, J., Staron, L., Arnim, von, A.G., and Golz, J.F. (2009). YABBYs and the transcriptional corepressors LEUNIG and LEUNIG_HOMOLOG maintain leaf polarity and meristem activity in Arabidopsis. Plant Cell *21*, 3105–3118.

Stepanova, A.N., Robertson-Hoyt, J., Yun, J., Benavente, L.M., Xie, D.-Y., Doležal, K., Schlereth, A., Jürgens, G., and Alonso, J.M. (2008). TAA1-Mediated Auxin Biosynthesis Is Essential for Hormone Crosstalk and Plant Development. Cell *133*, 177–191.

Steeves, T. A. and I. M. Sussex (1989). Patterns in plant development. Cambridge [England]; New York, Cambridge University Press.

Summerbell, D. (1974). A quantitative analysis of the effect of excision of the AER from the chick limb-bud. J Embryol Exp Morphol *32*, 651–660.

Sussex, I.M. (1951). Experiments on the Cause of Dorsiventrality in Leaves. Nature *167*, 651–652.

Swarup, S., and Verheyen, E.M. (2012). Wnt/Wingless Signaling in Drosophila. Cold Spring Harb Perspect Biol *4*, a007930–a007930.

Tabata, T., Schwartz, C., Gustavson, E., Ali, Z., and Kornberg, T.B. (1995). Creating a Drosophila wing de novo, the role of engrailed, and the compartment border hypothesis. Development *121*, 3359–3369.

Tabata, T., and Kornberg, T.B. (1994). Hedgehog is a signaling protein with a key role in patterning Drosophila imaginal discs. Cell *76*, 89–102.

Takahashi, T., Naito, S., and Komeda, Y. (1992). The Arabidopsis HSP18.2 promoter/GUS gene fusion in transgenic Arabidopsis plants: a powerful tool for the isolation of regulatory mutants of the heat-shock response. The Plant Journal *2*, 751–761.

Talbert, P.B., Adler, H.T., Parks, D.W., and Comai, L. (1995). The REVOLUTA gene is necessary for apical meristem development and for limiting cell divisions in the leaves and stems of Arabidopsis thaliana. Development *121*, 2723–2735.

Tanaka, M., Tamura, K., Noji, S., Nohno, T., and Ide, H. (1997). Induction of Additional Limb at the Dorsal–Ventral Boundary of a Chick Embryo. Developmental Biology *182*, 191–203.

Tao, Y., Ferrer, J.-L., Ljung, K., Pojer, F., Hong, F., Long, J.A., Li, L., Moreno, J.E., Bowman, M.E., Ivans, L.J., et al. (2008). Rapid Synthesis of Auxin via a New Tryptophan-Dependent Pathway Is Required for Shade Avoidance in Plants. Cell *133*, 164–176.

Tsukaya, H., and Uchimiya, H. (1997). Genetic analyses of the formation of the serrated margin of leaf blades in Arabidopsis : combination of a mutational analysis of leaf morphogenesis with the characterization of a specific marker gene expressed in hydathodes and stipules. Mol Gen Genet *256*, 231–238.

Villanueva, J.M., Broadhvest, J., Hauser, B.A., Meister, R.J., Schneitz, K., and Gasser, C.S. (1999). INNER NO OUTER regulates abaxial- adaxial patterning in Arabidopsis ovules. Genes Dev. *13*, 3160–3169.

Vogel, A., Rodriguez, C., and Warnken, W. (1995). Dorsal cell fate specified by chick Lmx1 during vertebrate limb development. Nature.

Waites, R., and Hudson, A. (1995). phantastica: a gene required for dorsoventrality of leaves in Antirrhinum majus. Development *121*, 2143–2154.

Waites, R., Selvadurai, H.R.N., Oliver, I.R., and Hudson, A. (1998). The PHANTASTICA Gene Encodes a MYB Transcription Factor Involved in Growth and Dorsoventrality of Lateral Organs in Antirrhinum. Cell *93*, 779–789.

Wenkel, S., Emery, J., Hou, B.H., Evans, M.M.S., and Barton, M.K. (2007). A Feedback Regulatory Module Formed by LITTLE ZIPPER and HD-ZIPIII Genes. The Plant Cell Online *19*, 3379–3390.

Williams, L., Carles, C.C., Osmont, K.S., and Fletcher, J.C. (2005). A database

analysis method identifies an endogenous trans-acting short-interfering RNA that targets the Arabidopsis ARF2, ARF3, and ARF4 genes. Proc Natl Acad Sci USA *102*, 9703–9708.

Wu, G., Lin, W.-C., Huang, T., Poethig, R.S., Springer, P.S., and Kerstetter, R.A. (2008). KANADI1 regulates adaxial-abaxial polarity in Arabidopsis by directly repressing the transcription of ASYMMETRIC LEAVES2. Proc. Natl. Acad. Sci. U.S.a. *105*, 16392–16397.

Xu, L., Xu, Y., Dong, A., Sun, Y., Pi, L., Xu, Y., Xu, Y., and Huang, H. (2003). Novel as1 and as2 defects in leaf adaxial-abaxial polarity reveal the requirement for ASYMMETRIC LEAVES1 and 2 and ERECTA functions in specifying leaf adaxial identity. Development *130*, 4097–4107.

Xu, L., Yang, L., Pi, L., Liu, Q., Ling, Q., Wang, H., Poethig, R.S., and Huang, H. (2006). Genetic interaction between the AS1-AS2 and RDR6-SGS3-AGO7 pathways for leaf morphogenesis. Plant Cell Physiol *47*, 853–863.

Yadav, R.K., Perales, M., Gruel, J., Ohno, C., Heisler, M., Girke, T., Jönsson, H., and Reddy, G.V. (2013). Plant stem cell maintenance involves direct transcriptional repression of differentiation program. Molecular Systems Biology *9*, 654–654.

Yan, J., Gu, Y., Jia, X., Kang, W., Pan, S., Tang, X., Chen, X., and Tang, G. (2012). Effective Small RNA Destruction by the Expression of a Short Tandem Target Mimic in Arabidopsis. The Plant Cell Online *24*, 415–427.

Yao, X., Wang, H., Li, H., Yuan, Z., Li, F., Yang, L., and Huang, H. (2009). Two types of cis-acting elements control the abaxial epidermis-specific transcription of the MIR165aand MIR166agenes. FEBS Letters *583*, 3711–3717.

Yoshida, K., Kasai, T., Garcia, M.R.C., Sawada, S., Shoji, T., Shimizu, S., Yamazaki, K., Komeda, Y., and Shinmyo, A. (1995). Heat-inducible expression system for a foreign gene in cultured tobacco cells using the HSP18.2 promoter of Arabidopsis thaliana. Appl Microbiol Biotechnol *44*, 466–472.

Zecca, M., Basler, K., and Struhl, G. (1995). Sequential organizing activities of engrailed, hedgehog and decapentaplegic in the Drosophila wing. Development.

Appendix

Transgenic plants	Generated by	Construct made by
KAN1p::KAN1-2×GFP *REVp::REV-2×YPet* *PIN1p::PIN1-CFP*	Carolyn Ohno	From (Yadav et al.,2013) Carolyn Ohno From (Gordon et al., 2009)
KAN2p::KAN2-2×GFP *REVp::REV-2×YPet* *PIN1p::PIN1-CFP*	Carolyn Ohno	Carolyn Ohno Carolyn Ohno From (Gordon et al., 2009)
KAN4p::KAN4-2×GFP *PIN1p::PIN1-CFP*	Carolyn Ohno	Carolyn Ohno From (Gordon et al., 2009)
UBQ10p>>STTM 165/166-88 *REVp::REV-2×YPet* *PIN1p::PIN1-CFP*	Monica Pia Caggiano	Monica Pia Caggiano Carolyn Ohno From (Gordon et al., 2009)
ATML1>>PHVr *REVp::REV-2×YPet* *PIN1p::PIN1-CFP*	Carolyn Ohno	Carolyn Ohno Carolyn Ohno From (Gordon et al., 2009)
AtML1p::LhGR_6Op:: KAN1-GFP *PIN1p::PIN1-GFP*	Carolyn Ohno	Carolyn Ohno (Heisler et al., 2005)
CLV3p::LhGR_6Op::KAN1-2×GFP *REVp::REV-2×YPet* *PIN1p::PIN1-CFP*	Carolyn Ohno	Carolyn Ohno Carolyn Ohno From (Gordon et al., 2009)
HSp::CRE-GR + *UBQ10p::lox spacer lox::* *REVr-Ypet* *PIN1p::PIN1-GFP*	Monica Pia Caggiano	Monica Pia Caggiano (Heisler et al., 2005)
HSp::CRE-GR + *UBQ10p::lox spacer lox::* *REVr-Ypet* *KAN1p::KAN1-2×GFP* *PIN1p::PIN1-CFP*	Xiulian Yu	Monica Pia Caggiano From (Yadav et al.,2013) From (Gordon et al., 2009)
HSp::CRE-GR + *UBQ10p::lox spacer lox::* *REVr-Ypet* *ML1::KAN1GR* *PIN1p::PIN1-GFP*	Xiulian Yu	Monica Pia Caggiano AtML1p::KAN1-GR_BJ36 from J.Bowman then subcloned by C. Ohno (Heisler et al., 2005)
kan1kan2 *PIN1p::PIN1-GFP* *REVp::REV-2×VENUS*	Carolyn Ohno	A gift from John Bowman (Heisler et al., 2005) Carolyn Ohno

kan1kan2 *HSp::CRE-GR +* *UBQ10p::lox spacer lox::* *REVr-Ypet* *PIN1p::PIN1-GFP*	Carolyn Ohno	Kindly provided from John Bowman Carolyn Ohno Carolyn Ohno (Heisler et al., 2005)
HSp::CRE-GR + *UBQ10p::lox spacer lox::* *REVr-Ypet* *35S::MAP4-GFP*	Xiulian Yu	Monica Pia Caggiano A gift from Richard J. Cyr
TAA1p::GFP-TAA1 *REVp::REV-2×YPet* *PIN1p::PIN1-CFP*	Xiulian Yu	(Stepanova et al., 2008)
HSp::CRE-GR + *UBQ10p::lox spacer lox::* *REVr-Ypet* *TAA1p::GFP-TAA1*	Xiulian Yu	Monica Pia Caggiano (Stepanova et al., 2008)
HSp::CRE-GR + *UBQ10p::lox spacer lox::* *REVr-Ypet* *TAA1p::GFP-TAA1* *PIN1p::PIN1-CFP*	Xiulian Yu	Monica Pia Caggiano (Stepanova et al., 2008) From (Gordon et al., 2009)
WOX1p::2GFP-WOX1 *PIN1p::PIN1-CFP*	Carolyn Ohno	Carolyn Ohno From (Gordon et al., 2009)
HSp::CRE-GR + *UBQ10p::lox spacer lox::* *REVr-Ypet* *PIN1p::PIN1-GFP* *WOX1p::2GFP-WOX1*	Carolyn Ohno	Monica Pia Caggiano (Heisler et al., 2005) Carolyn Ohno
PRSp::PRS-2×GFP *REVp::REV-2×YPet* *PIN1p::PIN1-CFP*	Carolyn Ohno	Carolyn Ohno Carolyn Ohno From (Gordon et al., 2009)
HSp::CRE-GR + *UBQ10p::lox spacer lox::* *REVr-Ypet* *PRSp::tdTOMATO-NLS* *PIN1p::PIN1-GFP*	Xiulian Yu	Monica Pia Caggiano Carolyn Ohno (Heisler et al., 2005)
HSp::CRE-GR + 35S::lox spacer lox::KAN1-GFP *REVp::REV-2×YPet* *PIN1p::PIN1-CFP*	Carolyn Ohno	Carolyn Ohno Carolyn Ohno From (Gordon et al., 2009)